University of Catania
PhD Program in Neuroscience

Maria Rosaria Tropea

Role of Aβ at the synapse in physiological conditions and in Alzheimer's disease: crosstalk with α7-nAChRs and cyclic nucleotides

4/12/2021

Department of Biomedical and Biotechnological Sciences
University of Catania School of Medicine
International PhD Program in Neuroscience
XXXIV Cycle

Maria Rosaria Tropea

Role of Amyloid-β peptide at the synapse in physiological conditions and in Alzheimer's disease: crosstalk with a7-nAChRs and cyclic nucleotides

Ph.D. THESIS

Coordinator: *Prof. Claudio Bucolo*
Tutor: *Prof. Daniela Puzzo*

Academic Year 2020-21

INDEX

“You have to begin to lose your memory, if only in bits and pieces, to realise that memory is what makes our lives. Life without memory is no life at all... Our memory is our coherence, our reason, our feeling, even our action. Without it, we are nothing”

Luis Bunuel

General Introduction

BACKGROUND

Alzheimer's Disease is a neurodegenerative disorder representing the most common form of dementia in the elderly. It is characterized by a deficit of memory function associated with the impairment of at least another cognitive domain (language, praxis, gnosis, executive function, judgment, and abstract thought) leading to the inability to conduct basic daily activities and, ultimately, to death.

Despite decades of intensive research, AD pathophysiology remains elusive, and several hypotheses have been proposed to explain the complex cascade of events leading to dementia. Among these, an extensive attention has been devoted to the so-called "Amyloid-beta (Aβ) hypothesis" based on the increase of soluble and insoluble aggregates of this protein in AD brains (for a review see Selkoe & Hardy 2016). Over the years, this hypothesis has been reshaped from an early version mainly focusing on the pathological significance of insoluble fibrils and senile plaques, to the concept that soluble oligomers of Aβ alter glutamatergic synaptic function and cause synapse loss (Li et al., 2011). On the other hand, a variety of *in vitro* and *in vivo* studies have demonstrated that, when at low concentrations, Aβ exerts a

physiological function in the healthy brain by regulating synaptic plasticity and memory (Morley et al., 2010; Puzzo et al., 2008). Aβ is physiologically produced in the healthy brain where it acts as an antimicrobial and neurotrophic factor (Yankner et al., 1990) and as a neuromodulator. In fact, Aβ is secreted at the synapse in an activity-dependent fashion (Cirrito et al., 2005; Kamenetz et al., 2003), and it has been demonstrated to enhance neurotransmitter release acting through the α7nAChRs. Indeed, low pM concentrations of Aβ interact with α7nAChRs with high binding affinity (Wang et al., 2000) showing an agonist-like effect in the regulation of synaptic function (Gulisano et al., 2019; Lawrence et al., 2014; Lazarevic et al., 2017; Oz et al., 2013; Mura et al., 2012; Puzzo et al., 2011; Dineley et al., 2002).

Interestingly, either in the healthy or diseased brain, Aβ interferes with molecular signaling pathways fundamental for the occurrence of long-term potentiation (LTP), a type of synaptic strengthening that is thought to underlie learning and memory. In particular, Aβ is likely to interfere with the second messenger systems leading to the phosphorylation of the transcription factor cAMP response element-binding protein (CREB), which is critical for memory formation (for a review see Teich et al, 2015).

AIM OF THE THESIS

The main aim of this thesis was to study the role of Amyloid-beta peptide (Aβ) at the synapse in physiological conditions and its involvement in the pathophysiology of AD.

Aim 1: To investigate how Aβ modulates hippocampal synaptic plasticity and memory.

Aim 2: To investigate whether the failure of Aβ physiological function might contribute to AD onset and progression.

THESIS ORGANIZATION AND MY CONTRIBUTION

I will discuss two of the projects I have carried out during my PhD program suggesting that Aβ needs α7nAChRs to modulate LTP and memory and that genetic deletion of α7nAChRs could represent one of the triggering events leading to AD. I will also report the results of a study aimed at clarifying some methodological issues encountered when performing behavioral studies to investigate memory on rodent models of AD.

In particular, the thesis is divided into different sections, as follows:

Chapter 1 reports a study investigating in depth the physiological role of oligomeric $A\beta_{42}$ at the hippocampus, assessing its neuromodulatory effect on different forms of synaptic plasticity and memory and

analyzing the cellular mechanisms and mediators involved (Gulisano et al., J Neurosci 2019).

I contributed to this work by conducting behavioral studies (from design to analyses of results) and some electrophysiological experiments. I also participate to conceptualization, discussion, writing, and revision of the manuscript. I presented data from this work at the "Annual Meeting of Young Researchers in Physiology" 2019 where I was awarded a Special Mention.

Chapter 2 reports a study aimed at understanding the impact of α7nAChRs in the pathophysiology of AD, demonstrating how their genetic deletion prevents Aβ to exert its physiological function triggering a compensatory increase of the peptide that, in turn, induces the functional and structural alterations related to AD (Tropea et al., Prog Neurobiol 2021).

As first author, I contributed to this work by conceiving the idea, carrying out experiments, analyzing results, writing and revising the manuscript. In particular, I conducted behavioral studies (from design to analyses of results) and contributed to electrophysiological experiments at the University of Catania. I also performed and analyzed microscopy studies during my PhD training at Università Politecnica delle Marche with the supervision of Prof. Fiorenzo Conti and Prof.

Marcello Melone. I presented data from this work as poster presenter at the Society for Neuroscience Meeting Global Connectome (Jan 2021, online); and as speaker at the 71st National Congress of the Italian Society of Physiology (Sept 2021, online).

Chapter 3 focuses on some methodological issues encountered when studying learning and memory in rodent models, indicating how a standardized test setting is needed to obtain reliable unbiased results in behavioral experiments (Tropea et al., J Alzheimers Dis, 2022).
As first author, I contributed to this work by conceiving the idea, analyzing results, writing and revising the manuscript. In particular, I supervised MD students that conducted behavioral studies and was co-tutor for their MD experimental thesis preparation based on this project.

A *General Discussion* will summarize the relevance of these findings giving new insights into possible future directions.

REFERENCES

Cirrito JR, Yamada KA, Finn MB, Sloviter RS, Bales KR, May PC, Schoepp DD, Paul SM, Mennerick S, Holtzman DM (2005) Synaptic activity regulates interstitial fluid amyloid-β levels in vivo. Neuron 48, 913–922.

Dineley, K.T., Bell, K.A., Bui, D., Sweatt, J.D., 2002. β-amyloid peptide activates a7 nicotinic acetylcholine receptors expressed in Xenopus oocytes. J. Biol. Chem. 277, 25056–25061. https://doi.org/10.1074/jbc.M200066200

Gulisano W, Melone M, Ripoli C, Tropea MR, Li Puma DD, Giunta S, Cocco S, Marcotulli D, Origlia N, Palmeri A, Arancio O, Conti F, Grassi C, Puzzo D (2019) Neuromodulatory Action of Picomolar Extracellular Aβ42 Oligomers on Presynaptic and Postsynaptic Mechanisms Underlying Synaptic Function and Memory. *J Neurosci* **39**, 5986–6000.

Kamenetz F, Tomita T, Hsieh H, Seabrook G, Borchelt D, Iwatsubo T, Sisodia S, Malinow R (2003) APP processing and synaptic function. Neuron 37, 925–937

Lawrence JLM, Tong M, Alfulaij N, Sherrin T, Contarino M, White MM, Bellinger FP, Todorovic C, Nichols RA (2014) Regulation of presynaptic Ca2+, synaptic plasticity and contextual fear conditioning by a N-terminal beta-amyloid fragment. *J Neurosci* 34, 14210–14218.

Lazarevic, V., Fieńko, S., Andres-Alonso, M., Anni, D., Ivanova, D., Montenegro-Venegas, C., Gundelfinger, E.D., Cousin, M.A., Fejtova, A., 2017. Physiological concentrations of amyloid beta regulate recycling of synaptic vesicles via alpha7 acetylcholine receptor and CDK5/calcineurin signaling. Front. Mol. Neurosci. https://doi.org/10.3389/fnmol.2017.00221

Li S, Jin MB, Koeglsperger T, Shepardson NE, Shankar GM, Selkoe D (2011) Soluble Aβ oligomers inhibit long-term potentiation through a mechanism involving excessive activation of extrasynaptic NR2B-containing NMDA receptors. J Neurosci 31:6627-6638.

Morley JE, Farr S A, Banks WA, Johnson SN, Yamada KA, Xu L (2010) A physiological role for amyloid-β protein: Enhancement of learning and memory. *J Alzheimers Dis* 19, 441–449.

Mura E, Zappettini S, Preda S, Biundo F, Lanni C, Grilli M, Cavallero A, Olivero G, Salamone A, Govoni S, Marchi M (2012) Dual effect of beta-amyloid on α7 and α4β2 nicotinic receptors controlling the release of glutamate, aspartate and GABA in rat hippocampus. PloS one 7:e29661

Oz, M., Lorke, D.E., Yang, K.S., Petroianu, G., 2013. On the Interaction of -Amyloid Peptides and 7-Nicotinic Acetylcholine Receptors in Alzheimer ' s Disease. Curr. Alzheimer Res. 10, 618–630.

Puzzo D, Privitera L, Leznik E, Fa M, Staniszewski A, Palmeri A, Arancio O (2008) Picomolar amyloid-beta positively modulates synaptic plasticity and memory in hippocampus. *J Neurosci* 28, 14537–14545.

Puzzo D, Privitera L, Fa' M, Staniszewski A, Hashimoto G, Aziz F, Sakurai M, Ribe EM, Troy CM, Mercken M, Jung SS, Palmeri A, Arancio O (2011) Endogenous amyloid-β is necessary for hippocampal synaptic plasticity and memory. Annals of neurology 69:819–830

Selkoe DJ, Hardy J. The amyloid hypothesis of Alzheimer's disease at 25 years. EMBO Mol Med. 2016;8(6):595-608. Published 2016 Jun 1. doi:10.15252/emmm.201606210

Teich, A.F., Nicholls, R.E., Puzzo, D. et al. Synaptic Therapy in Alzheimer's Disease: A CREB-centric Approach. Neurotherapeutics 12, 29–41 (2015). https://doi.org/10.1007/s13311-014-0327-5

Wang, H.Y., Lee, D.H., Davis, C.B., Shank, R.P., 2000. Amyloid peptide Abeta(1-42) binds selectively and with picomolar affinity to alpha7 nicotinic acetylcholine receptors. J. Neurochem. 75, 1155–61. https://doi.org/10.1046/j.1471-4159.2000.0751155.x

Chapter 1: Neuromodulatory action of picomolar extracellular Aβ42 oligomers on pre- and post-synaptic mechanisms underlying synaptic function and memory

Gulisano W[1], Melone M[2,3], Ripoli C[4,5], Tropea MR[1], Li Puma DD[4,5], Giunta S[1], Cocco S[4], Marcotulli D[2], Origlia N[6], Palmeri A[1], Arancio O[7], Conti F[2,3,8], Grassi C[4,5], Puzzo D[1,9].

[1]Dept. Biomedical and Biotechnological Sciences, University of Catania, Catania 95123, Italy; [2]Section of Neuroscience and Cell Biology, Dept. Experimental and Clinical Medicine, Università Politecnica delle Marche, Ancona 60020, Italy; [3]Center for Neurobiology of Aging, IRCCS INRCA, Ancona 60020, Italy; [4]Institute of Human Physiology, Università Cattolica del Sacro Cuore, Rome 00168, Italy; [5]Fondazione Policlinico Universitario A. Gemelli IRCCS, Rome, 00168, Italy; [6]Neuroscience Institute, Italian National Research Council, Pisa 56100, Italy; [7]Taub Institute for Research on Alzheimer's Disease and the Aging Brain, Columbia University, New York (NY) 10032, USA; [8]Foundation for Molecular Medicine, Università Politecnica delle Marche, Ancona 60020, Italy; [9]Oasi Research Institute-IRCCS, Troina, 94018, Italy.

In: J Neurosci. 2019 Jul 24;39(30):5986-6000.
doi: 10.1523 JNEUROSCI.0163-19.2019.

ABSTRACT

Failure of anti-amyloid-beta peptide (Aβ) therapies against Alzheimer's disease (AD), a neurodegenerative disorder characterized by high amounts of the peptide in the brain, raised the question of the physiological role of Aβ released at low concentrations in the healthy brain.

To address this question, here we studied the pre- and post-synaptic mechanisms underlying the neuromodulatory action of picomolar amounts of oligomeric $A\beta_{42}$ ($oA\beta_{42}$) on synaptic glutamatergic function in male and female mice.

We found that pM $oA\beta_{42}$ induces an increase of frequency of miniature excitatory postsynaptic currents and a decrease of paired pulse facilitation, associated with an increase in docked vesicle number, indicating that it augments neurotransmitter release at presynaptic level. $oA\beta_{42}$ also produced postsynaptic changes as shown by an increased length of postsynaptic density, accompanied by an increased expression of plasticity-related proteins such as cAMP-responsive element binding protein phosphorylated at Ser133, calcium-calmodulin-dependent kinase II phosphorylated at Thr286, and brain-derived neurotrophic factor, suggesting a role for Aβ in synaptic tagging. These changes resulted in the conversion of early into late long-term potentiation through the nitric oxide/cGMP/protein kinase G intracellular cascade

consistent with a cGMP-dependent switch from short to long-term memory observed *in vivo* after intrahippocampal administration of picomolar amounts of oAβ_{42}. These effects were present upon extracellular but not intracellular application of the peptide, and involved α7 nicotinic acetylcholine receptors.

These observations clarified the physiological role of oAβ_{42} in synaptic function and memory formation and provide solid fundamentals for investigating the pathological effects of Aβ occurring when it abnormally increases in the brain of AD patients.

Significance Statement

High levels of oligomeric amyloid-beta$_{42}$ (oAβ_{42}) induce synaptic dysfunction leading to memory impairment in Alzheimer's disease (AD). However, when at picomolar (pM) concentration, the peptide is needed to ensure long-term potentiation (LTP) and memory. Here we show that extracellular pM oAβ_{42} increases neurotransmitter release, number of docked vesicles, postsynaptic density length, and expression of plasticity-related proteins leading to the conversion of early-LTP into late-LTP and of short-term into long-term memory. These effects require α7 nicotinic acetylcholine receptors and are mediated through the nitric oxide/cGMP/protein kinase G pathway. The knowledge of Aβ function in the healthy brain might be useful to understand the causes leading to its increase and detrimental effect in AD.

INTRODUCTION

Abnormal elevation of amyloid-beta peptide (Aβ) in the brain is considered one of the main pathogenetic events in Alzheimer's disease (AD) (Hardy and Selkoe, 2002). Most of the studies in the field have focused on Aβ production, aggregation and degradation, resulting in therapeutic strategies aimed at decreasing Aβ levels in the brain. However, lack of correlation between insoluble Aβ deposits and cognitive impairment, presence of Aβ deposits in plaques or soluble oligomers in non demented individuals (Aizenstein et al., 2008; Maarouf et al., 2011; Lesné et al., 2013), and failure of Aβ reducing therapies (Gulisano et al., 2018a), have prompted the neuroscience community to reconsider the pathogenetic role of the peptide (Herrup, 2015; Puzzo et al., 2015; Gulisano et al., 2018a). To this end, the concept that Aβ is not solely a toxic product derived from Amyloid Precursor Protein (APP) processing, already proposed in the early nineties (Koo et al., 1993), has been strengthened by studies investigating the physiological role of the peptide in the CNS. Nonetheless, information regarding Aβ-dependent regulation of synaptic activity in the healthy brain is still fragmentary, precluding from a clear insight into the mechanisms underlying the switch from function to dysfunction (Koppensteiner et al., 2016).

Besides its neuroprotective activity (Pearson and Peers, 2006), Aβ is likely to act as a neuromodulator at the synapse where it is released during neuronal activity (Kamenetz et al., 2003; Brody et al., 2008) and is dynamically regulated by presynaptic mechanisms involving vesicle cycling (Cirrito et al., 2005, 2008). Our previous studies have shown that Aβ production increases during the induction of long-term potentiation (LTP) (Palmeri et al., 2017) and contextual fear learning (Puzzo et al., 2011), and that blocking its function in the healthy brain impairs LTP and memory (Garcia-Osta and Alberini, 2009; Morley et al., 2010; Puzzo et al., 2011). Moreover, administration of picomolar concentrations of the peptide, mimicking its physiological content in the brain (Schmidt et al., 2005; Puzzo et al., 2008), enhances LTP and memory (Morley et al., 2010; Puzzo et al., 2008), suggesting that Aβ acts in a hormetic fashion exerting a biphasic effect depending upon its concentration (Puzzo et al., 2012).

Recently, we have demonstrated that both the positive and negative effects exerted by $A\beta_{42}$ at the synapse need the presence of oligomers (Gulisano et al., 2018b), suggesting that oligomeric $A\beta_{42}$ ($oA\beta_{42}$) plays a key role in physiological synaptic function. These findings prompted us to investigate in depth how picomolar concentrations of $oA\beta_{42}$ affect the pre- and post-synaptic mechanisms underlying synaptic

transmission and plasticity, as well as memory, highlighting similarities and differences between the physiological and pathological roles of the peptide.

MATERIALS AND METHODS

Ethical approval

All experiments involving animals were approved by the University of Catania (#327/2013-B, #119-2017-PR) and the Università Cattolica del Sacro Cuore in Rome (#626-2016-PR), in accordance to the respective regulations of local Institutional Animal care and Use Committee (IACUC) and with the EU Directive 2010/63/EU. The experiments complied with the ARRIVE guidelines and were conducted to minimize the animals' pain and suffering.

Animals

Wild type (C57Bl/6J; RRID:IMSR_JAX:000664), *App*-KO (B6.129S7-App^{tm1Dbo}/J; RRID:IMSR_JAX:004133) and *α7*-KO (B6.129S7-Chrna7^{tm1Bay}/J; RRID:IMSR_JAX:003232) mice were purchased from the Jackson Laboratory (Bar Harbor, ME, USA) and bred in the animal facilities at University of Catania, and Università Cattolica del Sacro Cuore. Mice were maintained in stable hygrometric and thermic

conditions (50%; 21 °C ± 1 °C) on 12 hours light/dark cycle with *ad libitum* access to food and water. For electrophysiological recordings, male animals were used at 3-4 months of age (field recordings) or 21 days (whole-cell recordings). Dual patch experiments were performed on organotypic slices from P4-7 Wistar rats. For behavioral experiments, sex-balanced groups of mice were used at 3-4 months of age.

Aβ Preparation, Concentration and Characterization

Oligomeric Aβ was prepared as previously described (Stine et al., 2003; Puzzo et al., 2008; Ripoli et al., 2013). Briefly, the lyophilized peptide (American Peptide, Sunnyvale, USA) was suspended in 1,1,1,3,3,3-hexafluoro-2-propanol (HFIP; Sigma, St. Louis, MO, USA) to 1 mM. After the complete evaporation of HFIP to allow complete monomerization, the Aβ film was dissolved in dimethylsulfoxide (DMSO; Sigma), sonicated for 15 minutes, aliquoted, and stored at -20 °C. DMSO-Aβ solution was incubated in PBS at 4 °C for 12 hours to allow oligomerization. The oligomerized Aβ solution was then diluted in ACSF or saline solution (0.9% NaCl) to the final concentration, calculated based on the MW of the monomeric peptide.

Western blot of 200 pM and 200 nM Aβ solutions was routinely performed to assess oligomers presence (Gulisano et al., 2018b). Aβ

solutions were incubated for 20 minutes at 29 °C to reproduce experimental conditions of electrophysiological experiments. After this step, NuPAGE LDS sample buffer 4× was added and Aβ preparations (at the final concentration of 200 nM and 200 pM) were separated on 10%-20% Novex Tricine precast gels (Invitrogen). Proteins were then transferred onto 0.2 µm nitrocellulose membranes (Amersham Biosciences, Buckinghamshire,UK) that were incubated overnight at 4 °C with the mouse monoclonal antibody 6E10 (1:1000; Covance, Princeton, NJ, USA). The next day membranes were revealed with HRP-conjugated secondary antibodies (Cell Signaling Technology Inc., Danvers, MA) using the SuperSignal West Femto Maximum Sensitivity Substrate (Thermo Scientific, Waltham, MA, USA) and documented by using UVItec Cambridge Alliance. Low Range Rainbow Molecular Weight Markers (GE Healthcare Life Sciences) were used to assess the *protein* size.

Dose-response (DR) curves were performed to choose the dose of Aβ mimicking the physiological effects of oligomers on synaptic plasticity. Based on our previous work (Puzzo et al., 2012), hippocampal slices were treated with the following doses of Aβ: 2 pM, 20 pM, 200 pM, 2 nM, 20nM and 200 nM, for twenty minutes before to induce plasticity. Based on these results, we used 200 pM Aβ for *in vitro* experiments, corresponding to 0.903 pg for *in vivo* injections into each hippocampus.

DR curves were also performed with the same experimental design to assess the dose of Aβ capable to modify paired-pulse facilitation.

Drugs

Nω-Nitro-L-arginine methyl ester hydrochloride (L-NAME, Sigma; 100 μM) (Johnstone and Raymond, 2011), 8- Bromoguanosine- 3', 5'-cyclic monophosphorothioate, Rp-isomer (Rp-8-Br-cGMPS, Biolog, Bremen, Germany; 10 μM for electrophysiology and 1μg/1μl for behavioral studies) (Bollen et al., 2014), 1H-[1,2,4]Oxadiazolo[4,3-a]quinoxalin-1-one (ODQ, Sigma; 100 μM) (Puzzo et al., 2005), Anisomycin (ANI, Sigma; 20 μM) (Johnstone and Raymond, 2011), (2R)-amino-5-phosphonovaleric acid (APV, Tocris, Bristol, UK; 50 μM) (Puzzo et al., 2008), Methyllycaconitine (MLA, Sigma; 10 μM based on DR curves obtained in our laboratory) were dissolved in DMSO, aliquoted and stored at -20°C. All drugs were diluted in ACSF or saline solution (0.9% NaCl) to the desired final concentration right before electrophysiological or behavioral experiments. 6E10 (Covance, Princeton, NJ, USA, Cat# SIG-39320, RRID:AB_662798; 1:300) and M3.2 (Covance, Cat# SIG-39155, RRID:AB_2028758; 2 μg/ml) antibodies used for electrophysiological experiments were directly diluted in ACSF according to previous studies (Ripoli et al., 2014; Palmeri et al., 2017).

Dual whole-cell recordings

Hippocampal organotypic slice cultures were prepared from postnatal day 4-7 rats through a McIllwain tissue chopper and placed on semiporous membranes (Millipore) for 5–7 days before recordings, as previously described (Spinelli et al., 2017). Hippocampal subfields and electrode positions were identified with the aid of 4× and 40× water immersion objectives on an upright microscope equipped with differential interference contrast optics under infrared illumination (BX51WI; Olympus) and video observation (BTE-B050-U CMOS camera; Mightex). Neighbouring pairs of pyramidal cells were recorded simultaneously in CA1 by single stimulating bipolar tungsten electrode (FHC, Neural microTargeting Worldwide) placed on the Schaffer collateral fibers, as previously described (Barone et al., 2018). Slices were incubated in artificial cerebrospinal fluid (ACSF) containing (in mM): 119 NaCl, 2.5 KCl, 4 $CaCl_2$, 4 $MgCl_2$, 1 NaH_2PO_4, 26 $NaHCO_3$, 11 D-glucose, and 0.005 2-chloroadenosine, gassed with 95% O_2/5% CO_2. Whole-cell recording pipettes (3–4 MΩ) were filled with a solution containing (in mM): 135 $CsMeSO_3$, 8 NaCl, 10 HEPES, 0.25 EGTA, 2 Mg_2ATP, 0.3 Na_3GTP, 0.1 spermine, 7 phosphocreatine, and 5 QX-314, pH 7.25–7.30 (osmolarity 300 mOsm). Data were collected with a MultiClamp 700B amplifier (Molecular Devices), digitized at 10 kHz using the Digidata 1440A data acquisition system (Molecular

Devices) and analyzed off-line using pClamp 10 software (RRID:SCR_011323; Molecular Devices).

Experimental design

The AMPA/NMDA ratio was calculated as the peak averaged AMPAR-mediated EPSC at holding potential of −70 mV divided by the averaged NMDAR-mediated EPSC at holding potential of +40 mV at a latency at which AMPAR-mediated EPSC responses were fully decayed (50 ms after stimulation). Miniature EPSCs (mEPSCs) amplitude and frequency were evaluated in 60 s recordings in the presence of tetrodotoxin (TTX; 0.5 μM) at −70 mV.

We used two different experimental settings to evaluate whether oAβ_{42} exerted an extracellular and/or intracellular effect. To study the extracellular effect, slices were perfused with extracellular 200 pM oAβ_{42} whereas one patch-pipette was filled with vehicle and the other with 6E10 antibody that blocks the possible effect due to intracellular oAβ_{42}. To study the intracellular effect, slices were perfused with extracellular vehicle whereas one patch-pipette was filled with vehicle and the other with 200 pM oAβ_{42}. This design also allowed us to concurrently compare the effects of vehicle and 200 pM oAβ_{42} injected into adjacent neurons through patch-pipettes.

To confirm the ability of 6E10 to block oAβ_{42} action, slices were perfused with extracellular 200 pM oAβ_{42} paired with 6E10, 6E10 alone

or 200 pM oAβ_{42} alone whereas the patch-pipette was filled with vehicle.

Whole-cell LTP recordings in hippocampal brain slices

Experiments examining LTP were performed from single CA1 pyramidal cells after stimulating the Schaffer collateral fibers by means of a bipolar tungsten electrode (FHC, Neural microTargeting Worldwide) in acute hippocampal brain slices (300 μm thick) obtained by 21-d-old male C57BL/6 mice, as previously described (Ripoli et al., 2013, 2014). Animals were anesthetized with isoflurane, decapitated and the brains were rapidly placed in ice-cold cutting solution containing the following (in mM): 124 NaCl, 3.2 KCl, 1 NaH_2PO_4, 2 $MgCl_2$, 1 $CaCl_2$, 26 $NaHCO_3$, 10 glucose, 2 Na-pyruvate, and 0.6 ascorbic acid, pH 7.4, 95% O_2/5% CO_2. Slices were sectioned on a Leica Microsystems vibratome (VT1200S; Leica Microsystems) and rapidly transferred to an incubation chamber filled with ACSF containing the following (in mM): 124 NaCl, 3.2 KCl, 1 NaH_2PO_4, 1 $MgCl_2$, 2 $CaCl_2$, 26 $NaHCO_3$, and 10 glucose, pH 7.4, gassed with 95% O_2/5% CO_2. Slices were allowed to recover at 32 °C for 1 h before equilibration at room temperature. During recordings, slices were placed in a recording chamber perfused with heated ACSF (32 °C) and bubbled with 95% O_2/5% CO_2. All recordings were made with the $GABA_A$ receptor

antagonist picrotoxin (50 μM) added to the ACSF. Whole-cell recording pipettes (3–5 MΩ) were filled with the same internal solution used for dual-patch recordings in organotypic hippocampal slices. Whole-cell recordings were carried out with a Multiclamp 700B amplifier (Molecular Devices). A Digidata 1440A series interface and pClamp 10 software were used for data acquisition and stimulation protocols. Data were filtered at 1 kHz, digitized at 10 kHz, and analyzed on-line and off-line.

Experimental design

To study LTP in CA1 pyramidal cells, the stimulation intensity that elicited one-third of the maximal response amplitude of AMPAR EPSC was used for delivering test pulses every 20 s. CA1 pyramidal cells were held at -60 mV. LTP was induced by two trains of HFS (100 Hz, 1 s) separated by 20 s, with the patched cells depolarized to 0 mV. This induction protocol was always applied within 5–7 min of achieving whole-cell configuration, to avoid "wash-out" of LTP. Responses to test pulse were recorded for 30 min to assess LTP. The magnitude of LTP was calculated on basis of the averaged EPSC values during the last 5 min of post-HFS recordings (from minute 25 to minute 30). LTP magnitude was expressed as the percentage change in the mean EPSC peak amplitude normalized to baseline values, taken as 100% (i.e., mean values for the 5 min of recording before HFS).

Electrophysiological field recordings

Extracellular electrophysiological field recordings were performed on 400 μm transverse hippocampal slices as previously described (Puzzo et al., 2008). After cutting procedure by using a manual tissue-chopper, slices were transferred to a recording chamber and perfused (1-2 ml/min) with artificial cerebrospinal fluid (ACSF; composition in mM: 124 NaCl, 4.4 KCl, 1 Na_2HPO_4, 25 $NaHCO_3$, 2 $CaCl_2$, 2 $MgCl_2$, 10 Glucose) kept at 29 °C and continuously bubbled with an O_2/CO_2 mixture at 95% and 5%. After 120 minute recovery, field excitatory postsynaptic potentials (fEPSPs) were recorded in CA1 *stratum radiatum* by a glass electrode filled with ACSF in response to Schaffer collaterals stimulation by a bipolar tungsten electrode.

Experimental design

Recordings were performed and analyzed in pClamp 10. We first measured basal synaptic transmission (BST) by stimulating with a series of increasing voltage pulses (from 5 to 35 V). This allowed us to preliminarily select healthy slices to be used for electrophysiological recordings. For LTP, baseline was recorded every minute by stimulating at a voltage able to evoke a response of 35% of the maximum evoked response in BST. After 30-45 minutes, slices with a stable baseline (slope variation ± 5%) were used. We recorded for 15 min, and then

perfused with vehicle or drugs for the appropriate time. LTP was induced by a theta-burst stimulation (TBS), i.e. trains of 10 × 100 Hz bursts with five pulses per burst with a 200-msec inter burst interval, at the test pulse intensity. To elicit E-LTP we delivered a single TBS train (weak tetanic stimulation), whereas for L-LTP we delivered 3 TBS trains with a 15 second inter-train interval (strong tetanic stimulation). Analysis of fEPSP slope was performed off-line and results were expressed by normalizing on the first 15 min of baseline recordings. In another series of experiments, we evaluated paired-pulse facilitation (PPF). After BST assessment, slices were perfused with the NMDA receptor antagonist (2R)-amino-5-phosphonovaleric acid (APV; 50 μM) for 45 min, and then treated with vehicle or drugs in APV for the appropriate time. Two paired pulses within a time interval of 10, 20, 30, 40, 50, 100, 200, 500 and 1,000 ms were delivered. PPF was measured as percentage of the synaptic response of the second against the first delivered stimulus.

Intrahippocampal injections of oAβ_{42}

Mice underwent stereotaxic surgery for cannulas implantation. After anesthesia with Tiletamine + Zolazepam (60 mg/kg) and Medetomidine (40 μg/kg), mice were implanted with a 26-gauge guide cannula into the dorsal part of the hippocampi (coordinates from bregma: posterior =

2.46 mm, lateral = 1.50 mm to a depth of 1.30 mm). The cannulas were fixed to the skull with acrylic dental cement (RelyXTM Unicem) and mice were allowed to recover for a minimum of 6-8 days. Twenty minutes before the training phase (T1), mice were bilaterally infused with oAβ_{42} solution or vehicle or oAβ_{42} + Rp-8-Br-cGMPS in a final volume of 1 µl over 1 min with a microsyringe connected to the cannulas via polyethylene tubing. During infusion, animals were handled gently to minimize stress. After infusion, the needle was left in place for another minute to allow diffusion. In some animals, after behavioral studies, a solution of 4% methylene blue was infused for localization of infusion cannulas.

Novel Object Recognition

Novel Object Recognition test (NOR) was performed as described (Bollen et al., 2014; Palmeri et al., 2017) in sex-balanced WT mice. Mice underwent 3 days of habituation to the arena, objects and intrahippocampal injections, 1 day of training (T1) and 1 day of testing (T2). The arena was a plastic white box (50 x 35 x 45 cm), and objects (e.g. pyramid, cube, truncated sphere, etc.) were designed by a computer aided design software (Solidworks, France) and printed in polylactic acid with a Prusa-inspired 3D printer of our design. After each trial, the

box and the objects were cleaned with 70% ethanol and dried with absorbent paper.

Experimental design

During the first day of habituation the mouse was put into the empty arena and allowed to explore it for 5 min. During the second and the third day (familiarization with objects), the mouse was put into the arena containing two different objects, randomly chosen among our object collection and changed from day to day, for 5 min. During the fourth day, NOR training session (T1) was performed with two different protocols: short T1 and long-T1. The mouse was put into the arena and allowed to explore two identical objects placed in the central part of the box, equally distant from the perimeter and the center, for 3 min (short T1) or 10 min (long T1). During the fifth day, the mouse underwent the second trial (T2) to test memory retention for 10 min. The long delay interval of 24 h between T1 and T2 did not allow storage of memory information (natural forgetting) in mice that were previously exposed to a short T1 (no discrimination between the familiar and the novel objects). Conversely, long-term memory could be formed in mice that were previously exposed to a long T1. In T2, mice were presented with two different objects, respectively a “familiar” (i.e., the one used for T1) and a “novel” object. Animal exploration - defined as the mouse pointing its nose toward the object from a distance not >2 cm and was

measured in T2 to analyze: 1) discrimination (D) index, “exploration of novel object minus exploration of familiar object/total exploration time”; 2) total exploration time. The time spent exploring the objects was scored using a personal computer by an experimenter who was blinded to the conditions tested. We excluded from the analyses mice with a total exploration time <5 s.

Electron microscopy of hippocampal slices

Hippocampal slices (n = 2 for each conditions from 8 animals) were quickly immersed (within ~30 seconds after 120 minutes of electrophysiological recording) in a solution containing 4% paraformaldehyde and 0.5% glutaraldehyde in phosphate buffer (PB) and, then stored for 6 weeks in the same fixative solution at 4 °C. Subsequently, slices were exposed to embedding procedure according to previous studies (Melone et al., 2011, 2015). Briefly, they were post-fixed in 1% osmium tetroxide in PB for 45 min, and contrasted with 1% uranyl acetate in maleate buffer (pH 6.0; 1 hour). Dehydrated sections were immersed in propylene oxide, infiltrated with a mixture of Epon/Spurr resins (Electron Microscopy Sciences) sandwiched between Aclar films, and polymerized at 60 °C for 48 hours. Small block of tissue containing CA1 *stratum radiatum* was selected by light microscopic inspection, glued to blank epoxy and sectioned with an ultramicrotome

(MTX; Research and Manufacturing Company Inc.). Ultrathin sections (~60 nm; for a total of 20-25 ultrathin sections for each small selected block) were mounted on 200 mesh copper grids, stained with Sato's lead and examined with Philips EM 208 and/or CM10 electron microscopes coupled to a MegaView-II high resolution CCD camera (Soft Imaging System).

Experimental design

Electron microscopy was performed on hippocampal slices treated with vehicle, vehicle + 1 TBS, oAβ_{42} 200 pM, or Aβ 200 pM + 1 TBS. These slices were randomly collected during electrophysiological field recording experiments 120 minutes after tetanic stimulation and analysis of recordings was performed for each sample following the sample protocol described above. Quantitative analysis of vesicle pool, number of docked vesicles, area of spines, length of the post synaptic density (PSD), and of the proportion of perforated synapses (Shepherd and Harris, 1998; Pozzo-Miller et al., 1999; Geinisman, 2000; Bourne et al., 2013; Babits et al., 2016) was carried out. Randomly selected electron microscopical fields of the stratum radiatum (vehicle n = 87, vehicle + 1 TBS n = 116, oAβ42 200 pM n = 92, oAβ42 200 pM + 1 TBS n = 113) with at least an identifiable axo-spinous synapse (Shepherd and Harris, 1998) were acquired at original magnification of 36,000x.

Axo-spinous synapses were identified by the presence of a presynaptic terminal with vesicles, including those nearby the presynaptic density (i.e., the active zone), a synaptic cleft displayed electrodense material, postsynaptic membrane associated with a prominent PSD within the post-synaptic spines (Peters et al., 1991; DeFelipe et al., 1999). The distinction between vesicle pools (which comprise the reserve vesicle pool) and docked vesicles (which are thought to be part of the readily releasable pool), was made according to Shepherd and Harris 1998, Pozzo-Miller et al. 1999; Bourne et al. 2013. Briefly, vesicle pools were determined by counting the total number of small vesicles (~50 nm) per terminal; the docked vesicles pool by counting the vesicles touching the membrane of the presynaptic active zone. Spines profile area and PSD length were measured by Image J software tools measurement (Schneider et al., 2012; Babits et al., 2016). Spine profiles and PSD were traced along the membranes and measured; PSD length corresponded to the distance between the edges of PSD. Perforated synapses were identified based on the presence of a discontinuous PSD (Geinisman, 2000; Babits et al., 2016). Ultrathin sections and microscopical features of axo-spinous synapses were examined and analyzed in a blinded manner.

Western Blot on hippocampal slices

Western blot (WB) analysis was performed as previously described (Caraci et al., 2015). Tissues were homogenized in RIPA buffer (Thermoscientific) in the presence of phosphatase and protease inhibitors (Thermoscientific), and sonicated 3 times for 10 minutes. Protein concentrations were determined by Pierce BCA protein assay kit (Thermoscientific) and equal amounts of proteins (30-50 μg) were then loaded onto 10% or 12% Tris-glycine polyacrylamide gels for electrophoretic separation. Membranes were blocked for 1 hour, at room temperature, in a solution of 5% nonfat dry milk in Tris-buffered saline containing 0.1% Tween-20 or SEAblock (Thermoscientific) before incubation overnight at 4°C with the following primary antibodies: mouse anti-nNOS (Thermo Fisher Scientific, Waltham, MA, USA; Cat# 37-2800, RRID:AB_2533308; 1:1000); rabbit anti-p-CREB (ser133) (Millipore, Billerica, MA, USA; Cat# 06-519, RRID:AB_310153; 1:1000); mouse anti-CREB (Cell Signaling, Danvers, MA, USA; Cat# 9104, RRID:AB_490881; 1:500); rabbit anti-p-CaMKII (thr286) (Cell Signaling, Cat# 12716, RRID:AB_2713889; 1:1000); mouse anti-CaMKIIα (Cell Signaling; Cat# 50049, RRID:AB_2721906; 1:1000); rabbit anti-BDNF (Millipore, # AB1534, RRID:AB_90746; 1:500). Mouse anti tubulin (Sigma Aldrich; Cat# T5293, RRID:AB_477580; 1:1000) was used as loading control. Molecular weights for immunoblot

analysis were determined using precision Plus Protein™ Dual color Standards (Biorad; Hercules, CA, USA), PAGE-MASTER Protein Standard (Genscript; Piscataway, NJ, USA). Protein detection was performed by using a secondary infrared fluorescent dye conjugated antibody absorbing at 800 or 680 nm. The secondary antibody goat anti-Rabbit IRDye 680 (Li-Cor Biosciences; Cat #926-68021, RRID:AB_10706309) and goat anti-Mouse IRDye 800CW (Li-Cor Biosciences; Cat #926-32210, RRID:AB_621842) were used at 1:20,000 and 1:30,000, respectively. Blots were visualized using an Odyssey Infrared Imaging Scanner (Li-Cor Science Tec, Milan, Italy). In other experiments after incubation with appropriate secondary horseradish peroxidase-conjugated antibodies (1:2500; Cell Signaling), visualization was performed with ECL plus (GE Healthcare, Amersham Place, Buckinghamshire, UK) using UVItec Cambridge Alliance. Densitometric analysis was carried out with either Odyssey Infrared Imaging Scanner or UVItec or ImageJ software after normalization with loading controls.

Experimental design

We collected slices from electrophysiological field recordings experiments 120 min after tetanic stimulation. For each experimental condition (vehicle, 1 TBS, Aβ, Aβ + 1 TBS; or vehicle, 3 TBS for nNOS) 4 slices from different animals were collected to obtain a sample;

2-3 samples for a total of 8-12 slices were used to evaluate the expression of each protein of interest.

Statistical analyses

For each experiment, sample size relied on power analyses ($\alpha = 0.05$, power $1-\beta = 0.80$) calculated by G-Power 3.1 software suggesting for each condition a minimum of 6 slices (electrophysiology) and 8 mice (behavioral studies) to obtain an effect size = 0.62. Experimenters were "blind" with respect to treatment. All data were expressed as mean ± SEM.

After data collection, statistical analysis was performed by SigmaPlot 12.0 (RRID:SCR_003210), Systat 9 (RRID:SCR_010455) and GraphPad Prism 7 (RRID:SCR_00279) software. A preliminary analysis of normal distribution was performed by Shapiro-Wilk normality test. We used: i) ANOVA for repeated measures to analyze PPF and LTP (120 min after tetanus) curves; ii) one-way ANOVA with Bonferroni's or Tukey's post-hoc correction for LTP graphs displaying residual potentiation (average of the last five minutes of LTP recording), for analyses of D index and total exploration time among conditions in NOR, and for WB; 3) two-samples t-test to compare conditions in dual-patch recording; 4) one-sample t-test to compare D index with zero.

Given the non-normal distribution of electron microscopical data, as assessed by D'Agostino & Pearson normality test, comparison of the number of pool vesicles, docked vesicles, area of spines, and PSD length between all groups was made by non-parametric Kruskal-Wallis with Dunn's multiple comparison test. The percentages of non-perforated and perforated synapses were compared using non-parametric contingency analysis with Fisher test. The level of significance was set at $p < 0.05$.

RESULTS

Picomolar concentrations of extracellular oAβ_{42} affect spontaneous neurotransmitter release and synaptic plasticity

Intraneuronal uptake and accumulation of high doses of oAβ_{42} are key events leading to impairment of synaptic transmission, LTP and memory (Ripoli et al., 2014; Puzzo et al., 2017). However, it is not known whether the capability of oAβ_{42} to enhance synaptic function when at low concentrations is triggered by an extracellular mechanism or it requires protein internalization.

To address this issue, we first characterized our oAβ_{42} preparations confirming that they contained both monomers and oligomers (**Fig. 1A**), as recently shown (Gulisano et al., 2018b). DR curves obtained by

treating hippocampal slices with different doses of oAβ_{42} (from 2 pM to 200 nM) for twenty minutes before tetanus, confirmed that 200 pM oAβ_{42} was the concentration inducing the maximum enhancement of LTP (**Fig. 1B**), consistently with our previous findings (Puzzo et al., 2008, 2012).

Next, we studied the effect of extra- and intra-cellular 200 pM oAβ_{42} on glutamatergic basal synaptic transmission through dual patch-clamp whole-cell recordings of adjacent CA1 pyramidal neurons of organotypic slice cultures in the following experimental conditions: i) extracellular 200 pM oAβ_{42}, with a patch-pipette filled with vehicle and the other one with an antibody raised against human Aβ42 (6E10); ii) extracellular vehicle, with a patch-pipette filled with vehicle and the other one with 200 pM oAβ_{42} (**Fig. 1C**). We found no effect of oAβ_{42} onto AMPA- and NMDA glutamatergic receptor evoked currents when the peptide was administered either extracellularly or intracellularly (**Fig. 1D-E**). Conversely, extracellular administration of oAβ_{42} increased the spontaneous release of neurotransmitter from the presynaptic terminal measured through the miniature excitatory postsynaptic current (mEPSC) frequency, without altering their amplitude at 20 min after its application (**Fig. 1F-G**). Remarkably, intracellular application of 6E10 did not block the effect of extracellular oAβ_{42}, confirming that the oAβ_{42}-induced modification of glutamatergic

transmission does not require peptide internalization. Control experiments confirmed that blocking oAβ_{42} with extracellular 6E10 prevented oAβ_{42} to increase mEPSC frequency (**Fig. 1H**), whereas 6E10 did not affect mEPSC *per se*.

Further experiments in which LTP was studied through patch-clamp technique showed that 200 pM oAβ_{42} increased EPSC amplitude recorded for 30 min after a high-frequency stimulation (two trains at 100 Hz for 1 s separated by 20 s), only when extracellularly applied, but not when injected into CA1 pyramidal neurons through the patch pipette (**Fig. 1I**). Altogether these findings demonstrate that picomolar oAβ_{42} extracellularly modulates glutamatergic transmission and plasticity, and it does not act through a direct intracellular mechanism.

Picomolar concentrations of oAβ_{42} affect paired-pulse facilitation and convert early-LTP into late-LTP, and short-term into long-term memory

The increase of mEPSC frequency prompted us to investigate whether oAβ_{42} affects paired-pulse facilitation (PPF), a presynaptic form of short-term plasticity linked with changes in release probability (Zucker and Regehr, 2002). We found that 20 min perfusion with 200 pM oAβ_{42} decreased PPF (**Fig. 2A**), thus suggesting an increase of the release

probability (Dobrunz and Stevens, 1997). A DR curve confirmed that 200 pM was the dose capable to affect PPF (**Fig. 2B**).

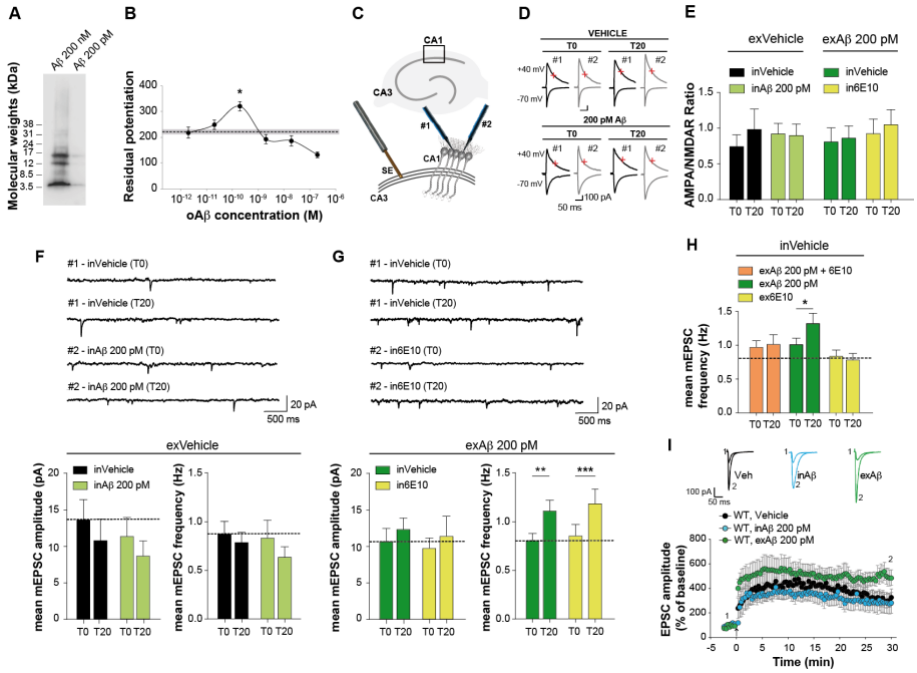

Figure 1. Extracellular, but not intracellular, pM concentrations of oAβ$_{42}$ affect spontaneous release of neurotransmitter and synaptic plasticity. A) Characterization of synthetic human oAβ$_{42}$ solutions by WB analysis shows the presence of monomers, dimers, trimers, and tetramers for 200 nM oAβ$_{42}$ solution, and the presence of monomers and tetramers for 200 pM oAβ$_{42}$. **B)** DR curve for the effect of oAβ$_{42}$ (from 2 pM to 200 nM, n = 5 for each concentration) on CA1-LTP indicates that the peptide has a maximum stimulatory effect at 200 pM (321.04 ± 17.92 % of baseline vs. 228.63 ± 20.29 % of baseline; $F_{(6,28)} = 9.882$, $p < 0.0001$; Bonferroni's $p = 0.031$) and an inhibitory effect at 200 nM (133.25 ± 11.59 % of baseline; Bonferroni's $p = 0.023$). The dotted horizontal line corresponds to treatment with vehicle. The residual potentiation was calculated by averaging the last 5 minutes of LTP. **C)** Schematic representation of dual whole-cell recordings from adjacent (namely #1 and #2) CA1 hippocampal pyramidal neurons (see methods for details).

D) Representative AMPAR- and NMDAR-EPSCs at time 0 (T0) and 20 min after extracellular application of vehicle or 200 pM oAβ_{42} (T20). The amplitude of NMDA currents recorded at +40 mV (holding potential) was measured at 50 ms post-stimulus (red crosses). **E)** Neither intraneuronal (in) nor extracellular (ex) 200 pM oAβ_{42} affected AMPAR/NMDAR ratios. Slices perfused with exVehicle: inVehicle T0 = 0.74 ± 0.16, T20 = 0.97 ± 0.28, n = 10; in 200 pM oAβ_{42} T0 = 0.92 ± 0.14, T20 = 0.90 ± 0.16, n = 10. Slices perfused with ex 200 pM oAβ_{42}: inVehicle T0 = 0.80 ± 0.19, T20 = 0.86 ± 0.16, n = 15; in6E10 T0 = 0.92 ± 0.20, T20 = 1.04 ± 0.21, n = 15. **F)** Representative mEPSC traces recorded in neurons treated with vehicle and 200 pM inAβ_{42} at T0 and T20. Intraneuronal 200 pM oAβ_{42} had no significant effect on mEPSC frequency (from 0.82 ± 0.18 Hz at T0 to 0.63 ± 0.10 Hz at T20, n = 14; p = 0.10) or amplitude (from 11.33 ± 2.58 pA at T0 to 8.64 ± 2.06 pA at T20, n = 14; p = 0.07) compared with slices in which cells were injected with vehicle and extracellularly perfused with vehicle (mEPSC frequencies from 0.87 ± 0.13 Hz at T0 to 0.78 ± 0.10 Hz at T20, n = 14; p = 0.07; mEPSC amplitudes from 13.58 ± 2.77 pA at T0 to 10.73 ± 2.97 pA at T20, n = 14; p = 0.19). **G)** Extracellular application of 200 pM oAβ_{42} significantly increased mEPSC frequency both in vehicle injected (from 0.79 ± 0.08 Hz at T0 to 1.10 ± 0.10 Hz, n = 14; p = 0.002 at T20) and adjacent 6E10 injected neurons (from 0.85 ± 0.11 Hz at T0 to 1.18 ± 0.15 Hz, n = 14; p = 0.0008 at T20), without altering the mEPSC amplitude (mean amplitude of: i) vehicle: T0 = 10.6 ± 1.9 pA, T20 = 12.2 ± 1.6 pA, n = 14; p = 0.20; ii) 6E10: T0 = 9.7 ± 1.4 pA, T20 = 11.2 ± 2.7 pA, n = 14; p = 0.51). **H)** Extracellular application of 200 pM oAβ_{42} paired with 6E10 or 6E10 alone did not modify mEPSC frequency in vehicle injected neurons (exAβ+6E10: from 0.96 ± 0.08 Hz at T0 to 1.00 ± 0.15 Hz, n = 18; p = 0.746 at T20; 6E10: from 0.83 ± 0.07 Hz at T0 to 0.77 ± 0.10 Hz, n = 10; p = 0.543 at T20). In interleaved experiments, extracellular 200 pM oAβ_{42} was still capable to increase mEPSC frequency (from 1.00 ± 0.10 Hz at T0 to 1.31 ± 0.15 Hz, n = 8; p = 0.029 at T20). **I)** Extracellular oAβ_{42} (n = 11) enhanced LTP elicited through a high-frequency stimulation (two trains at 100 Hz for 1 s separated by 20 s) compared to vehicle (n = 10) (Bonferroni's p = 0.003). By contrast, intracellular oAβ_{42} did not modify potentiation (Bonferroni's p > 0.05). ANOVA among all: $F_{(2,28)} = 10.846$; p = 0.001. ** = p < 0.005; *** = p < 0.001. Data expressed as mean ± SEM.

To further investigate the role of Aβ in PPF, we suppressed endogenous Aβ through the anti-Aβ antibody M3.2, specifically targeting murine Aβ. This induced the opposite effect, i.e. an enhancement of PPF, that was rescued by concomitant perfusion with human 200 pM oAβ_{42} (**Fig. 2C**), not recognized by M3.2.

Altogether these findings are consistent with a positive modulatory role of Aβ onto neurotransmitter release probability.

Next, we investigated whether 200 pM oAβ_{42} influenced the early phase of LTP (E-LTP), a form of protein synthesis independent plasticity that involves a change in presynaptic neurotransmitter release and short-term kinase activity (Huang, 1998). We found that pre-treatment with 200 pM oAβ_{42} converted E-LTP obtained through a weak tetanic stimulation (1 theta-burst stimulation, TBS) into late phase LTP (L-LTP) (**Fig. 2D**). The potentiation induced by pairing 200 pM oAβ_{42} with 1 TBS was comparable to that induced by a strong tetanic stimulation consisting of 3 TBSs elicited with a 15 s inter-train interval. To confirm that 200 pM oAβ_{42} converted E-LTP into the traditional protein-synthesis dependent L-LTP (Johnstone and Raymond, 2011), slices were continuously perfused with the translation inhibitor anisomycin (ANI, 20 μM; 30 min before and 25 after tetanus) that prevented the oAβ_{42}-induced L-LTP (**Fig. 2E**). Additionally, we confirmed that ANI

perfusion inhibits 3-TBS-induced L-LTP without affecting 1 TBS-induced E-LTP (**Fig. 2E**), as the latter is known to not involve new protein synthesis (Johnstone and Raymond, 2011). Taken together, these observations support a role for oAβ_{42} in triggering new protein synthesis and gene transcription.

Because LTP represents the cellular surrogate of memory, we assessed whether bilateral intrahippocampal injections with 200 pM oAβ_{42} 20 minutes before training were able to convert short-term into long-term memory. To this end, we used a novel object recognition (NOR) protocol where the short time exposure (3 min) during the training phase (T1) does not allow animals to discriminate between the old and the new object after a 24-hrs long-term interval, due to natural forgetting (Bollen et al., 2014; Palmeri et al., 2017). The analyses of the discrimination index indicated that mice receiving a weak stimulus (i.e., short exposure in T1) paired with 200 pM oAβ_{42} were able to discriminate between the old and the familiar object after 24 hrs compared with vehicle-treated animals showing natural forgetting. This oAβ_{42}-induced long-term memory was comparable to that induced by a stronger training stimulus (10 min of exposure in T1) (**Fig. 2F**). Total exploration time was similar in all groups (**Fig. 2F**). Thus, 200 pM oAβ_{42} converts short-term into long-term memory.

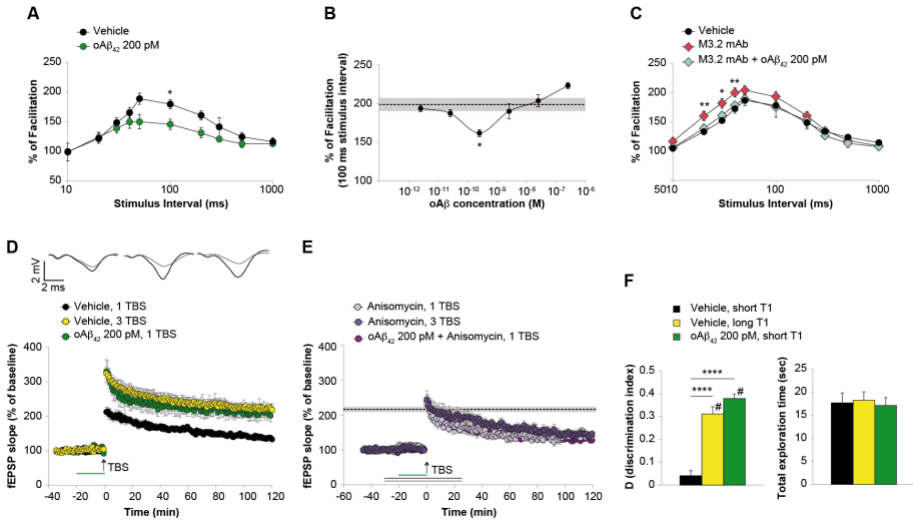

Figure 2. pM oAβ$_{42}$ decreases PPF and converts E-LTP into L-LTP, as well as short-term into long-term memory. A) Paired pulse facilitation (PPF) was decreased in slices perfused with 200 pM oAβ$_{42}$ for 20 min compared with control slices (% facilitation at 100 msec interval here and in following panels: vehicle = 179.58 ± 7.47 %, n = 9; 200 pM oAβ$_{42}$ = 145.67 ± 8.74 %, n = 10 for each condition). ANOVA for repeated measures for the entire curve $F_{(1,17)} = 6.262$, p = 0.023; Bonferroni's p = 0.041 at 100 msec. **B)** DR curve for the effect of oAβ$_{42}$ (from 2 pM to 200 nM, n = 7 for each concentration) on PPF indicates that the peptide has a maximum stimulatory effect at 200 pM. Curve showing the % of facilitation at 100 msec stimulus interval (Bonferroni's p = 0.022 between vehicle and 200 pM oAβ$_{42}$). The dotted horizontal line corresponds to treatment with vehicle. **C)** The increase of PPF caused by the anti-murine Aβ antibody M3.2 mAb (193.75 ± 8.43 %, n = 11; $F_{(1,18)} = 4.749$, p = 0.043 vs. vehicle; Bonferroni's p = 0.007, 0.011 and 0.006 at 20, 30 and 40 msec) was rescued by 200 pM human oAβ$_{42}$ (175.39 ± 17.22 %, n = 10; $F_{(1,19)} = 5.111$, p = 0.036 vs. M3.2 mAb; $F_{(1,17)} = 0.006$, p = 0.939 vs. vehicle). **D)** Twenty minute perfusion with 200 pM oAβ$_{42}$ converted E-LTP elicited through a weak tetanic stimulation (1 theta-burst stimulation, TBS) to L-LTP (134.24 ± 5.44 % of baseline vs. 220.10 ± 17.74 % of baseline, n = 7/7; $F_{(1,12)} = 9.883$, p = 0.008), inducing a potentiation similar to that obtained with a strong tetanic stimulation (3 TBS) (219.91 ± 7.75 % of baseline, n = 7; $F_{(1,12)} = 0.321$, p = 0.582 comparing oAβ$_{42}$ + 1 TBS vs. Vehicle + 3 TBS). **E)** A perfusion (30 min before and 25 min after tetanus) with the translation inhibitor

anisomycin (ANI) blocked the oAβ_{42}-induced L-LTP (127.48 ± 8.71 % of baseline, n = 7; $F_{(1,12)}$ = 11.946, p = 0.005 vs. oAβ_{42} + 1 TBS). ANI did not modify E-LTP induced by 1 TBS (137.92 ± 8.05 % of baseline, n = 7; $F_{(1,11)}$ = 3.091; p = 0.106 vs. Vehicle + 1 TBS) but blocked L-LTP induced by 3 TBS (146.41 ± 14.77 % of baseline, n = 6; $F_{(1,12)}$ = 25.976, p < 0.0001 vs. Vehicle + 3 TBS). Shaded area with dashed line corresponds to mean + SEM of the 5 last recorded point in slices treated with vehicle + 3 TBS as in panel C. **F)** Evaluation of recognition memory indicated a difference in Discrimination Index (D = exploration of novel object minus exploration of familiar object/total exploration time) between vehicle-treated mice that underwent a 3 min exposition in T1 (short T1) or a 10 min exposition in T1 (long T1) (0.04 ± 0.02 vs. 0.31 ± 0.03 comparing short T1 vs. long T1, n = 10/10 sex-balanced mice; Bonferroni's p < 0.0001). Comparison of D with zero confirmed that a long T1 was able to induce long-term memory in a 24-h-delay novel object recognition task ($t_{(9)}$ = 9.604, p < 0.0001), whereas a short T1 did not ($t_{(9)}$ = 1.62, p = 0.140). Intrahippocampal injections with 200 pM oAβ_{42} 20 min before a short T1 converted short-term into long-term memory (D = 0.38 ± 0.01, n = 10 sex-balanced mice; $t_{(9)}$ = 19.79, p < 0.0001 comparing D with zero in oAβ_{42} + Short T1). One-way ANOVA with Bonferroni's post-hoc corrections confirmed the significant difference between D in vehicle- and oAβ_{42}-treated mice previously exposed to a short T1 (p < 0.0001). The increase of D induced by treatment with oAβ_{42} was similar to that obtained in vehicle-treated mice that spent a longer period in T1 (p = 0.314 comparing D in oAβ_{42} + short T1 vs. vehicle + long T1). On the right, total exploration time was comparable in the 3 groups of mice ($F_{(2,27)}$ = 0.086, p = 0.918). * p < 0.05, ** p < 0.01, **** p < 0.0001; # difference from 0. Data expressed as mean ± SEM.

Picomolar concentrations of oAβ_{42} induce ultrastructural changes of hippocampal CA1 synapses at both pre- and post-synaptic levels

Synaptic plasticity is accompanied by structural changes occurring at both pre- and post-synaptic levels (Bourne et al., 2013). We therefore investigated whether oAβ_{42} determines specific ultrastructural changes (i.e, vesicle pool, number of docked vesicles, area of spines, PSD length,

and percentage of perforated synapses; **Table 1**) at axo-spinous synapses of the CA1 *stratum radiatum* in slices used for electrophysiological experiments collected and stored at 120 min after Aβ treatment. Quantitative electron microscopy showed an increase of docked vesicles in axon terminals from slices treated with 200 pM oAβ_{42}, and of PSD length in spines from slices treated with oAβ_{42} paired with a weak stimulation (**Fig. 3**). Taken together, these ultrastructural changes robustly support the electrophysiological data. Most importantly, this body of evidence indicates that synapses undergo a series of coordinated changes occurring both at the pre- and post-synaptic site following application of oAβ_{42} at pM concentrations.

The effect of picomolar concentrations of oAβ_{42} on short- and long-term synaptic plasticity and memory requires α7 nicotinic acetylcholine receptors (α7nAChRs)

Because recent studies indicated that high nanomolar concentrations of extracellular oAβ_{42} require APP to impair LTP and memory (Puzzo et al., 2017; Wang et al., 2017), we tested whether the plasticity enhancing effect of extracellular pM oAβ_{42} was APP-dependent. We used APP knock out (KO) mice to understand if the absence of endogenous APP prevented 200 pM oAβ_{42} to exert its effects on PPF and LTP. We found that 200 pM oAβ_{42} was still able to decrease PPF (**Fig. 4A**) and convert

E-LTP into L-LTP (**Fig. 4B**) in APP KO mice. Thus, differently than nanomolar Aβ, pM concentrations of the peptide did not require APP to produce their synaptic effects.

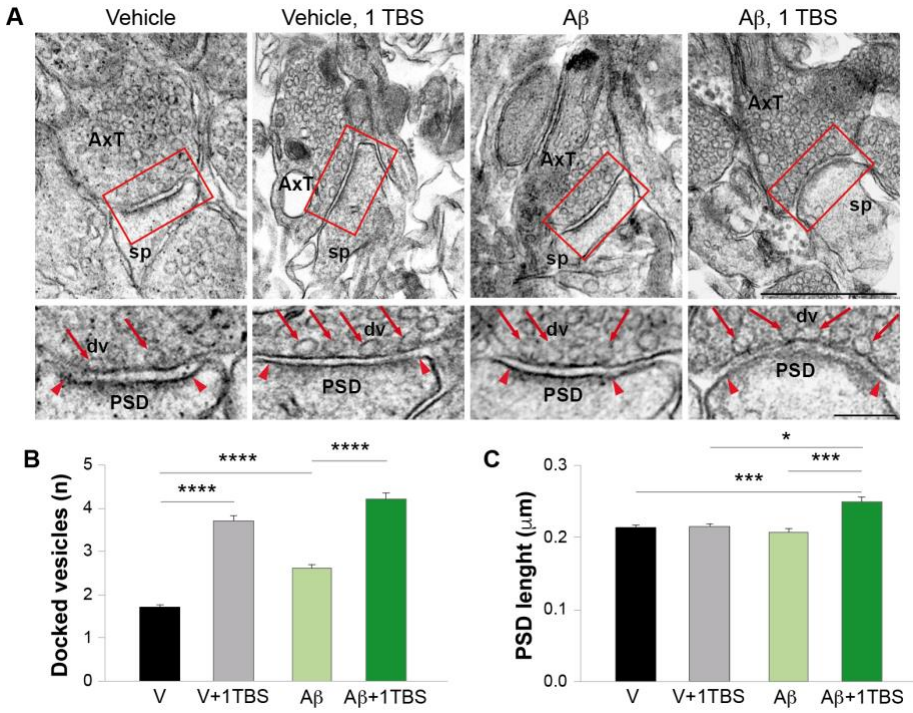

Figure 3. pM oAβ$_{42}$ increases number of docked vesicles and PSD length. A) Representative asymmetric axo-spinous synapses of CA1 *stratum radiatum* from hippocampal slices previously treated for electrophysiological recordings. Framed regions enlarged (bottom) show the synaptic contact for each synapse from different experimental conditions. Arrows = docked vesicles (dv) at the active zone of axon terminals; arrowheads = edges of postsynaptic density (PSD). AxT, axon terminal; sp, spine. Bars: 500 nm for upper panels, 100 nm for bottom panels. **B)** oAβ$_{42}$ alone increased the number (n) of docked vesicles compared to vehicle ($p < 0.0001$). The number of docked vesicles increased in tetanized slices treated with oAβ$_{42}$ compared to non-tetanized slices treated with the peptide, as well as tetanized slices treated with

vehicle vs. vehicle-treated non-tetanized ones ($p < 0.0001$). **C)** $oA\beta_{42}$ paired with a weak tetanic stimulation (1 TBS) increased PSD length compared to other conditions. See **Table 1** for detailed results and statistical analyses. V = Vehicle, Aβ = 200 pM $oA\beta_{42}$, 1 TBS = weak tetanic stimulation. * $p < 0.05$; *** $p < 0.005$; **** $p < 0.0001$. Data expressed as mean ± SEM.

Experimental Condition	**V**	**V+T**	**Aβ**	**Aβ+T**	**Statistical analyses°** (P value)					
Asymmetric synapses (n)	n=172	n=151	n=124	n=113	**V *vs* V+T**	**V *vs* Aβ**	**V *vs* Aβ+T**	**V+T *vs* Aβ**	**Aβ *vs* Aβ+T**	**V+T *vs* Aβ+T**
Vesicle pool (n)	74.8 ± 2.4	70.2 ± 2.9	72.9 ± 3.1	77.3 ± 3.0	0.48	> 0.99	> 0.99	> 0.99	> 0.99	0.73
Docked vesicles (n)	1.7 ± 0.08	3.7 ± 0.12	2.6 ± 0.10	4.2 ± 0.14	<0.0001	<0.0001	<0.0001	<0.0001	<0.0001	0.13
Area of spines (μm^2)	0.09 ± 0.004	0.11 ± 0.006	0.10 ± 0.005	0.10 ± 0.006	0.08	0.055	> 0.99	> 0.99	0.32	0.51
PSD length (µm)	0.212 ± 0.005	0.214 ± 0.005	0.207 ± 0.006	0.249 ± 0.008	> 0.99	> 0.99	0.0037	> 0.99	0.0041	0.0398
Perforated PSD	4.07%	11.26%	5.65%	14.20%	0.018§	0.58§	0.0013§	0.132§	0.021§	0.508§

Table 1 - Detailed results of TEM performed on hippocampal slices stored at 120 min after electrophysiological recordings in the following experimental conditions: vehicle (V), vehicle + 1 TBS tetanus (V + T), $oA\beta_{42}$ 200 pM (Aβ), $oA\beta_{42}$ 200 pM + 1 TBS tetanus (Aβ + T). °Statistical analyses performed by non parametric Kruskal-Wallis test with Dunn's test for multiple comparison. Number of microscopical fields: V (n = 87); V+T (n = 116); Aβ (n = 92); Aβ + T (n = 113). For vesicle pool, docked vesicles, area of spines, PSD length values are mean ± SEM. For perforated PSD, % indicates the proportion of asymmetric synapses with perforated PSD. § Statistical analysis performed by contingengy analysis with Fisher test.

We then turned on α7nAChRs because of their interplay with Aβ in physiological conditions (Lawrence et al., 2014; Puzzo et al., 2008, 2011; Zappettini et al., 2012). When slices from α7nAChRs KO (α7 KO) mice were treated with 200 pM oAβ$_{42}$, the decrease of PPF and the conversion of E-LTP to L-LTP were not elicited (**Fig. 4C-D**). To confirm that the effects of 200 pM oAβ$_{42}$ were mediated by α7nAChRs, we acutely blocked these receptors by the selective antagonist methyllycaconitine (MLA). This prevented 200 pM oAβ$_{42}$ to affect PPF and LTP (**Fig. 4E-F**), suggesting that oAβ$_{42}$ needs α7nAChRs to exert its enhancing effects.

To corroborate our findings indicating that α7nAChRs, but not APP, were needed for 200 pM oAβ$_{42}$ to enhance plasticity, we repeated experiments after the acute block of α7nAChR function with MLA that prevented the 200 pM oAβ$_{42}$-mediated decrease of PPF and conversion of E-LTP into L-LTP in slices from APP KO mice (**Fig. 4G-H**).

Next, we validated our *in vitro* and *ex vivo* results *in vivo* by studying whether APP and/or α7nAChRs were needed for 200 pM oAβ$_{42}$ to convert short-term into long-term memory. APP-KO and α7-KO mice were injected intrahippocampally with vehicle or 200 pM oAβ$_{42}$ before training (short exposure in T1) and memory was evaluated after 24 hrs. Analyses of the discrimination index revealed that 200 pM oAβ$_{42}$ was

capable to induce long-term memory in APP-KO but not in α7-KO mice (**Fig. 4I**), without modifying total exploration time (**Fig. 4J**). Thus, α7nAChRs, but not APP, were necessary for pM oAβ_{42} to convert short- into long-term memory.

The oAβ_{42}-induced conversion of early-LTP into late-LTP and short-term into long-term memory depends upon the NO/cGMP/PKG pathway and involves plasticity-related proteins (PRPs)

To get an insight into the intracellular mechanisms involved in the oAβ_{42}-induced enhancement of LTP, we focused on the nitric oxide (NO)/cGMP/PKG pathway, that plays a key role in pre- and postsynaptic mechanisms of plasticity and in the conversion from E-LTP to L-LTP (Bon and Garthwaite, 2003; Johnstone and Raymond, 2011). To this end, hippocampal slices were treated with 200 pM oAβ_{42} paired with drugs able to inhibit NO or cGMP production, or PKG activation. When preventing NO production by using the inhibitor of neuronal nitric oxide synthase (nNOS) L-NAME, or the inhibitor of soluble guanylyl cyclase *ODQ*, or the cGMP analog Rp-8-Br-cGMPS, oAβ_{42} failed to induce a long-lasting potentiation (**Fig. 5A**).

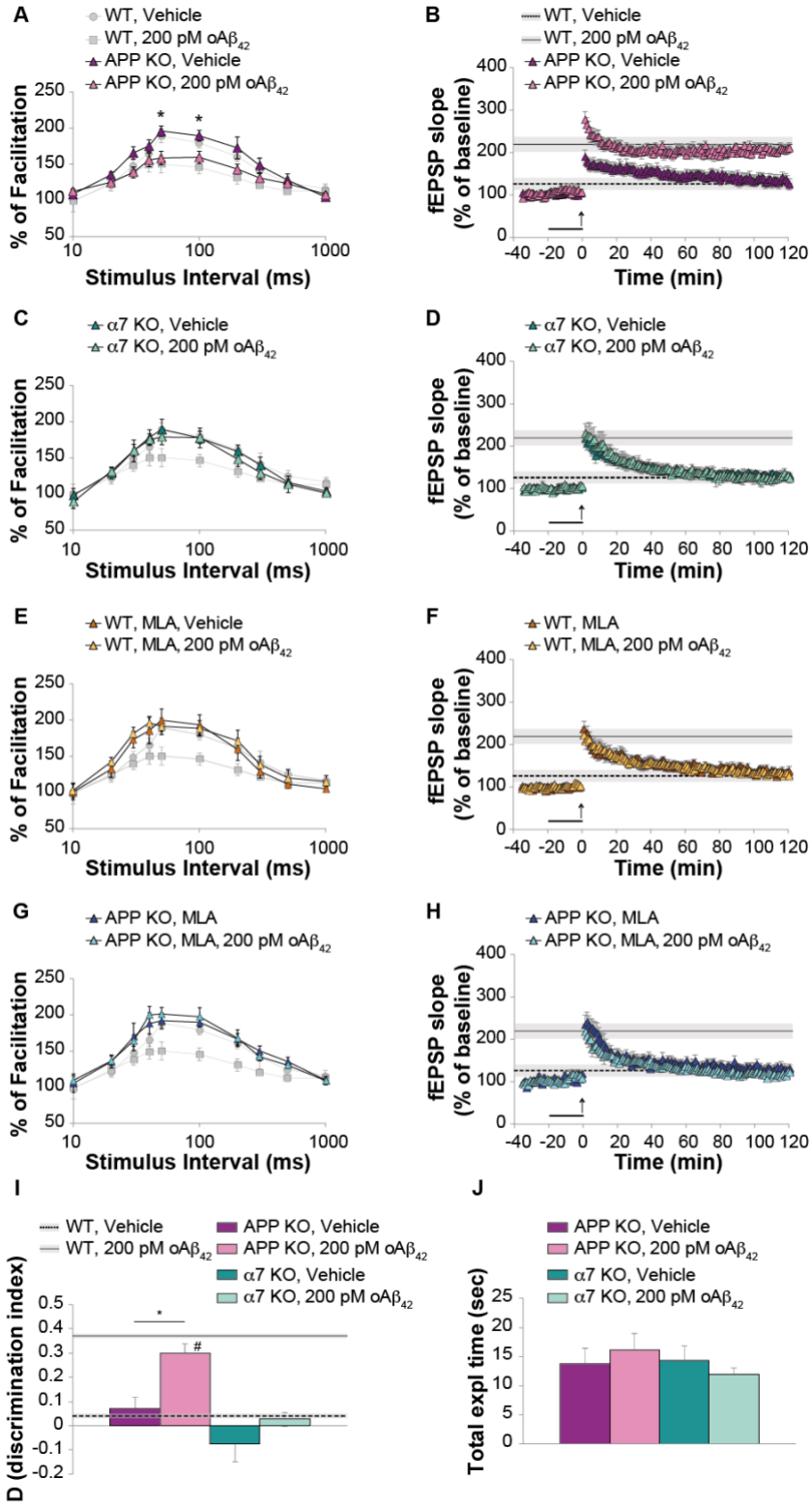
A
WT, Vehicle
WT, 200 pM oAβ42
APP KO, Vehicle
APP KO, 200 pM oAβ42
% of Facilitation
Stimulus Interval (ms)
B
fEPSP slope (% of baseline)
Time (min)
C
α7 KO, Vehicle
α7 KO, 200 pM oAβ42
D
E
WT, MLA, Vehicle
WT, MLA, 200 pM oAβ42
F
WT, MLA
WT, MLA, 200 pM oAβ42
G
APP KO, MLA
APP KO, MLA, 200 pM oAβ42
H
I
D (discrimination index)
J
Total expl time (sec)

Figure 4. The α7-nAChR, but not APP, is needed for pM oAβ_{42} to decrease PPF, and convert both E-LTP into L-LTP and short-term into long-term memory.

A) Twenty minute perfusion with 200 pM oAβ_{42} was capable to decrease PPF in slices from APP KO mice (% facilitation at 100 msec interval here and in following panels: APP KO + vehicle = 189.34 ± 7.51 %, n = 8; 200 pM oAβ_{42} = 159.57 ± 8.32 %, n = 8; ANOVA for repeated measures $F_{(1,14)} = 5.234$, p = 0.038; Bonferroni's p = 0.013 at 50 msec and 0.044 at 100 msec). Grey shaded curves represent mean + SEM of PPF curves in WT slices treated with vehicle or 200 pM oAβ_{42} as shown in Figure 2. **B)** 200 pM oAβ_{42} converted E-LTP into L-LTP in slices from APP KO mice (124.69 ± 13.13 % of baseline vs. 210.28 ± 12.60 % of baseline, n = 7/7; ANOVA for repeated measures $F_{(1,12)} = 14.77$, p = 0.002). Grey shaded areas with lines represent mean + SEM of the last recorded point of 1 TBS-induced LTP in WT slices treated with vehicle or 200 pM oAβ_{42} as shown in Figure 2; the arrow indicates 1 TBS in this and the following panels. **C)** 200 pM oAβ_{42} did not affect PPF in slices from α7 KO mice (177.42 ± 13.67% vs. 178.03 ± 8.52 %, n = 8/8; $F_{(1,16)} = 0.388$, p = 0.542). **D)** 200 pM oAβ_{42} did not convert E-LTP into L-LTP in slices from α7-KO mice (131.12 ± 3.46 % of baseline vs. 124.43 ± 11.09 % of baseline, n = 7/7; $F_{(1,12)} = 0.002$, p = 0.964). **E)** 200 pM oAβ_{42} did not affect PPF in slices from WT mice treated with the α7nAChRs antagonist MLA (10 nM, 10 min before tetanus) (192.99 ± 13.84 % vs. 188.02 ± 10.54 %, n = 11/11; $F_{(1,20)} = 0.154$, p = 0.699). **F)** 200 pM oAβ_{42} did not convert E-LTP into L-LTP in slices from WT mice treated with MLA (137.45 ± 12.25 % of baseline vs. 128.57 ± 3.81 % of baseline, n = 6/7; $F_{(1,11)} = 0.009$, p = 0.927). **G)** 200 pM oAβ_{42} did not modify PPF in APP-KO mice treated with MLA (189.90 ± 6.86 % vs. 197.38 ± 12.64 %, n = 6/10; $F_{(1,14)} = 0.001$, p = 0.973). **H)** 200 pM oAβ_{42} did not convert E-LTP into L-LTP in slices from APP KO mice treated with MLA (130.70 ± 9.68 % of baseline vs. 121.18 ± 7.35 % of baseline, n = 6/7; $F_{(1,11)} = 0.589$, p = 0.459). **I)** Intrahippocampal injections with 200 pM oAβ_{42} 20 min before a short T1 converted short-term into long-term memory in APP KO mice (D = 0.06 ± 0.04 vs. 0.30 ± 0.03; n = 10/10 sex-balanced mice; Bonferroni's p = 0.022 comparing APP KO mice treated with vehicle or 200 pM oAβ_{42}; $t_{(9)} = 7.645$, p < 0.0001 comparing D vs. zero in APP KO + 200 pM oAβ_{42}). Conversely, 200 pM oAβ_{42} administration did not induce long-term memory in α7 KO mice (D = - 0.07 ± 0.07 vs. 0.02 ± 0.02; n = 10/10 sex-balanced mice; Bonferroni's p = 1 comparing α7 KO mice treated with vehicle or 200 pM oAβ_{42}; $t_{(9)} = 0.999$, p = 0.344 comparing D vs. zero in α7 KO + 200 pM oAβ_{42}). **J)** Total

exploration time was comparable in the 4 groups of mice ($F_{(3,36)} = 0.515$, $p = 0.674$). * $p < 0.05$; # difference from 0. Data expressed as mean ± SEM.

Control experiments showed that L-NAME, ODQ and Rp-8-Br-cGMPS did not disrupt LTP evoked by a weak tetanic stimulation *per se* (**Fig. 5B**), whereas they impaired L-LTP induced by a 3 TBS stimulation (**Fig. 5C**), further suggesting that pM oAβ_{42} acts through a pathway that is physiologically involved in L-LTP formation.

Because electrophysiological data showed an involvement of the NO/cGMP/PKG pathway, we performed western blots on slices from electrophysiology experiments to evaluate whether oAβ_{42} triggers NO production by affecting nNOS expression. We found a significant increase of nNOS in slices treated with 200 pM oAβ_{42} paired with a weak tetanus (**Fig. 5D**), similar to that obtained in slices treated with vehicle paired with a strong tetanus (**Fig. 5E**).

Furthermore, we explored the molecular mechanisms underlying oAβ_{42}-induced L-LTP by analyzing the expression of PRPs, known to be involved in synaptic plasticity and memory (Puzzo et al., 2016), including cAMP-responsive element binding protein (CREB), calcium-calmodulin-dependent protein kinase II α (CaMKII), and Brain Derived

Neurotrophic Factor (BDNF), in the same hippocampal slices used for electrophysiological experiments. We found that cAMP-responsive element binding protein (CREB) phosphorylated at Ser 133 (p-CREB) was increased in slices treated with oAβ_{42} alone or oAβ_{42} paired with a weak tetanic stimulation without affecting total CREB levels (**Fig. 5F-H**). oAβ_{42} also increased the expression of the calcium-calmodulin-dependent protein kinase II α (CaMKII) phosphorylated at Thr 286 (p-CaMKII) (**Fig. 5F, I-J**) and Brain Derived Neurotrophic Factor (BDNF) (**Fig. 5F, K**).

Finally, since the NO/cGMP/PKG pathway has been widely demonstrated to intervene in memory processes and previous studies have suggested that PKG activity maintains CREB phosphorylation at Ser133 during memory consolidation (Puzzo et al., 2016), we studied whether the oAβ_{42}-induced conversion of short-term into long-term memory depends upon PKG activity. As for LTP, we found that treatment with the cGMP analog, Rp-8-Br-cGMPS, prevented oAβ_{42} to induce long-term memory in mice that underwent a short-exposure during the training phase (**Fig. 5L**), whereas Rp-8-Br-cGMPS did not affect short-term memory *per se* (**Fig. 5L**). Thus, PKG activation mediates oAβ_{42}-induced conversion of short-term into long-term memory.

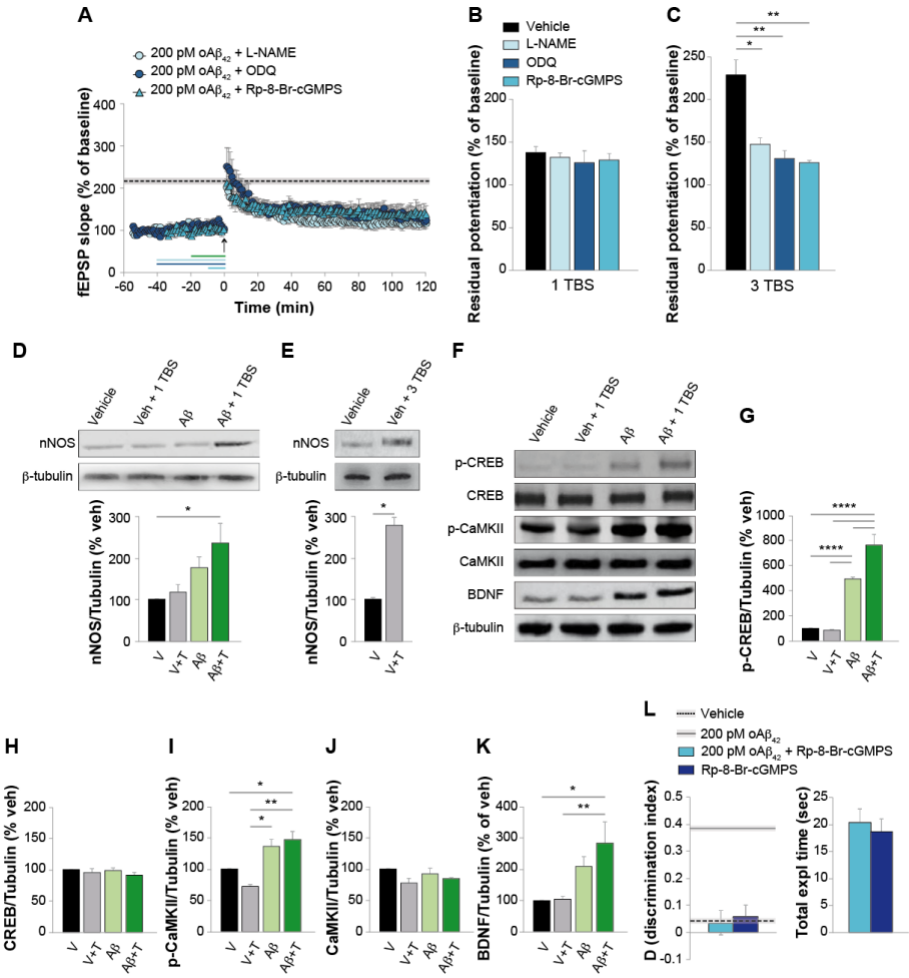

Figure 5 – Conversion of E-LTP into L-LTP and short-term into long-term memory by pM oAβ$_{42}$ is mediated through the NO/cGMP/PKG cascade. A) 200 pM oAβ$_{42}$ did not induce L-LTP in slices treated with the nNOS inhibitor N-v-nitro-L-arginine methyl ester (L-NAME; 100 µM for 40 min) (118.96 ± 12.57 % of baseline, n = 7; $F_{(1,12)}$ = 18.645, p = 0.001 vs. 200 pM oAβ$_{42}$ + 1 TBS), the sGC inhibitor 1H-[1,2,4]Oxadiazol[4,3-a]quinoxalin-1-one (ODQ; 100 µM for 40 min) (125.84 ± 13.39 % of baseline, n = 6; $F_{(1,11)}$ = 8.903, p = 0.012), and the PKG inhibitor Rp-8-Br-cGMPS (10 µM for 10 min) (140.48 ± 19.61 % of baseline, n = 7; $F_{(1,12)}$ = 9.161, p = 0.011). Shaded area with line corresponds to mean + SEM of the last recorded point in WT

slices treated with 200 pM oAβ_{42} + 1 TBS as in Figure 2. **B)** A treatment with L-NAME, ODQ or Rp-8Br-cGMPS alone did not modify residual potentiation induced by a weak tetanic stimulation compared to vehicle (n = 4 for each condition, $F_{(1,12)}$ = 0.315, p = 0.814). **C)** Blocking the NO/cGMP/PKG pathway inhibits L-LTP induced by a strong tetanic stimulation compared to vehicle (n = 4 for each condition, $F_{(3,14)}$ = 13.391, p < 0.0001 among all; Vehicle: 228.15 ± 18.80 % of baseline; L-NAME: 148.44 ± 7.45 % of baseline, Bonferrroni's p = 0.006; ODQ: 131.24 ± 9.22 % of baseline, Bonferrroni's p = 0.001; Rp-8Br-cGMPS: 126.15 ± 2.54 % of baseline, Bonferrroni's p = 0.001). **D)** On top, representative images of WB assay (cropped images based on MW) performed on hippocampal slices (n = 4 for each lane) treated for electrophysiological experiments, collected and stored at 120 min after treatment (V = vehicle; T = 1 TBS; Aβ = oAβ_{42} 200 pM). On bottom, bar graph obtained by the average of 2-3 different membranes here and in D. β-Tubulin expression is shown as one example of loading control. An increase of nNOS expression ($F_{(3,8)}$ = 4.570; p = 0.038; Tukey's p = 0.042) was detected in slices treated with Aβ and a 1TBS stimulation. **E)** nNOS expression increased in slices treated with vehicle and 3TBS ($F_{(1,2)}$ = 52.412; p = 0.019). **F)** WB assay of plasticity-related proteins. **G)** p-CREB expression was increased after treatment with Aβ alone and further enhanced in Aβ +T ($F_{(3,12)}$ = 61.713; p < 0.0001; Tukey's p < 0.0001). **H)** No changes were detected in total CREB expression among different conditions ($F_{(3,4)}$ = 0.930; p = 0.504). **I)** Aβ paired with 1 TBS increased p-CaMKII levels ($F_{(3,8)}$ = 11.746; p = 0.003) compared to V (p = 0.017) or V+T (p = 0.004), whereas **J)** CaMKII expression was not modified ($F_{(3,4)}$ = 2.758; p = 0.176). **K)** Aβ paired with 1 TBS increased BDNF levels ($F_{(3,8)}$ = 5.686; p = 0.022) compared to V (p = 0.034) and V+T (p = 0.038). **L)** Evaluation of recognition memory indicated that 200 pM oAβ_{42} did not induce long-term memory in mice concurrently treated with the PKG inhibitor Rp-8-Br-cGMPS (D = 0.03 ± 0.044, n = 10 sex-balanced mice for each condition; $t_{(9)}$ = 0.735, p = 0.481 comparing D vs. zero; Bonferroni's p < 0.0001 comparing D between 200 pM oAβ_{42} vs. 200 pM oAβ_{42} + Rp-8-Br-cGMPS). Rp-8-Br-cGMPS alone did not affect short-term memory (Bonferroni's p = 1 vs. vehicle). Total exploration time (right panel) was not modified by treatments ($F_{(2,27)}$ = 0.086, p = 0.667). Shaded area with lines corresponds to mean + SEM of D in mice treated with vehicle or 200 pM oAβ_{42} 20 min before a short T1 exposure. * p < 0.05; ** p < 0.01; **** p < 0.0001. Data expressed as mean ± SEM.

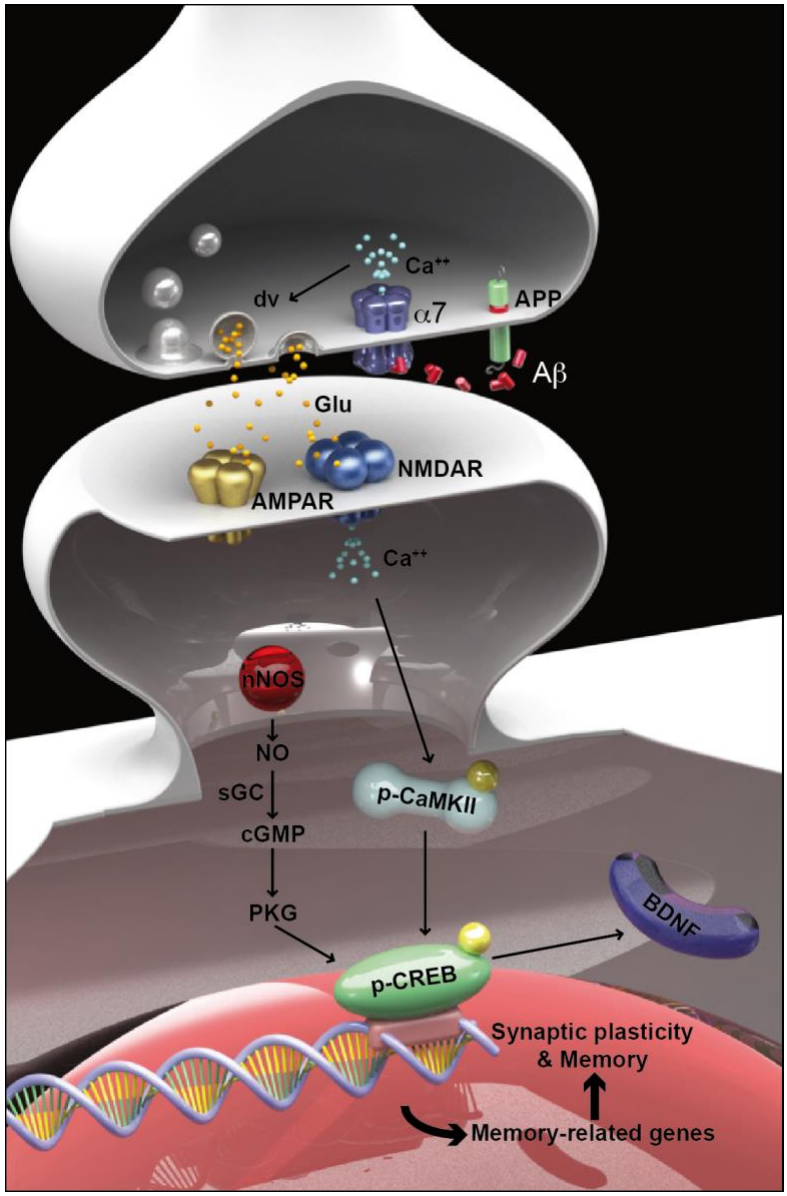

Figure 6 - Aβ-mediated events occurring at the synapse in physiological conditions: a working hypothesis. In physiological conditions Aβ activates α7nAChRs leading to Ca^{2+} entry thus increasing neurotransmitter release. This, in turn, would trigger a cascade of intracellular events involving the NO/cGMP/PKG pathway and the plasticity-related molecules p-CREB, p-CaMKII and BDNF leading to the enhancement of synaptic plasticity and memory.

Overall, our findings indicate that oAβ_{42} mainly acts through an intracellular signaling pathway involving the NO/cGMP/PKG pathway leading to PRPs activation, synaptic potentiation and memory formation as summarized in **Figure 6**.

DISCUSSION

In this manuscript we focused on the role of picomolar concentrations of oAβ_{42} at hippocampal synapses in the healthy rodent brain. We found that 200 pM oAβ_{42} increases neurotransmitter release, induces pre- and post-synaptic ultrastructural changes, and increases PRPs expression leading to the conversion of E-LTP into L-LTP and of short-term memory into long-term memory.

This study was inspired by previous observations indicating that oAβ_{42} exerts opposite effects onto synaptic plasticity and memory depending upon its concentration (Puzzo et al., 2012; Gulisano et al., 2018b). Here, we first performed a DR curve to confirm that 200 pM oAβ_{42} was the dose capable to enhance LTP, whereas 200 nM impaired it, consistently

with previous works (Puzzo et al., 2008, 2011, 2012; Garcia-Osta and Alberini, 2009; Morley et al., 2010; Lazarevic et al., 2017).

Next, because high concentrations of extracellular oAβ_{42} enter neurons (Ripoli et al., 2014; Puzzo et al., 2017) leading to synaptic dysfunction through direct intracellular targets (Ripoli et al., 2014), we investigated whether pM oAβ_{42} acts at extracellular and/or intracellular levels when enhancing synaptic transmission and plasticity. We demonstrated that the effect of pM oAβ_{42} is exerted only when the peptide is applied extracellularly, since its administration inside neurons did not affect LTP. Dual-patch experiments, in which we applied oAβ_{42} from the extracellular space while one of the two adjacent neurons was injected with the 6E10 antibody to neutralize human oAβ_{42} possibly accumulated inside neurons, confirmed that only extracellular oAβ_{42} enhances mEPSC frequency.

The increase in mEPSC frequency and the decrease of PPF suggest a pre-synaptic mechanism of neurotransmitter release, in line with previous electrophysiological findings showing that pM oAβ_{42} affect basal synaptic transmission inducing an increase of fiber volley amplitude, an index of presynaptic recruitment (Gulisano et al., 2018b), and post-tetanic potentiation, a form of short-term plasticity due to

presynaptic calcium entry (Puzzo et al., 2008). Furthermore, it has been recently demonstrated that Aβ exerts an opposite effect on synaptic vesicle recycling depending upon the dose (Lazarevic et al., 2017), in line with other studies showing a sustained increase of mEPSC frequency after prolonged exposure to 200 pM oAβ_{42} (Koppensteiner et al., 2016) or treatment with inhibitors of Aβ degradation (Abramov et al., 2009). In these circumstances, high levels of Aβ may maintain neurotransmitter release for a longer period leading to vesicle depletion (Parodi et al., 2010), or enter neurons directly, affecting presynaptic proteins such as synaptophysin, VAMP2 or synapsin I (Russell et al., 2012; Koppensteiner et al., 2016).

In this manuscript we show that both exogenously applied human Aβ at low concentrations or endogenous Aβ are involved in neurotransmitter release. This is consistent with previous studies demonstrating that endogenous Aβ is needed for synaptic plasticity and memory to occur (Garcia-Osta and Alberini, 2009; Morley et al., 2010; Puzzo et al., 2011) and that Aβ production physiologically increased during neuronal activity and memory induction (Kamenetz et al., 2003; Cirrito et al., 2005; Brody et al., 2008; Puzzo et al., 2011; Palmeri et al., 2017). Interestingly, we have previously demonstrated that the impairment of LTP and memory due to the inhibition of endogenous Aβ could be

rescued by concomitant application of exogenous 200 pM Aβ, with 300 pM Aβ producing a more pronounced enhancement similar to that obtained with the administration of 200 pM exogenous Aβ alone (Puzzo et al., 2011). In the same work, we demonstrated that the threshold of Aβ needed for normal synaptic plasticity and memory is around 330-380 pM. Thus, considering that $A\beta_{42}$ levels in basal conditions are equal to 180-200 pM (Puzzo et al., 2008), adding 200 pM of exogenous Aβ is likely to induce a further enhancement of synaptic plasticity and memory. Even if we cannot exclude that exogenously applied and endogenous Aβ might use different mechanisms to act, previous works have suggested that a common target might be represented by α7-nAchRs (Puzzo et al., 2008, 2011), whose genetic or pharmacological deletion prevented both endogenous or exogenous Aβ to exert its effects at the synapse.

Because the probability of transmitter release contributes to LTP induction and maintenance (Kleschevnikov et al., 1996), we studied whether $oA\beta_{42}$ converted E-LTP into L-LTP, two different forms of plasticity characterized by different temporal and mechanistic features (Huang, 1998). E-LTP can be induced by a weak tetanic stimulation, decays in one or two hours, does not depend on new protein synthesis and is mostly due to activation of kinases. Conversely, L-LTP needs a

stronger stimulation to be induced, lasts several hours and requires new protein synthesis and gene transcription (Bliss and Collingridge, 1993; Nguyen et al., 1994; Huang, 1998). Several studies have demonstrated that adequate physiological or pharmacological stimuli might convert E-LTP into L-LTP, a mechanism that parallels transformation of short-term memory into long-term memory [for a review see (Puzzo et al., 2016)]. Here, we found that a treatment with pM oAβ_{42} before a weak tetanic stimulation converted E-LTP and short-term memory into L-LTP and long-term memory, respectively, suggesting that at this concentration the peptide acts as a cognitive-enhancer and further begging the question on how its removal from the brain might be beneficial.

Ultrastructural analyses of hippocampal slices treated as for electrophysiology revealed that oAβ_{42} produces a series of concomitant changes occurring both pre- and post-synaptically, as one would expect for long-term normal synaptic plasticity to occur (Antonova, 2001). Indeed, oAβ_{42} alone elevated the fraction of vesicles available for release (i.e., docked vesicles) during the induction of plasticity (Bourne et al., 2013), whereas a longer PSD, which is suggestive of plastic changes occurring at the post-synaptic site (Babits et al., 2016), was observed in slices treated with oAβ_{42} paired with a weak tetanus.

In the present study we have also sought to explore the possible extracellular targets used by pM oAβ_{42} to affect PPF and convert E-LTP into L-LTP. We first focused on APP because it binds different Aβ species (Lorenzo et al., 2000; Shaked et al., 2006; Fogel et al., 2014), and it is involved in the enhancement of neurotransmitter release leading to hippocampal hyperactivity in AD (Bakker et al., 2012; Busche et al., 2012).

Furthermore, recent studies have shown that, when at high concentrations, extracellular Aβ needs APP to impair synaptic plasticity and memory (Puzzo et al., 2017; Wang et al., 2017). Here, we used APP KO mice at young age, when the impairment of LTP and memory is not yet manifested (Dawson et al., 1999; Tyan et al., 2012), to investigate whether Aβ needs APP to enhance synaptic plasticity and memory when at low concentration. Because pM oAβ_{42} still enhanced neurotransmitter release, synaptic plasticity and memory in APP KO mice, we concluded that APP intervenes in Aβ detrimental effects when the peptide is present at high concentrations (Puzzo et al., 2017), but is not needed for oAβ_{42} at low concentrations to enhance synaptic plasticity.

Since Aβ induces a series of events mediated by an increase of Ca^{2+} entry in the presynaptic terminal (Puzzo et al., 2008; Lawrence et al.,

2014), we focused on α7nAChRs, ionotropic channels permeable to calcium that are highly expressed in the hippocampus and implicated in a variety of cognitive functions such as learning and memory, attention and reward [reviewed in (Picciotto et al., 2000)]. The link between Aβ and α7nAChRs has been widely studied, and it is known that Aβ binds α7nAChRs with high affinity, exerting an agonistic or antagonistic effect in a dose-dependent manner (Wang et al., 2000; Mura et al., 2012). Using genetic and pharmacological approaches, we showed that α7nAChRs are needed for pM oAβ_{42} to increase neurotransmitter release and to consolidate LTP. Experiments performed in hippocampal slices from APP KO mice treated with the α7nAChR antagonist MLA further confirmed that, at low concentrations, oAβ_{42} exerts its effect through α7nAChRs and not APP, in agreement with previous studies (Puzzo et al., 2008, 2011; Mura et al., 2012; Lawrence et al., 2014).

The *in vitro* observation showing that α7nAChRs but not APP are necessary for pM oAβ_{42} to produce L-LTP was further confirmed by *in vivo* studies demonstrating that the oAβ_{42}-induced conversion of short-term into long-term memory relies upon α7nAChRs and does not involve APP.

Here we also demonstrated that oAβ_{42} effects are mediated by the NO/cGMP/PKG cascade, already known to be involved in LTP and

memory induction and maintenance (Johnstone and Raymond, 2011; Bollen et al., 2014). In fact, inhibition of this pathway prevented the oAβ_{42}-induced L-LTP and long-term memory. Interestingly, we have recently demonstrated that in physiological conditions cGMP stimulates Aβ production to induce L-LTP and memory (Palmeri et al., 2017). This, together with the present results, indicates that the NO/cGMP pathway acts both upstream and downstream of Aβ, suggesting the existence of a cGMP-Aβ-cGMP loop as a preferential intracellular mechanism involved in Aβ-mediated plastic effects.

Additionally, pM oAβ_{42} increased the expression of nNOS, which, on the other hand, is decreased by high concentrations of the peptide (Venturini et al., 2002). This effect might be due to direct or indirect mechanisms. Indeed, previous studies have demonstrated that Aβ fragments can bind nNOS (Padayachee and Whiteley, 2011), suggesting the possibility of a direct interaction between the two proteins. On the other hand, the oAβ_{42}-induced increase of neurotransmitter release might enhance Ca^{2+} influx at the post-synaptic level triggering increased nNOS expression (Sasaki et al., 2000).

The oAβ_{42}-induced conversion of E-LTP into L-LTP suggests a possible role for Aβ in synaptic tagging mechanism. Synapses that have received a weak stimulation enter a receptive state (tagging) that, if associated

with the synthesis of PRPs, will lead to LTP maintenance. The initial changes in the synaptic weight are given by the efficacy of the pre- and postsynaptic elements, and require a third factor to persist (Redondo and Morris, 2011). Consistent with this possibility, pre-treatment of hippocampal slices with oAβ_{42} induced the synaptic changes underlying L-LTP, such as the increased phosphorylation of CREB known to lead to PRPs expression needed for L-LTP appearance (Bourtchuladze et al., 1994). Moreover, p-CREB further increased in slices where oAβ_{42} was paired with a weak tetanus, confirming that CREB phosphorylation continues to rise during LTP maintenance (Leutgeb et al., 2005), and that the NO/cGMP/PKG cascade can trigger gene expression through CREB phosphorylation during L-LTP (Lu et al., 1999).

Interestingly, pairing oAβ_{42} with a weak tetanus induced an increase of CaMKII phosphorylation and BDNF expression, molecules known to stimulate CREB activation thus inducing L-LTP and long-term memory. In particular, p-CaMKII, like nNOS, responds to NMDA-receptors mediated Ca^{2+} entry during LTP, and is involved in tag signaling (Lisman et al., 2012) and metaplasticity (Deisseroth et al., 1995); BDNF is responsible for upregulating gene transcription and promoting structural changes during L-LTP (Bekinschtein et al., 2007).

This further suggests that oAβ_{42} may prime the synapse to be more responsive, as also indicated by ultrastructural results.

In conclusion, our findings evidenced interesting differences and similarities between low versus high oAβ_{42} concentrations. Indeed, the effects of pM oAβ_{42} are exerted at extracellular level and depend upon α7nAChRs, whereas nM oAβ_{42} requires APP and intraneuronal internalization (Ripoli et al., 2014; Puzzo et al., 2017), even if it is not possible to exclude an extracellular effect mediated by different receptors. On the other side, low and high oAβ_{42} levels affect the same key intracellular pathways involved in synaptic plasticity and memory (i.e., NO/cGMP/PKG/p-CREB cascade, CaMKII, BDNF), leading to their stimulation when at pM concentrations, or inhibition when at nM concentrations (Puzzo et al., 2005, 2009; Ghosh and Giese, 2015; Song et al., 2015; Opazo et al., 2018). The capability of oAβ_{42} to induce opposite effects depending upon its dose is consistent with previous studies (Calabrese, 2001; Puzzo et al., 2012), and this biphasic behavior characterized by low-dose stimulation and high-dose inhibition might be framed into the "hormesis" phenomenon (Calabrese, 2008; Mattson, 2008). Indeed, even if the most used approach to model a DR curve is the linear Hill model, several studies have pointed out that it might not be sufficient to explain the multi-phasic response exerted by a variety

of endogenous or exogenous compounds [reviewed in (Prickaerts et al., 2017)]. Although different mechanisms may underlie the hormetic effect (Mattson, 2008), it is widely accepted that a compound might interact with a certain target depending upon its concentration. Consistently, Aβ binds different targets in a concentration-dependent manner (Xie et al., 2002; Moreth et al., 2013; Mura et al., 2012) and, recently, it has been shown that Aβ directly affects α7-nAchRs conformation and function by acting as an agonist when at pM concentrations or an antagonist when at nM concentrations (Lasala et al., 2019). It should be also considered that at high Aβ concentrations, the amount of oligomerization proportionally increases overrunning the physiological level (Gulisano et al., 2018). This, in turn, might determine the interaction of Aβ oligomers with different targets, including APP (Puzzo et al., 2017).

These observations might be useful to understand the mechanisms switching the positive into the negative effects exerted by oAβ, and might constitute the bases for further studies to ensure novel, safe and rational personalized therapeutic approaches to cure patients affected by AD.

REFERENCES

Abramov E, Dolev I, Fogel H, Ciccotosto GD, Ruff E, Slutsky I (2009) Amyloid-beta as a positive endogenous regulator of release probability at hippocampal synapses. Nature neuroscience 12:1567–1576 Available at: http://www.nature.com/doifinder/10.1038/nn.2433.

Aizenstein HJ, Nebes RD, Saxton JA, Price JC, Mathis CA, Tsopelas ND, Ziolko SK, James JA, Snitz BE, Houck PR, Bi W, Cohen AD, Lopresti BJ, DeKosky ST, Halligan EM, Klunk WE (2008) Frequent amyloid deposition without significant cognitive impairment among the elderly. Archives of neurology 65:1509–1517 Available at: http://europepmc.org/abstract/MED/19001171, http://europepmc.org/articles/PMC2636844/?report=abstract%0Ahttp://europepmc.org/articles/PMC2636844?pdf=render%0Ahttp://www.ncbi.nlm.nih.gov/pubmed/19001171%0Ahttp://europepmc.org/articles/PMC2636844.

Antonova I (2001) Rapid Increase in Clusters of Presynaptic Proteins at Onset of Long-Lasting Potentiation. Science 294:1547–1550 Available at: http://www.sciencemag.org/cgi/doi/10.1126/science.1066273.

Babits R, Szőke B, Sótonyi P, Rácz B (2016) Food restriction modifies ultrastructure of hippocampal synapses. Hippocampus 26:437–444 Available at: http://www.ncbi.nlm.nih.gov/pubmed/26386363.

Bakker A, Krauss GL, Albert MS, Speck CL, Jones LR, Stark CE, Yassa MA, Bassett SS, Shelton AL, Gallagher M (2012) Reduction of hippocampal hyperactivity improves cognition in amnestic mild cognitive impairment. Neuron 74:467–474 Available at: http://www.ncbi.nlm.nih.gov/pubmed/22578498.

Barone E, Tramutola A, Triani F, Calcagnini S, Di Domenico F, Ripoli C, Gaetani S, Grassi C, Butterfield DA, Cassano T, Perluigi M (2018) Biliverdin Reductase-A Mediates the Beneficial Effects of Intranasal Insulin in Alzheimer Disease. Molecular Neurobiology Available at: http://link.springer.com/10.1007/s12035-018-1231-5.

Bekinschtein P, Cammarota M, Igaz LM, Bevilaqua LRM, Izquierdo I, Medina JH (2007) Persistence of long-term memory storage requires a late protein synthesis- and BDNF- dependent phase in the hippocampus. Neuron 53:261–277 Available at: http://www.ncbi.nlm.nih.gov/pubmed/17224407.

Bliss T, Collingridge G (1993) A synaptic model of memory: long-term potentiation

in the hippocampus. Nature 361:31–39.

Bollen E, Puzzo D, Rutten K, Privitera L, De Vry J, Vanmierlo T, Kenis G, Palmeri A, D'Hooge R, Balschun D, Steinbusch HMW, Blokland A, Prickaerts J (2014) Improved long-term memory via enhancing cGMP-PKG signaling requires cAMP-PKA signaling. Neuropsychopharmacology : official publication of the American College of Neuropsychopharmacology 39:2497–2505 Available at: http://www.ncbi.nlm.nih.gov/pubmed/24813825.

Bon CLM, Garthwaite J (2003) On the Role of Nitric Oxide in Hippocampal Long-Term Potentiation. J Neurosci 23:1941–1948 Available at: http://www.jneurosci.org/cgi/content/abstract/23/5/1941.

Bourne JN, Chirillo MA, Harris KM (2013) Presynaptic ultrastructural plasticity along CA3→CA1 axons during long-term potentiation in mature hippocampus. The Journal of comparative neurology 521:3898–3912 Available at: http://www.ncbi.nlm.nih.gov/pubmed/23784793%5Cnhttp://onlinelibrary.wiley.com/doi/10.1002/cne.23384/abstract.

Bourtchuladze R, Frenguelli B, Blendy J, Cioffi D, Schutz G, Silva AJ (1994) Deficient long-term memory in mice with a targeted mutation of the cAMP-responsive element-binding protein. Cell 79:59–68 Available at: http://www.ncbi.nlm.nih.gov/pubmed/7923378.

Brody DL, Magnoni S, Schwetye KE, Spinner ML, Esparza TJ, Stocchetti N, Zipfel GJ, Holtzman DM (2008) Amyloid-beta dynamics correlate with neurological status in the injured human brain. Science (New York, NY) 321:1221–1224 Available at: http://www.ncbi.nlm.nih.gov/pubmed/18755980.

Busche MA, Chen X, Henning HA, Reichwald J, Staufenbiel M, Sakmann B, Konnerth A (2012) Critical role of soluble amyloid-β for early hippocampal hyperactivity in a mouse model of Alzheimer's disease. Proceedings of the National Academy of Sciences of the United States of America 109:8740–8745 Available at: http://www.ncbi.nlm.nih.gov/pubmed/22592800%5Cnhttp://www.pubmedcentral.nih.gov/articlerender.fcgi?artid=PMC3365221.

Calabrese EJ (2001) Amyloid beta-peptide: biphasic dose responses. Critical reviews in toxicology 31:605–606 Available at: http://www.ncbi.nlm.nih.gov/pubmed/11504184.

Calabrese EJ (2008) Hormesis and medicine. British Journal of Clinical

Pharmacology.

Caraci F, Gulisano W, Guida CA, Impellizzeri AAR, Drago F, Puzzo D, Palmeri A (2015) A key role for TGF-β1 in hippocampal synaptic plasticity and memory. Scientific reports 5:11252 Available at: http://www.ncbi.nlm.nih.gov/pubmed/26059637%5Cnhttp://www.pubmedcentral.nih.gov/articlerender.fcgi?artid=PMC4462026.

Cirrito JR, Kang J-E, Lee J, Stewart FR, Verges DK, Silverio LM, Bu G, Mennerick S, Holtzman DM (2008) Endocytosis is required for synaptic activity-dependent release of amyloid-beta in vivo. Neuron 58:42–51 Available at: http://www.ncbi.nlm.nih.gov/pubmed/18400162.

Cirrito JR, Yamada KA, Finn MB, Sloviter RS, Bales KR, May PC, Schoepp DD, Paul SM, Mennerick S, Holtzman DM (2005) Synaptic Activity Regulates Interstitial Fluid Amyloid-β Levels In Vivo. Neuron 48:913–922.

Dawson GR, Seabrook GR, Zheng H, Smith DW, Graham S, O'Dowd G, Bowery BJ, Boyce S, Trumbauer ME, Chen HY, Van Der Ploeg LHT, Sirinathsinghji DJS (1999) Age-related cognitive deficits, impaired long-term potentiation and reduction in synaptic marker density in mice lacking the β-amyloid precursor protein. Neuroscience.

DeFelipe J, Marco P, Busturia I, Merchán-Pérez A (1999) Estimation of the number of synapses in the cerebral cortex: methodological considerations. Cerebral cortex (New York, NY : 1991) 9:722–732 Available at: http://www.ncbi.nlm.nih.gov/pubmed/10554995.

Deisseroth K, Bito H, Schulman H, Tsien RW (1995) Synaptic Plasticity: A molecular mechanism for metaplasticity. Current Biology 5:1334–1338.

Dobrunz LE, Stevens CF (1997) Heterogeneity of Release Probability, Facilitation, and Depletion at Central Synapses. Neuron 18:995–1008 Available at: http://linkinghub.elsevier.com/retrieve/pii/S0896627300803384.

Fogel H, Frere S, Segev O, Bharill S, Shapira I, Gazit N, O'Malley T, Slomowitz E, Berdichevsky Y, Walsh DM, Isacoff EY, Hirsch JA, Slutsky I (2014) APP homodimers transduce an amyloid-β-mediated increase in release probability at excitatory synapses. Cell reports 7:1560–1576 Available at: http://www.ncbi.nlm.nih.gov/pubmed/24835997.

Garcia-Osta A, Alberini CM (2009) Amyloid beta mediates memory formation. Learning & memory (Cold Spring Harbor, NY) 16:267–272 Available at:

papers3://publication/doi/10.1101/lm.1310209.

Geinisman Y (2000) Structural synaptic modifications associated with hippocampal LTP and behavioral learning. Cerebral cortex (New York, NY : 1991) 10:952–962 Available at: http://www.ncbi.nlm.nih.gov/pubmed/11007546%5Cnhttp://cercor.oxfordjournals.org/content/10/10/952.short.

Ghosh A, Giese KP (2015) Calcium/calmodulin-dependent kinase II and Alzheimer's disease. Molecular brain 8:78 Available at: http://molecularbrain.biomedcentral.com/articles/10.1186/s13041-015-0166-2.

Gulisano W, Maugeri D, Baltrons MA, Fà M, Amato A, Palmeri A, D'Adamio L, Grassi C, Devanand DP, Honig LS, Puzzo D, Arancio O (2018a) Role of Amyloid-β and Tau Proteins in Alzheimer's Disease: Confuting the Amyloid Cascade. Journal of Alzheimer's disease : JAD 136:1383–1398 Available at: http://www.ncbi.nlm.nih.gov/pubmed/23576130%5Cnhttp://www.pubmedcentral.nih.gov/articlerender.fcgi?artid=PMC3634198.

Gulisano W, Melone M, Li Puma DD, Tropea MR, Palmeri A, Arancio O, Grassi C, Conti F, Puzzo D (2018b) The effect of amyloid-β peptide on synaptic plasticity and memory is influenced by different isoforms, concentrations, and aggregation status. Neurobiology of Aging 71:51–60 Available at: https://linkinghub.elsevier.com/retrieve/pii/S0197458018302306.

Hardy J, Selkoe DJ (2002) The Amyloid Hypothesis of Alzheimer ' s Disease : Progress and Problems on the Road to Therapeutics. Science 297:353–357.

Herrup K (2015) The case for rejecting the amyloid cascade hypothesis. Nature Neuroscience 18:794–799 Available at: http://www.nature.com/doifinder/10.1038/nn.4017.

Huang EP (1998) Synaptic plasticity: Going through phases with LTP. Current Biology 8:R350–R352 Available at: http://linkinghub.elsevier.com/retrieve/pii/S0960982298702192.

Johnstone VP a., Raymond CR (2011) A protein synthesis and nitric oxide-dependent presynaptic enhancement in persistent forms of long-term potentiation. Learning & memory (Cold Spring Harbor, NY) 18:625–633 Available at: http://www.ncbi.nlm.nih.gov/pubmed/21933902.

Kamenetz F, Tomita T, Hsieh H, Seabrook G, Borchelt D, Iwatsubo T, Sisodia S, Malinow R (2003) APP processing and synaptic function. Neuron 37:925–937

Available at: http://www.ncbi.nlm.nih.gov/pubmed/12670422%5Cnhttp://ac.els-cdn.com/S0896627303001247/1-s2.0-S0896627303001247-main.pdf?_tid=84f34ca6-67b8-11e6-9a34-00000aab0f01&acdnat=1471795468_de7bad86612e8577c795987ff33791b2.

Kleschevnikov AM, Sokolov M V., Kuhnt U, Dawe GS, Stephenson JD, Voronin LL (1996) Changes in paired-pulse facilitation correlate with induction of long-term potentiation in area CA1 of rat hippocampal slices. Neuroscience 76:829–843.

Koo EH, Park L, Selkoe DJ (1993) Amyloid β-Protein as a Substrate Interacts with Extracellular Matrix to Promote Neurite Outgrowth. Proceedings of the National Academy of Sciences 90:4748–4752 Available at: http://www.pubmedcentral.nih.gov/articlerender.fcgi?artid=46590&tool=pmcentrez&rendertype=abstract.

Koppensteiner P, Trinchese F, Fà M, Puzzo D, Gulisano W, Yan S, Poussin A, Liu S, Orozco I, Dale E, Teich AF, Palmeri A, Ninan I, Boehm S, Arancio O (2016) Time-dependent reversal of synaptic plasticity induced by physiological concentrations of oligomeric Aβ42: an early index of Alzheimer's disease. Scientific reports 6:32553 Available at: http://www.nature.com/articles/srep32553.

Lasala M, Fabiani C, Corradi J, Antollini S, Bouzat C (2019) Molecular Modulation of Human α7 Nicotinic Receptor by Amyloid-β Peptides. Frontiers in cellular neuroscience 13:37 Available at: http://www.ncbi.nlm.nih.gov/pubmed/30800059.

Lawrence JLM, Tong M, Alfulaij N, Sherrin T, Contarino M, White MM, Bellinger FP, Todorovic C, Nichols RA (2014) Regulation of presynaptic Ca2+, synaptic plasticity and contextual fear conditioning by a N-terminal β-amyloid fragment. The Journal of neuroscience : the official journal of the Society for Neuroscience 34:14210–14218 Available at: http://www.jneurosci.org/cgi/doi/10.1523/JNEUROSCI.0326-14.2014.

Lazarevic V, Fieńko S, Andres-Alonso M, Anni D, Ivanova D, Montenegro-Venegas C, Gundelfinger ED, Cousin MA, Fejtova A (2017) Physiological Concentrations of Amyloid Beta Regulate Recycling of Synaptic Vesicles via Alpha7 Acetylcholine Receptor and CDK5/Calcineurin Signaling. Frontiers in

molecular neuroscience 10:221 Available at: http://journal.frontiersin.org/article/10.3389/fnmol.2017.00221/full.

Lesné SE, Sherman MA, Grant M, Kuskowski M, Schneider JA, Bennett DA, Ashe KH (2013) Brain amyloid-β oligomers in ageing and Alzheimer's disease. Brain : a journal of neurology 136:1383–1398 Available at: http://www.ncbi.nlm.nih.gov/pubmed/23576130.

Leutgeb JK, Frey JU, Behnisch T (2005) Single cell analysis of activity-dependent cyclic AMP-responsive element-binding protein phosphorylation during long-lasting long-term potentiation in area CA1 of mature rat hippocampal-organotypic cultures. Neuroscience 131:601–610 Available at: http://www.ncbi.nlm.nih.gov/pubmed/15730866.

Lisman J, Yasuda R, Raghavachari S (2012) Mechanisms of CaMKII action in long-term potentiation. Nature reviews Neuroscience 13:169–182 Available at: http://www.nature.com/doifinder/10.1038/nrn3192.

Lorenzo A, Yuan M, Zhang Z, Paganetti PA, Sturchler-Pierrat C, Staufenbiel M, Mautino J, Vigo FS, Sommer B, Yankner BA (2000) Amyloid beta interacts with the amyloid precursor protein: a potential toxic mechanism in Alzheimer's disease. Nature neuroscience 3:460–464 Available at: http://www.ncbi.nlm.nih.gov/pubmed/10769385.

Lu YF, Kandel ER, Hawkins RD (1999) Nitric oxide signaling contributes to late-phase LTP and CREB phosphorylation in the hippocampus. The Journal of neuroscience : the official journal of the Society for Neuroscience 19:10250–10261 Available at: http://www.ncbi.nlm.nih.gov/pubmed/10575022.

Maarouf CL, Daugs ID, Kokjohn TA, Walker DG, Hunter JM, Kruchowsky JC, Woltjer R, Kaye J, Castaño EM, Sabbagh MN, Beach TG, Roher AE (2011) Alzheimer's disease and non-demented high pathology control nonagenarians: comparing and contrasting the biochemistry of cognitively successful aging. PloS one 6:e27291 Available at: http://www.ncbi.nlm.nih.gov/pubmed/22087282.

Mattson MP (2008) Hormesis defined. Ageing research reviews 7:1–7 Available at: http://www.ncbi.nlm.nih.gov/pubmed/18162444.

Melone M, Bellesi M, Ducati A, Iacoangeli M, Conti F (2011) Cellular and Synaptic Localization of EAAT2a in Human Cerebral Cortex. Frontiers in Neuroanatomy 4:151 Available at:

http://journal.frontiersin.org/article/10.3389/fnana.2010.00151/abstract.

Melone M, Ciappelloni S, Conti F (2015) A quantitative analysis of cellular and synaptic localization of GAT-1 and GAT-3 in rat neocortex. Brain structure & function 220:885–897.

Morley JE, Farr SA, Banks WA, Johnson SN, Yamada KA, Xu L (2010) A physiological role for amyloid-beta protein:enhancement of learning and memory. Journal of Alzheimer's disease : JAD 19:441–449 Available at: http://www.ncbi.nlm.nih.gov/pubmed/19749407.

Mura E, Zappettini S, Preda S, Biundo F, Lanni C, Grilli M, Cavallero A, Olivero G, Salamone A, Govoni S, Marchi M (2012) Dual effect of beta-amyloid on α7 and α4β2 nicotinic receptors controlling the release of glutamate, aspartate and GABA in rat hippocampus. PloS one 7:e29661 Available at: http://www.ncbi.nlm.nih.gov/pubmed/22253754.

Nguyen P V., Abel T, Kandel ER (1994) Requirement of a critical period of transcription for induction of a late phase of LTP. Science (New York, NY) 265:1104–1107 Available at: http://www.ncbi.nlm.nih.gov/pubmed/8066450.

Opazo P, Viana da Silva S, Carta M, Breillat C, Coultrap SJ, Grillo-Bosch D, Sainlos M, Coussen F, Bayer KU, Mulle C, Choquet D (2018) CaMKII Metaplasticity Drives Aβ Oligomer-Mediated Synaptotoxicity. Cell reports 23:3137–3145 Available at: http://www.jneurosci.org/cgi/doi/10.1523/JNEUROSCI.2086-05.2005.

Padayachee ER, Whiteley CG (2011) Spectrofluorimetric analysis of the interaction of amyloid peptides with neuronal nitric oxide synthase: implications in Alzheimer's disease. Biochimica et biophysica acta 1810:1136–1140 Available at: http://www.ncbi.nlm.nih.gov/pubmed/21930189.

Palmeri A, Ricciarelli R, Gulisano W, Rivera D, Rebosio C, Calcagno E, Tropea MR, Conti S, Das U, Roy S, Pronzato MA, Arancio O, Fedele E, Puzzo D (2017) Amyloid-β Peptide Is Needed for cGMP-Induced Long-Term Potentiation and Memory. The Journal of neuroscience : the official journal of the Society for Neuroscience 37:6926–6937 Available at: http://www.jneurosci.org/lookup/doi/10.1523/JNEUROSCI.3607-16.2017.

Parodi J, Sepúlveda FJ, Roa J, Opazo C, Inestrosa NC, Aguayo LG (2010) Beta-amyloid causes depletion of synaptic vesicles leading to neurotransmission failure. The Journal of biological chemistry 285:2506–2514 Available at:

http://www.ncbi.nlm.nih.gov/pubmed/19915004.

Pearson HA, Peers C (2006) Physiological roles for amyloid beta peptides. The Journal of physiology 575:5–10 Available at: http://doi.wiley.com/10.1113/jphysiol.2006.111203.

Peters A, Palay SL, deF Webster H (1991) The fine structure of the nervous system neurons and their supportive cells. Oxford University Press, New York.

Picciotto MR, Caldarone BJ, King SL, Zachariou V (2000) Nicotinic receptors in the brain. Links between molecular biology and behavior. Neuropsychopharmacology : official publication of the American College of Neuropsychopharmacology 22:451–465 Available at: http://www.ncbi.nlm.nih.gov/pubmed/10731620.

Pozzo-Miller LD, Gottschalk W, Zhang L, McDermott K, Du J, Gopalakrishnan R, Oho C, Sheng ZH, Lu B (1999) Impairments in high-frequency transmission, synaptic vesicle docking, and synaptic protein distribution in the hippocampus of BDNF knockout mice. The Journal of neuroscience : the official journal of the Society for Neuroscience 19:4972–4983 Available at: http://eutils.ncbi.nlm.nih.gov/entrez/eutils/elink.fcgi?dbfrom=pubmed&id=10366630&retmode=ref&cmd=prlinks%5Cnpapers2://publication/uuid/0120F81C-C1AF-40BC-B5F5-1BB132CD7B01.

Prickaerts J, Van Goethem NP, Gulisano W, Argyrousi EK, Palmeri A, Puzzo D (2017) Physiological and pathological processes of synaptic plasticity and memory in drug discovery: Do not forget the dose-response curve. European journal of pharmacology 817:59–70 Available at: http://dx.doi.org/10.1016/j.ejphar.2017.05.058.

Puzzo D, Fiorito J, Purgatorio R, Gulisano W, Palmeri A, Arancio O, Nicholls R (2016) Molecular Mechanisms of Learning and Memory.

Puzzo D, Gulisano W, Arancio O, Palmeri A (2015) The keystone of Alzheimer pathogenesis might be sought in Aβ physiology. Neuroscience 307:26–36 Available at: http://www.ncbi.nlm.nih.gov/pubmed/26314631.

Puzzo D, Piacentini R, Fá M, Gulisano W, Li Puma DD, Staniszewski A, Zhang H, Tropea MR, Cocco S, Palmeri A, Fraser P, D'Adamio L, Grassi C, Arancio O (2017) LTP and memory impairment caused by extracellular Aβ and Tau oligomers is APP-dependent. eLife 6:1–21 Available at: http://elifesciences.org/lookup/doi/10.7554/eLife.26991 [Accessed September

18, 2017].

Puzzo D, Privitera L, Fa' M, Staniszewski A, Hashimoto G, Aziz F, Sakurai M, Ribe EM, Troy CM, Mercken M, Jung SS, Palmeri A, Arancio O (2011) Endogenous amyloid-β is necessary for hippocampal synaptic plasticity and memory. Annals of neurology 69:819–830 Available at: http://www.ncbi.nlm.nih.gov/pubmed/21472769.

Puzzo D, Privitera L, Leznik E, Fà M, Staniszewski A, Palmeri A, Arancio O (2008) Picomolar amyloid-beta positively modulates synaptic plasticity and memory in hippocampus. The Journal of neuroscience : the official journal of the Society for Neuroscience 28:14537–14545 Available at: http://www.jneurosci.org/cgi/doi/10.1523/JNEUROSCI.2692-08.2008.

Puzzo D, Privitera L, Palmeri A (2012) Hormetic effect of amyloid-β peptide in synaptic plasticity and memory. Neurobiology of aging 33:1484.e15-24 Available at: http://dx.doi.org/10.1016/j.neurobiolaging.2011.12.020.

Puzzo D, Staniszewski A, Deng SX, Privitera L, Leznik E, Liu S, Zhang H, Feng Y, Palmeri A, Landry DW, Arancio O (2009) Phosphodiesterase 5 inhibition improves synaptic function, memory, and amyloid-beta load in an Alzheimer's disease mouse model. The Journal of neuroscience : the official journal of the Society for Neuroscience 29:8075–8086 Available at: http://www.jneurosci.org/cgi/doi/10.1523/JNEUROSCI.0864-09.2009.

Puzzo D, Vitolo O, Trinchese F, Jacob JP, Palmeri A, Arancio O (2005) Amyloid-beta peptide inhibits activation of the nitric oxide/cGMP/cAMP-responsive element-binding protein pathway during hippocampal synaptic plasticity. The Journal of neuroscience : the official journal of the Society for Neuroscience 25:6887–6897 Available at: http://www.jneurosci.org/cgi/doi/10.1523/JNEUROSCI.5291-04.2005.

Redondo RL, Morris RGM (2011) Making memories last: the synaptic tagging and capture hypothesis. Nature reviews Neuroscience 12:17–30 Available at: http://www.nature.com/doifinder/10.1038/nrn2963.

Ripoli C, Cocco S, Li Puma DD, Piacentini R, Mastrodonato A, Scala F, Puzzo D, D'Ascenzo M, Grassi C (2014) Intracellular accumulation of amyloid-β (Aβ) protein plays a major role in Aβ-induced alterations of glutamatergic synaptic transmission and plasticity. The Journal of neuroscience : the official journal of the Society for Neuroscience 34:12893–12903 Available at:

http://www.jneurosci.org/cgi/doi/10.1523/JNEUROSCI.1201-14.2014.

Ripoli C, Piacentini R, Riccardi E, Leone L, Li Puma DD, Bitan G, Grassi C (2013) Effects of different amyloid β-protein analogues on synaptic function. Neurobiology of aging 34:1032–1044 Available at: http://www.ncbi.nlm.nih.gov/pubmed/23046860.

Russell CL, Semerdjieva S, Empson RM, Austen BM, Beesley PW, Alifragis P (2012) Amyloid-β acts as a regulator of neurotransmitter release disrupting the interaction between synaptophysin and VAMP2. PloS one 7:e43201 Available at: http://www.ncbi.nlm.nih.gov/pubmed/22905234.

Sasaki M, Gonzalez-Zulueta M, Huang H, Herring WJ, Ahn SY, Ginty DD, Dawson VL, Dawson TM (2000) Dynamic regulation of neuronal NO synthase transcription by calcium influx through a CREB family transcription factor-dependent mechanism. Proceedings of the National Academy of Sciences of the United States of America.

Schmidt SD, Nixon RA, Mathews PM (2005) ELISA Method for Measurement of Amyloid-β Levels. In: Amyloid Proteins, pp 279–298. New Jersey: Humana Press. Available at: http://link.springer.com/10.1385/1-59259-874-9:279.

Schneider CA, Rasband WS, Eliceiri KW (2012) NIH Image to ImageJ: 25 years of image analysis. Nature methods 9:671–675 Available at: http://www.ncbi.nlm.nih.gov/pubmed/22930834.

Shaked GM, Kummer MP, Lu DC, Galvan V, Bredesen DE, Koo EH (2006) Abeta induces cell death by direct interaction with its cognate extracellular domain on APP (APP 597-624). FASEB journal : official publication of the Federation of American Societies for Experimental Biology 20:1254–1256 Available at: http://www.ncbi.nlm.nih.gov/pubmed/16636103.

Shepherd GM, Harris KM (1998) Three-dimensional structure and composition of CA3-->CA1 axons in rat hippocampal slices: implications for presynaptic connectivity and compartmentalization. The Journal of neuroscience : the official journal of the Society for Neuroscience 18:8300–8310 Available at: http://www.ncbi.nlm.nih.gov/pubmed/9763474.

Song J-H, Yu J-T, Tan L (2015) Brain-Derived Neurotrophic Factor in Alzheimer's Disease: Risk, Mechanisms, and Therapy. Molecular neurobiology 52:1477–1493 Available at: http://link.springer.com/10.1007/s12035-014-8958-4.

Spinelli M, Fusco S, Mainardi M, Scala F, Natale F, Lapenta R, Mattera A, Rinaudo

M, Li Puma DD, Ripoli C, Grassi A, D'Ascenzo M, Grassi C (2017) Brain insulin resistance impairs hippocampal synaptic plasticity and memory by increasing GluA1 palmitoylation through FoxO3a. Nature communications 8:2009 Available at: http://www.ncbi.nlm.nih.gov/pubmed/29222408.

Stine WB, Dahlgren KN, Krafft GA, LaDu MJ (2003) In vitro characterization of conditions for amyloid-beta peptide oligomerization and fibrillogenesis. The Journal of biological chemistry 278:11612–11622 Available at: http://www.ncbi.nlm.nih.gov/pubmed/12499373.

Tyan S-H, Yu-Jung Shih A, Walsch JJ, Murayama H, Sarsoza F, Ku L, Eggert S, Hof PR, Koo EH, Dickstein DL (2012) Amyloid precursor protein (APP) regulates synaptic structure and function. MolCell Neurosci 51:43–52.

Venturini G, Colasanti M, Persichini T, Fioravanti E, Ascenzi P, Palomba L, Cantoni O, Musci G (2002) Beta-amyloid inhibits NOS activity by subtracting NADPH availability. The FASEB journal : official publication of the Federation of American Societies for Experimental Biology.

Wang HY, Lee DH, Davis CB, Shank RP (2000) Amyloid peptide Abeta(1-42) binds selectively and with picomolar affinity to alpha7 nicotinic acetylcholine receptors. Journal of neurochemistry 75:1155–1161 Available at: http://www.ncbi.nlm.nih.gov/pubmed/10936198.

Wang Z, Jackson RJ, Hong W, Taylor WM, Corbett GT, Moreno A, Liu W, Li S, Frosch MP, Slutsky I, Young-Pearse TL, Spires-Jones TL, Walsh DM (2017) Human Brain-Derived Aβ Oligomers Bind to Synapses and Disrupt Synaptic Activity in a Manner That Requires APP. The Journal of neuroscience : the official journal of the Society for Neuroscience 37:11947–11966 Available at: http://www.ncbi.nlm.nih.gov/pubmed/29101243.

Zappettini S, Grilli M, Olivero G, Mura E, Preda S, Govoni S, Salamone A, Marchi M (2012) Beta Amyloid Differently Modulate Nicotinic and Muscarinic Receptor Subtypes which Stimulate in vitro and in vivo the Release of Glycine in the Rat Hippocampus. Frontiers in pharmacology 3:146 Available at: http://www.ncbi.nlm.nih.gov/pubmed/22866037.

Zucker RS, Regehr WG (2002) Short-Term Synaptic Plasticity. Annual Review of Physiology 64:355–405 Available at: http://www.annualreviews.org/doi/10.1146/annurev.physiol.64.092501.11454.

Chapter 2: Genetic deletion of α7 nicotinic acetylcholine receptors induces an age-dependent Alzheimer's disease-like pathology

Tropea MR[1], Li Puma DD[2,3], Melone M[4,5], Gulisano W[1], Arancio O[6], Grassi C[2,3], Conti F[4,5,7], Puzzo D[1,8].

[1]Dept. Biomedical and Biotechnological Sciences, University of Catania, Catania 95123, Italy; [2]Department of Neuroscience, Università Cattolica del Sacro Cuore, 00168 Rome, Italy; [3]Fondazione Policlinico Universitario A. Gemelli IRCCS, 00168 Rome, Italy; [4]Section of Neuroscience and Cell Biology, Dept. Experimental and Clinical Medicine, Università Politecnica delle Marche, Ancona 60020, Italy; [5]Center for Neurobiology of Aging, National Institute of Science and Health for Aging (INRCA-IRCCS), Italy; [6]Dept. Pathology and Cell Biology, Taub Institute for Research on Alzheimer's Disease and the Aging Brain, and Dept. Medicine, Columbia University, New York, NY, United States; [7]Foundation for Molecular Medicine, Università Politecnica delle Marche, Ancona 60020, Italy; [8]Oasi Research Institute-IRCCS, Troina, 94018, Italy.

In: Prog Neurobiol. 2021 Nov; 206:102154.

doi: 10.1016/j.pneurobio.2021.102154.

ABSTRACT

The accumulation of amyloid-beta peptide (Aβ) and the failure of cholinergic transmission are key players in Alzheimer's disease (AD). However, in the healthy brain, Aβ contributes to synaptic plasticity and memory acting through α7 subtype nicotinic acetylcholine receptors (α7nAChRs). Here, we hypothesized that the α7nAChR deletion blocks Aβ physiological function and promotes a compensatory increase in Aβ levels that, in turn, triggers an AD-like pathology.

To validate this hypothesis, we studied the age-dependent phenotype of α7 knock out mice. We found that α7nAChR deletion caused an impairment of hippocampal synaptic plasticity and memory at 12 months of age, paralleled by an increase of Amyloid Precursor Protein expression and Aβ levels. This was accompanied by other classical AD features such as a hyperphosphorylation of tau at residues Ser 199, Ser 396, Thr 205, a decrease of GSK-3β at Ser 9, the presence of paired helical filaments and neurofibrillary tangles, neuronal loss and an increase of GFAP-positive astrocytes.

Our findings suggest that α7nAChR malfunction might precede Aβ and tau pathology, offering a different perspective to interpret the failure of anti-Aβ therapies against AD and to find novel therapeutical approaches aimed at restoring α7nAChRs-mediated Aβ function at the synapse.

INTRODUCTION

Alzheimer's disease (AD) is the most common neurodegenerative disorder affecting the elderly, but its intricate pathophysiology has prevented the discovery of effective therapies. The Cholinergic and the Amyloid-β (Aβ) Hypotheses represent the two main etiopathological theories proposed to explain the onset and progression of the disease. The Cholinergic Hypothesis (Appel, 1981) has been supported by several evidences indicating that cholinergic transmission is affected in early AD. Indeed, loss of cholinergic neurons in the nucleus basalis of Meynert, decrease of choline acetyltransferase (ChAT) activity and reduction of nicotinic receptors (nAChRs) have been highly correlated with dementia and its progression (Burghaus et al., 2000; Dickson et al., 1995; Engidawork et al., 2001; Kuhn et al., 2015; Mufson et al., 2007; Strada et al., 1992; Whitehouse et al., 1981).

On the other hand, the Aβ Hypothesis (Hardy and Allsop, 1991) posits that the increase and accumulation of Aβ represent the *primum movens* in AD pathophysiology, responsible of synaptic dysfunction triggering downstream events leading to dementia [reviewed in (Gulisano et al., 2018a)].

A third leading actor in this conundrum is tau, a microtubule-associated protein involved in microtubule assembly and stabilization (Wang and Mandelkow, 2015) whose activity and function is regulated by different

types of post-translational modifications such as phosphorylation, ubiquitination or glycosylation (Martin et al., 2011). Interestingly, tau shares numerous characteristics with Aβ since both proteins form insoluble deposits, i.e. senile plaques and neurofibrillary tangles (NFTs), respectively (Glenner and Wong, 1984; Grundke-Iqbal et al., 1986), and can aggregate in soluble oligomers whose increase has been highly related to AD severity (Fá et al., 2016; Hölttä et al., 2013; Lasagna-Reeves, 2012; Sengupta et al., 2017). According to the classic Aβ Hypothesis, tau hyperphosphorylation is triggered by Aβ but, recently, it has been demonstrated that the two proteins might act independently or concomitantly to impair synaptic plasticity and memory (Fá et al., 2016; Puzzo et al., 2020), probably converging onto common targets such as amyloid precursor protein (APP) (Puzzo et al., 2017; Wang et al., 2017).

Although pre-clinical and clinical data continue to support both the Cholinergic and the Aβ hypotheses, therapeutic strategies aimed at increasing ACh transmission are not able to act as disease-modifying drugs, and approaches expected to cure the disease by decreasing Aβ levels have failed so far. In particular, cholinesterase inhibitors used to treat cognitive symptoms in early to moderate AD patients (Anand and Singh, 2013) do not induce a long-term improvement of cognition and

the treatment is not always effective (Connelly et al., 2005; Lemstra et al., 2007). Also, a variety of nAChR agonists, although promising in preclinical studies, had a limited efficacy when experimented in clinical trials, probably for the rapid nAChRs desensitization (Picciotto, 2000). The outcome of clinical trials with anti-Aβ drugs is even more puzzling since the success obtained in animal models of AD has not been replicated in humans. Active and passive immunization against Aβ as well as the use of drugs aimed at preventing Aβ formation have failed, either not showing efficacy or inducing severe side effects [for a review see (Gulisano et al., 2018a)]. Notwithstanding these discouraging results, anti-Aβ therapies are still under investigation with the intent to treat patients in the very early asymptomatic phase of the disease, or to select Aβ-responders based on a personalized approach. However, the latest unsuccessful trials with the anti-Aβ antibody aducanumab and the BACE inhibitor elenbecestat (see www.alzforum.org) are emblematic and confirmed that the Occam's razor strategy "if Aβ increases in AD patients, clearing Aβ from the brain is the solution" might not be the right choice against AD (Gulisano et al., 2018a; Herrup, 2015; Puzzo et al., 2015).

It is undeniable that AD patients present an increase of Aβ and hyperphosphorylated tau, as well as an impairment of cholinergic

transmission (Gulisano et al., 2018a; Ferreira-Vieira et al., 2016; Selkoe and Hardy, 2016). On the other hand, the observation that in the healthy brain Aβ exerts a physiological function mediated by cholinergic receptors (Gulisano et al., 2019) might offer a new perspective to tackle the intricate pathophysiology of AD (Puzzo et al., 2015). Indeed, a variety of studies have demonstrated that Aβ enhances neurotransmitter release (Gulisano et al., 2019; Koppensteiner et al., 2016; Lazarevic et al., 2017) – for a review see (Puzzo et al., 2015) - and facilitates long-term potentiation (LTP) and memory formation (Garcia-Osta and Alberini, 2009; Morley et al., 2010; Palmeri et al., 2017; Puzzo et al., 2011, 2008; Ricciarelli et al., 2014) through α7nAChRs. In fact, picomolar concentrations of Aβ bind α7nAChRs with high affinity (Wang et al., 2000) exerting an agonist-like action that regulates synaptic function (Dineley et al., 2002; Gulisano et al., 2019; Lawrence et al., 2014; Lazarevic et al., 2017; Mura et al., 2012; Oz et al., 2013; Puzzo et al., 2011, 2008). Therefore, a genetic or pharmacological deletion of α7nAChRs prevents the Aβ-induced enhancement of short- and long-term synaptic plasticity as well as memory (Gulisano et al., 2019; Puzzo et al., 2011, 2008).

These observations inspired this work that aimed at understanding whether the Cholinergic and Aβ hypotheses might be unified looking at

the disease from a different perspective summarized in one question: what are the consequences of a failure of Aβ physiological function when its endogenous receptor, i.e. α7nAChR, does not work properly?

MATERIAL AND METHODS

Animals

We used WT (C57BL/6J; RRID:IMSR_JAX:000664) and α7-KO (B6.129S7-Chrna7tm1Bay/J; RRID:IMSR_JAX:003232) purchased from The Jackson Laboratory. Histology was also performed on hippocampal slices from 3×Tg mice (APPSwe, PS1M146V, and tauP301L) genetically engineered by LaFerla and colleagues at the Department of Neurobiology and Behaviour, University of California, Irvine (Oddo et al., 2003). Colonies were established in the animal facilities at University of Catania and Università Cattolica del Sacro Cuore. Housing conditions were controlled maintaining stable hygrometric and thermic conditions (50%; 21°C ± 1°C) on 12 h light/dark cycle with ad libitum access to food and water.

All the experiments were performed according to the local Institutional Animal care and Use Committee (approval #327/2013-B, #119-2017-PR, #626-2016-PR) and the European Communities Council Directives (2010/63/EU). Experiments complied with the ARRIVE guidelines and

were conducted to minimize animal suffering. To reduce number of animals, we used males for electrophysiological recordings, sex-balanced animals for behavioral experiments, western blotting and ELISA, females for histology and immunohistochemistry. Animals were used at different ages according to our scientific work plan, as detailed in the specific sections.

Electrophysiological field recordings

Extracellular electrophysiological field recordings were performed on 400 mm transverse hippocampal slices as previously described (Gulisano et al., 2019; Puzzo et al., 2017). After cervical dislocation, hippocampi were removed and cut (400 μm thickness) by a manual tissue chopper. Slices were transferred to a recording chamber and perfused (1-2 mL/min) with ACSF (composition in mM: 124.0 NaCl, 4.4 KCl, 1.0 Na_2HPO_4, 25.0 $NaHCO_3$, 2.0 $CaCl_2$, 2.0 $MgCl_2$, 10.0 Glucose) kept at 29 °C and continuously bubbled with an O_2/CO_2 mixture at 95% and 5%. Slices were allowed to recover for 120 minutes prior to recording. Field excitatory postsynaptic potentials (fEPSPs) were recorded in CA1 *stratum radiatum* by a glass capillary filled with ACSF in response to stimulation of the Schaffer collaterals by a bipolar tungsten electrode. Basal synaptic transmission (BST) was assessed by stimulating with a series of increasing voltage pulses (from 5 to 35 V)

to select healthy slices to be used for electrophysiological recordings. For Paired pulse facilitation (PPF) experiments, slices were perfused with the NMDA receptor antagonist (2R)-amino-5-phosphonovaleric acid (APV; 50 μM) for 45 min. Two pulses with a time interval of 10, 20, 30, 40, 50, 100, 200, 500, and 1000 ms were delivered and fEPSP responses were recorded. In another series of experiments, we studied LTP. Baseline was elicited every minute, by stimulating at a voltage able to evoke a response of 35% of the maximum evoked response in BST. After 30-45 min, slices with a stable baseline (slope variation ± 5%) were recorded for 15 min before to induce LTP by a theta-burst (TBS) stimulation, i.e. 3 TBS trains delivered with a 15 seconds inter-train interval with each train consisting in 10 × 100 Hz bursts with 5 pulses per burst with a 200-ms interburst interval, at the test pulse intensity. Recordings were performed and analyzed offline in pClamp 10 (Molecular Devices, Sunnyvale, CA, USA). PPF was plotted as the percentage of the synaptic response of the second against the first delivered stimulus. LTP was plotted as fEPSP (normalized as % of baseline) vs. time (min).

Drugs

In a series of experiments, hippocampal slices were treated with α-bungarotoxin (α-BTX; Sigma-Aldrich, 10 μM), methyllycaconitine

(MLA, Sigma-Aldrich, 10 μM), murine anti-Aβ antibody M3.2 (Covance, catalog #SIG-39155, 2 μg/ml) before tetanic stimulation. MLA was dissolved in DMSO, aliquoted, stored at -20°C. All drugs were diluted in ACSF to the desired final concentration right before electrophysiological experiments, according to previous studies (Gulisano et al., 2019; Puzzo et al., 2008).

Behavioral studies

Fear Conditioning (FC) was performed as previously described (Puzzo et al., 2017). The apparatus consisted in a conditioning chamber, connected to an interface (Kinder Scientific, USA), located in a sound-attenuating box (Campden Inst., UK) with a computer fan installed in one side to provide a background white noise. A webcam mounted on the top of the chamber allowed video recording of the experiment. The floor, made of 36-bar insulated shock grid, was cleaned after each test with 70% ethanol and water. The protocol lasted 3 days. Mice were handled every day for about 5 min before the experiment. During the first day the animal was placed in the conditioning chamber for 2 min prior to the conditioned stimulus (CS) delivery. CS was a tone (2800 Hz and 85 dB) delivered for 30 s. In the last 2 s of the tone, the mouse received a foot shock as an unconditioned stimulus (US) through the electrified grid floor (0.7 mA for 2 s). After the CS/US pairing, the

mouse was left into the chamber for 30 s before to be placed in the home cage. Twenty-four hours after training (day 2), the mouse was placed back in the conditioning chamber for 5 min to evaluate contextual fear memory. Forty-eight hours after training (day 3) animals were placed in the conditioning chamber to evaluate cued fear memory. To this end, a novel context was created by using an acrylic black box with a smooth flat floor sprayed with vanilla odorant. After 2 min (pre-CS test), the mouse was exposed to the same tone used during the training for 3 min (CS test). Freezing (absence of movement except for that needed for breathing) was manually scored during the three days by two different operators and the averaged value was used to perform the analyses.

Novel Object Recognition (NOR) was performed as previously described (Gulisano et al., 2018b). The arena was a white plastic box (50 x 35 x 45 cm) placed on a lab bench. A webcam, connected to the computer, was fixed on the wall. The NOR protocol was performed in 5 days: 3 days of habituation, 1 day of training (T1) and 1 day of testing (T2). Objects were designed by a computer aided design software (Solidworks, France) and printed in polylactic acid with a Prusa i3-inspired 3D printer of our design. After each trial, the box and the objects were cleaned with 70% ethanol and dried with absorbent paper. During the first day (habituation to the arena), the mouse was put into the empty arena and allowed to explore it for 10 min. During the second

and the third day (familiarization with objects), the mouse was put into the arena containing two different objects, randomly chosen among our object collection and changed from day to day, for 10 min. During the fourth day, NOR training session (T1) was performed. The mouse was put into the arena and allowed to explore for 10 min two identical objects placed in the central part of the box, equally distant from the perimeter and the center. During the fifth day (24 h after T1), the mouse underwent the second trial (T2) to test memory retention for 10 min. Mice were presented with two different objects, respectively a "familiar" (i.e. the one used for T1) and a "novel" object. For Novel Object Location (NOL), the mouse was put into the arena and allowed to explore for 10 min two identical objects placed in one side of the box. On the day after, the location of one object was changed and the mouse underwent the T2 for 10 min. For both NOR and NOL experiments, animal exploration - defined as the mouse pointing its nose toward the object from a distance not > 2 cm - was measured in T2. We analyzed: i) percentage exploration of familiar vs. novel object; ii) discrimination (D) index, "exploration of novel object minus exploration of familiar object/total exploration time"; and iii) total exploration time. Mice with a total exploration time < 5 s were excluded from analysis.

Determination of Aβ levels

Briefly, hippocampal tissues from 12M α7 KO and WT mice were sonicated in lysis buffer (10 µl/mg tissue) containing 5M guanidine-HCl/50mM Tris, pH 8.0). Sonicates were then diluted ten- fold with Dulbecco's PBS containing 1× protease inhibitor cocktail (Sigma). Levels of murine Aβ (1–42) were measured by enzyme-linked immunosorbent assay (ELISA) using commercial kits (Thermo Fisher Scientific, cat# KMB3441) following manufacturer's instructions. All assays were performed on F-bottom 96-well plates (Nunc, Wiesbaden, Germany). Tertiary antibodies were conjugated to horseradish peroxidase. Wells were developed with tetramethylbenzidine and measured at 450 nm.

Western Blotting on hippocampal homogenates

Western blot (WB) analysis was performed as previously described (Gulisano et al., 2019; Li Puma et al., 2019) with minor modifications. Whole hippocampi from 9 and 12 months-old WT and α7 KO mice were homogenized in RIPA buffer (Thermoscientific) in the presence of phosphatase and protease inhibitors (Thermoscientific), and sonicated 3 times for 10 minutes on ice. Protein concentrations were determined by Bradford protein assay (Biorad) and 40µg of total proteins were then loaded onto 4-15% Tris-glycine polyacrylamide gels (Biorad) for

electrophoretic separation and then transferred onto 0.45 or 0.22 μm nitrocellulose membranes (Amersham Biosciences, Buckinghamshire,UK). Membranes were blocked for 1-hour, at RT, in either a solution of 5% nonfat dry milk in Tris-buffered saline containing 0.1% Tween-20 before incubation overnight at 4°C with the following primary antibodies: mouse 4G8, that recognizes residues 17–24 of Aβ and the same sequence in APP full length (BioLegend San Diego, California, USA; 1:1000); mouse C-term APP Y188 (Abcam; Cambridge UK; 1:1000); mouse M3.2 (BioLegend; 1:1000), that recognizes residues 10-15 of murine Aβ and the same sequence in APP full length; mouse pTau Ser199 (Thermo fisher Scientific; 1:1000); rabbit pTau Ser396 (SAB; Signalway Antibody Co., Ltd.; 1:1000); rabbit pTau Thr205 (SAB; 1:1000); rabbit pGSK-3β Ser9 (Cell Signaling; 1:1000). Mouse anti-GAPDH (Abcam; 1:5000), rabbit total GSK-3β (Cell signaling; 1:1000) and mouse Tau-5 (Thermo fisher Scientific; 1:1000) were used as loading controls. After incubation with HRP-conjugated secondary antibodies (Cell Signaling Technology) visualization was performed with ECL plus (Amersham Biosciences) using UVItec Cambridge Alliance. Molecular weights for immunoblot analysis were determined using Precision Plus Dual Color Standards (Biorad).

Tissue preparation for microscopy studies

For histology, NeuN and GFAP immunohistochemistry, fresh brains were removed, immersed in 10% formalin for 72 hrs and then transferred in 4% PFA in phosphate buffer until use. For PHF-1 immunohistochemistry, animals were anesthetized by intraperitoneal injection of a cocktail of Zolazepam plus Tiletamine (120 mg/Kg) and Medetomidine (80 μg/Kg), and perfused through the ascending aorta with a flush of physiological saline followed by 4% paraformaldehyde. Brains were removed and post-fixed in 4% PFA in phosphate buffer for 5 days.

Sections (50 μm thickness) were sequentially cut with a Vibratome within 2.350 and 1.725 mm lateral range and processed for immunohistochemistry or histological stains.

Congo Red stain

Congo Red stain was performed as previously described (Wilcock et al., 2006). Sections were incubated for 20 min in a fresh prepared alkaline saturated NaCl solution. Briefly, NaCl was added to an 80% ethanol solution while stirring, until the formation of an undissolved NaCl layer (about 5 mm thick) and 1% NaOH 1 M was added before use. Sections were then incubated in 0.2 % Congo Red solution (Sigma-Aldrich) for 30 min and rinsed five times in 95% ethanol.

Bielschowsky stain

Bielschowsky silver stain was performed as suggested by the manufacturer (Bielschowsky silver stain kit, VitroVivo Biotech, cat.#VB-3015). Briefly, sections were incubated in pre-warmed 40°C Silver Nitrate solution for 18 minutes, washed in distilled water and then incubated with silver ammonium solution at 40°C for 30 minutes. Subsequently, slices were placed in the developing solution for 75 seconds and in 1% ammonium hydroxide solution for 60 seconds. Slices were then washed in distilled water and incubated in 5% sodium thiosulfate solution for 5 minutes.

Immunohistochemistry

Antibodies. The following primary antibodies were used: mouse anti-PHF-1 (1:50) detecting tau Ser396/Ser404 phosphorylation sites (generous gift of Dr. Peter Davies); mouse anti-NeuN (1:100; Millipore, cat.#MAB377); mouse anti-GFAP (1:350; Sigma-Aldrich, cat.#G3893).

Immunofluorescence. Immunofluorescence was performed as previously described (Melone et al., 2019). Sections were incubated in 10% NDS (1 hr), followed by a solution containing PHF-1 primary antibody overnight at RT. Sections were rinsed in Tris (0.5 M buffered

saline, pH 7.4) incubated first in 10% NDS (15 min), and then in a solution containing the secondary antibody (Alexa Fluor 488, 1:230; Jackson) for 2 hrs at RT. Sections were washed in Tris, mounted, and coverslipped with propyl-gallate 0.1M in glycerol-PBS solution (9:1). Omission of the primary antibodies in sections from each experimental group resulted in a lack of specific staining in the corresponding channel (negative control). To quench lipofuscin autofluorescence, at the end of immunofluorescence protocols, sections were incubated for 5 min in 0.1% Sudan Black dissolved in 70% alcohol. To minimize procedural variability, sections from all experimental groups, were exposed to immunofluorescence procedure in parallel.

Immunoperoxidase. Immunoperoxidase was performed as previously described (Melone et al., 2019). For both NeuN and GFAP optimal detection (i.e. immunoreactivity against the background level) was determined by testing different conditions (e.g., inclusion or exclusion of detergents, and a range of dilutions for primary antibodies) in a set of pilot trials. Sections were treated with H_2O_2 (1% in Tris for 25 min) to remove endogenous peroxidase activity, rinsed in Tris and then incubated in 10% NGS (1 hr) followed by a solution containing NeuN or GFAP primary antibodies (overnight at RT). Sections were rinsed in Tris and incubated first in 10% NGS (15 min) and then in a solution containing biotinylated secondary antibody (1:180; Jackson) for 2 hrs at

RT. Subsequently, they were rinsed in Tris, incubated in avidin-biotin peroxidase complex (ABC Elite PK6100, Vector), washed in Tris, and incubated in 3,3'diaminobenzidine tetrahydrochloride (DAB; 0.05% in 0.05 M Tris buffer, pH 7.6 with 0.03% H_2O_2). Then, sections were washed, mounted, and coverslipped with dpx mounting medium. Method specificity was assessed by substituting NeuN and GFAP primary antibodies with Tris, resulting in the absence of immunoreactivity. To minimize procedural variability, sections from all experimental groups, were exposed to immunoperoxidase procedure in parallel.

Data collection and analysis.

For confocal microscopy, PHF-1 immunolabeled sections were scanned with a Leica SP2 TCS-SL microscope. For 20x of CA1, microscopical fields were acquired as 512 x 512 pixel images (pixel size of 750 nm) with pinhole 1.4 Airy unit, and to improve signal/noise ratio, 4 frames of each image were averaged. For quantitative microscopy of stratum oriens (so), stratum pyramidalis (sp), and stratum radiatum (sr), microscopical fields were acquired as 512 x 512 pixel images (pixel size of 465 nm) with a planapo 63 × objective (numerical aperture 1.4) and pinhole 1.0 Airy unit. To improve signal/noise ratio, 4 frames of each image were averaged. CA1 microscopical fields were randomly selected (8 microscopical fields/layer/4 sections from 2 animals for each

experimental group). To avoid the influence of the acquisition parameters (i.e. photomultiplier gain and offset) on fluorescence intensity, all microscopical fields from all conditions were scanned and acquired with the same setting. As previously described (de Vivo, 2010), photomultiplier gain and offset were set so that the brightest pixel was just slightly below saturation, and the offset such that the darkest pixels were just above zero. To avoid the effects of the surface-depth gradient on immunodetection (Melone et al., 2005), all microscopical fields were acquired at a z-axis level yielding the maximum brightness of immunopositive profiles (de Vivo, 2010; Melone et al., 2005).

For quantitation of intensity, randomly selected subfields of 32 × 32 μm from the original microscopic fields (Melone et al., 2019) (32 for each experimental group/layer; with a total of 96 subfields for each condition) were used.

Optimal visualization of immunoreactivity was achieved by setting the threshold value to the mean pixel value over the field under study in WT and α7 KO groups (Melone et al., 2005). Intensity of threshold subfields was calculated by Image J (Schneider et al., 2012). Number and mean size of immunoreactive puncta of each subfield were obtained by transforming images to binary mode and calculated using Image J (Bozdagi et al., 2000; Bragina et al., 2006; Schneider et al., 2012). For PFH-1 positive neuronal-like cells, intensity of 2-4 regions of interested

(ROI) within the cytoplasm, was calculated (area between 30 and 40 μm^2) (de Vivo, 2010). For the intensity of PHF-1 positive dendritic-like profiles, value was extracted by plotting intensity pixel values along the major axis of profiles using Image J (Melone et al., 2019).

For light microscopy studies, hippocampus and CA1 of Congo Red and Bielschowsky stained sections were acquired at 4 × and 20 × and at 4 × and 40 × original magnifications, respectively (4-6 sections/2 animals for each experimental group). For NeuN and GFAP studies, hippocampi of immunostained sections were acquired at 4 ×, and at 40 × for quantitative studies in so, sp, sr. NeuN and GFAP positive cells were manually identified, and to estimate the density of cells, the area of microscopical fields (18 microscopical fields/layer/6 sections from 3 animals for each experimental group; with a total of 54 fields for each condition) was calculated by Image J.

Statistics

All experiments were performed by researchers blind with respect to treatment. All data were expressed as mean ± standard error mean (SEM). Statistical analysis was performed by using different tests, based on preliminary analyses of normal distribution. ANOVA for repeated measures was used to analyze PPF and LTP (120 minutes of recording after tetanus). One-way ANOVA with Bonferroni's post-hoc correction

was used for PPF single time intervals. Two-tailed t-test was used for analyses of behavioral parameters, NeuN and GFAP immunohistochemistry. One sample t-test was used to compare D with zero in NOR and NOL. Given the non-normal distribution of data, assessed by D'Agostino & Pearson normality, we used Mann-Whitney test for ELISA and PHF-1 immunoreactivity; Mann-Whitney and Kruskal-Wallis One Way tests for WB experiments. Systat 9, Graphpad Prism 8, and Sigmaplot 14 software were used for statistical analyses. The level of significance was set at $P < 0.05$.

RESULTS

Synaptic plasticity and memory are impaired in 12-month-old α7 KO mice

The role of α7nAChRs in cognitive functions (Picciotto, 2000) relies on their ability to modulate synaptic function through the regulation of glutamate release (Cheng and Yakel, 2015). Thus, we first evaluated whether their genetic deletion affected paired-pulse facilitation (PPF), a form of short-term plasticity that might reflect release probability. PPF resulted unchanged in slices from α7 KO mice at 3, 6 and 9 months of age, but was increased at 12 months (M) compared to slices from age-

matched WT animals (Figure 1A). We then investigated long-term plasticity by recording LTP at hippocampal CA3-CA1 synapses. Potentiation was normal in hippocampal slices from animals at 3M and 6M in both genotypes (Figure 1B). An initial deficiency of LTP was present at 9M, even if it was less pronounced in respect to the impairment found at 12M (Figure 1C). Thus, we chose to conduct the rest of this study on 12M animals.

The observation that release probability and plasticity were impaired in an age-dependent manner, prompted us to study different types of memory known to be impaired in AD (Puzzo et al., 2014a). Evaluation of contextual fear memory 24 hrs after training showed that the amount of freezing behavior was impaired in 12 M α7 KO compared to WT controls (Figure 1D), whereas no differences were found in amygdala-dependent cued fear memory (Figure 1E).

We then evaluated recognition and spatial memory through Novel Object Recognition (NOR) and Novel Object Location (NOL) tasks. Analyses of Discrimination index (D = exploration of novel object minus exploration of familiar object/total exploration time) showed an impairment of memory in 12 M α7 KO (Figure 1F). Comparison of D with zero confirmed that only WT mice were able to discriminate between the old and the novel object or its different spatial location. No

differences were detected in total exploration time between the two groups of mice (Figure 1G).

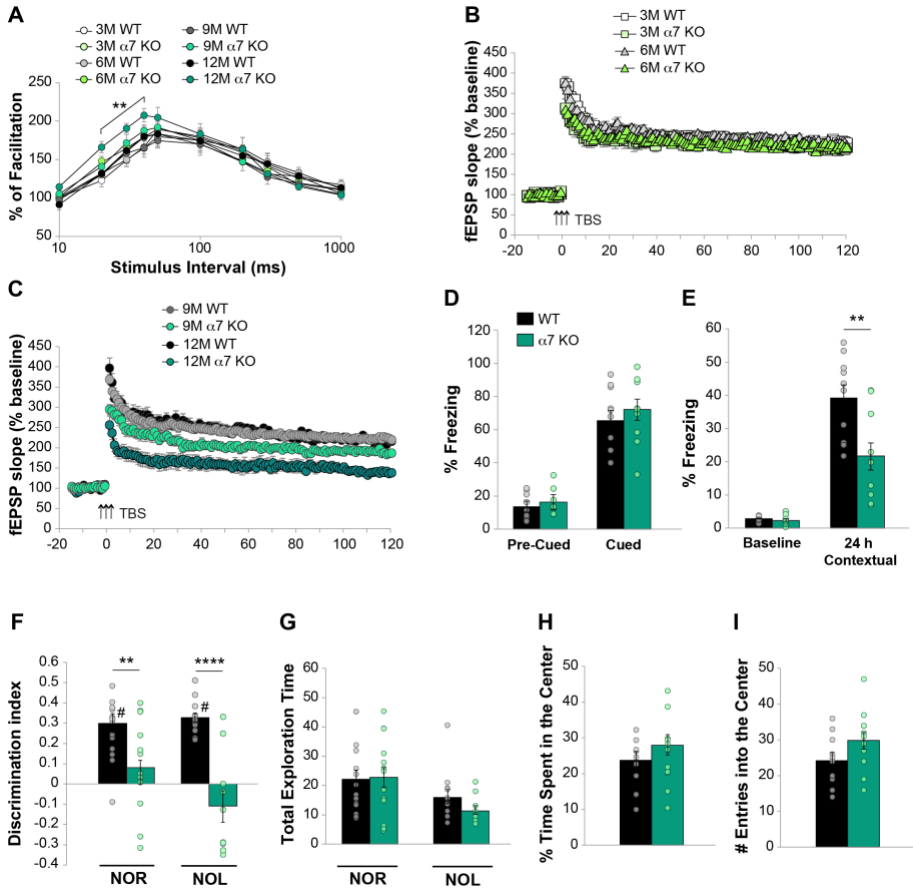

Figure 1 – Synaptic plasticity and memory are impaired in 12-month-old α7 KO mice.

A) PPF changed in slices from 12M α7 KO but was unaltered at other ages (P = 0.010 in 12M α7 KO vs. WT; N = 9 slices from 6-7 3-month-old animals; N = 7 slices from 5-6 animals at other ages). **B)** LTP was normal in slices from α7 KO at 3 M and 6 M (P > 0.05 compared with age-matched WT). TBS = theta-burst stimulation. N = 7 slices from 5-6 animals for each condition, here and in C. **C)** LTP was impaired in slices from 12 M α7 KO ($F_{(1,12)}$ = 35.1837, P < 0.0001) compared with age-matched

WT. A slight impairment of LTP was present at 9M ($F_{(1,12)}$ = 10.883, P < 0.006 vs. 9 M WT; $F_{1,12}$ = 12.212, p = 0.004 vs. 12 M α7 KO). **D)** Contextual fear memory was impaired in 12 M α7 KO mice ($t_{(18)}$ = 3.06, P = 0.007; N = 10/10. **E)** No differences were detected in cued fear memory ($t_{(18)}$ = 0.722, P = 0.479). **F)** Discrimination index (D) was impaired in 12 M α7 KO mice (NOR: $t_{(27)}$ = 2.92, P = 0.007; N = 15 WT/12 α7 KO; NOL: $t_{(27)}$ = 5.882, P < 0.0001; N = 12 WT/10 α7 KO). WT but not α7 KO mice were able to learn (P < 0.0001 D vs. zero). **G)** Total exploration time was similar among genotypes (NOR: $t_{(27)}$ = 0.143; P = 0.887; NOL: $t_{(20)}$ = 0.543; P = 0.887). **H-I)** No differences were present in exploratory and anxiety-like behavior tested by the open field task ($t_{(20)}$ = 1.081, P = 0.293 for % time spent into the center; $t_{(20)}$ = 1.632, P = 0.118 for number of entries into the center; N = 10 WT/12 α7 KO). *P < 0.05, **P < 0.01, ****P < 0.0001, #P ≠ 0. Data expressed as mean ± SEM.

Open field test showed that locomotor activity and anxiety-like behavior were not affected (Figure 1H,I), suggesting that the impairment of memory found in α7 KO was not due to motor or motivational defects. Thus, α7 KO mice showed an age-dependent impairment of hippocampal synaptic plasticity and memory.

The lack of endogenous α7nAChRs induces an increase of Aβ production and APP expression

The impairment of synaptic plasticity and memory found in α7 KO mice might be due to the sole alteration of cholinergic transmission. In fact, the impairment of LTP was also present in hippocampal slices from wild type mice acutely treated with drugs inhibiting α7-nAchRs, such as α-BTX and MLA (Supplementary Fig. 1). However, this scenario is also

compatible with the hypothesis that the cognitive phenotype is triggered by the failure of Aβ-mediated synaptic homeostasis. Indeed, in a situation in which Aβ is not able to adequately exert its physiological functions through α7nAChRs, a feedback mechanism might occur, inducing a compensatory increase of Aβ production overtime. High levels of Aβ might in turn be responsible for the impairment of synaptic plasticity and memory found in α7 KO mice. To test this hypothesis, we evaluated whether the age-dependent damage of LTP and memory was paralleled by changes in Aβ production. We performed the enzyme-linked immunosorbent assay (ELISA) for mouse $A\beta_{42}$ on hippocampal homogenates from 12M α7 KO and WT mice and confirmed that the deletion of α7nAChR induced a significant increase of the peptide levels (Figure 2A). Because Aβ is produced by APP cleavage, we next verified whether this feedback mechanism acted through a modification of APP expression. We found an increase of APP full-length expression in 12M α7 KO hippocampi (Figure 2B,C) that was confirmed by 3 different antibodies: Y188, 4G8, and M3.2. Furthermore, 4G8 (recognizing both human and murine Aβ) and M3.2 (specific for murine Aβ) allowed detecting a 24 KDa band, presumably corresponding to soluble aggregates (i.e., pentamers), that was significantly increased in α7 KO hippocampi (Figure 2D,E). However, Congo Red staining did not reveal the presence of hippocampal senile plaques (Figure 2F).

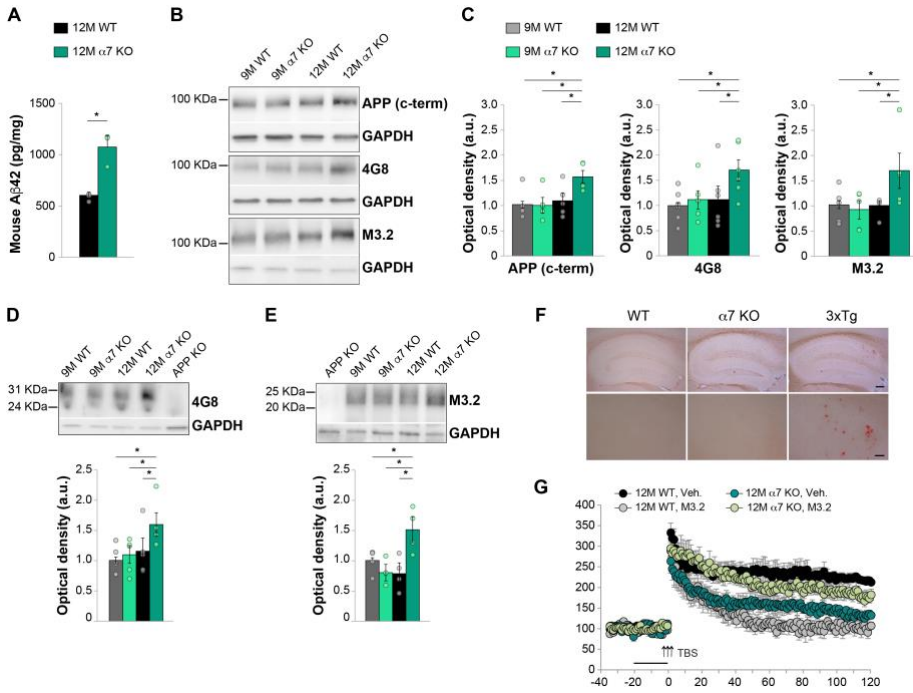

Figure 2 - Aβ levels and APP expression increase in 12M α7 KO mice.

A) ELISA revealed an increase of Aβ42 levels in hippocampal homogenates from α7 KO compared with WT mice (Mann-Whitney Rank Sum Test, P = 0.036, N = 3 and 4 animals, respectively). **B)** Western blot analysis comparing the expression of APP in hippocampi from WT and α7 KO animals at 9M and 12M assessed by 3 different antibodies, i.e. 4G8, Y188 and M3.2. **C)** Bar graphs showing the results of the densitometric analysis of the Western blots reported in (B) indicated a significant increase of APP expression in hippocampi from 12M α7 KO mice compared to WT (Kruskal-Wallis One Way Analysis of Variance on Ranks, P = 0.038 for Y188, N = 5 for each condition; P = 0.040 for 4G8, N = 6 for each condition and P = 0.046 for M3.2; N = 5 for each condition). GAPDH expression level was used as loading control here, in D and E. **D)** An increase of a ≈ 25 kDa band, presumably representing Aβ oligomers, was detected in 12M α7 KO hippocampi either when using the 4G8 (Kruskal-Wallis One Way Analysis of Variance on Ranks, P = 0.035, N = 5 for each condition) or **E)** the M3.2 antibody, specific for murine Aβ (Kruskal-Wallis One Way Analysis of Variance on Ranks; P = 0.030, N = 4 for each consition). APP KO mice

were used as negative controls both in D and E. **F)** No plaques were detected using Congo red staining in α7 KO hippocampal slices. Hippocampal slices from 3×Tg mice are used as a positive control. Upper panels: 4 × magnification, scale bar 100 μm; Lower panels: 20 × magnification, scale bar 50 μm. **G)** The anti-Aβ antibody M3.2 rescued LTP in 12 M α7 KO hippocampal slices ($F_{(1,12)}$ = 7.063, p = 0.021 vs. α7 KO vehicle-treated slices; N = 6/8 from 5-6 animals), whereas it impaired LTP in WT slices ($F_{(1,11)}$ = 21.730, p = 0.001 vs. WT vehicle-treated slices; N = 7/6 from 5-5 animals). TBS = theta-burst stimulation. *P < 0.05. Data expressed as mean ± SEM.

To further confirm that the increase of Aβ contributed to the impairment of synaptic plasticity found in hippocampal slices from 12M α7 KO mice, we investigated whether neutralization of Aβ by a treatment with the murine anti-Aβ antibody M3.2 rescued LTP. We found that M3.2 (2μg/ml for 20 min before tetanus) restored LTP in slices from 12M α7 KO mice (Figure 2G). Notably, the same treatment impaired LTP in slices from wild type mice (Figure 2G).

Overall, these findings suggest that the absence of α7nAChRs triggers an age-dependent increase of soluble Aβ and APP, which parallels the impairment of synaptic plasticity and memory, with no plaque formation.

The lack of endogenous α7nAChRs triggers tau hyperphosphorylation through GSK-3β modulation

Tau hyperphosphorylation and accumulation of paired helical filaments (PHF) leading to NFTs formation represent hallmarks of AD brain

lesion highly correlated with cognitive impairment (Iqbal et al., 2005). Here, we first investigated whether α7nAChRs deletion modified tau phosphorylation at different residues known to be associated with neurodegeneration and AD, i.e., Ser 199, Ser 396, and Thr 205 (De Chiara et al., 2019; Neddens et al., 2018). Western blotting analysis showed a significant increase of pTau expression at Ser 199 and Ser 396 (Figure 3A), and Thr 205 (Figure 3B) in hippocampi from 12M α7 KO mice compared to WT. In a series of complementary experiments, we found that p-Tau (Ser 199 and Thr 205) was not modified in hippocampi from 9M α7 KO mice compared with age-matched WT (Supplementary Figure 2).

We then turned our attention onto glycogen synthase kinase-3β (GSK-3β), considered a crucial molecule in AD, being a possible molecular link between Aβ and tau pathology (Llorens-MarÃ-tin et al., 2014). In particular, we focused on GSK-3β auto-inhibitory phosphorylation site on Ser 9 whose dysregulation induces an abnormal activation of GSK-3β leading, in turn, to tau hyperphosphorylation (Hanger and Noble, 2011). We found a decrease in Ser 9 phosphorylation of GSK-3β in hippocampi from α7 KO mice (Figure 3C) that paralleled the increase of tau phosphorylation.

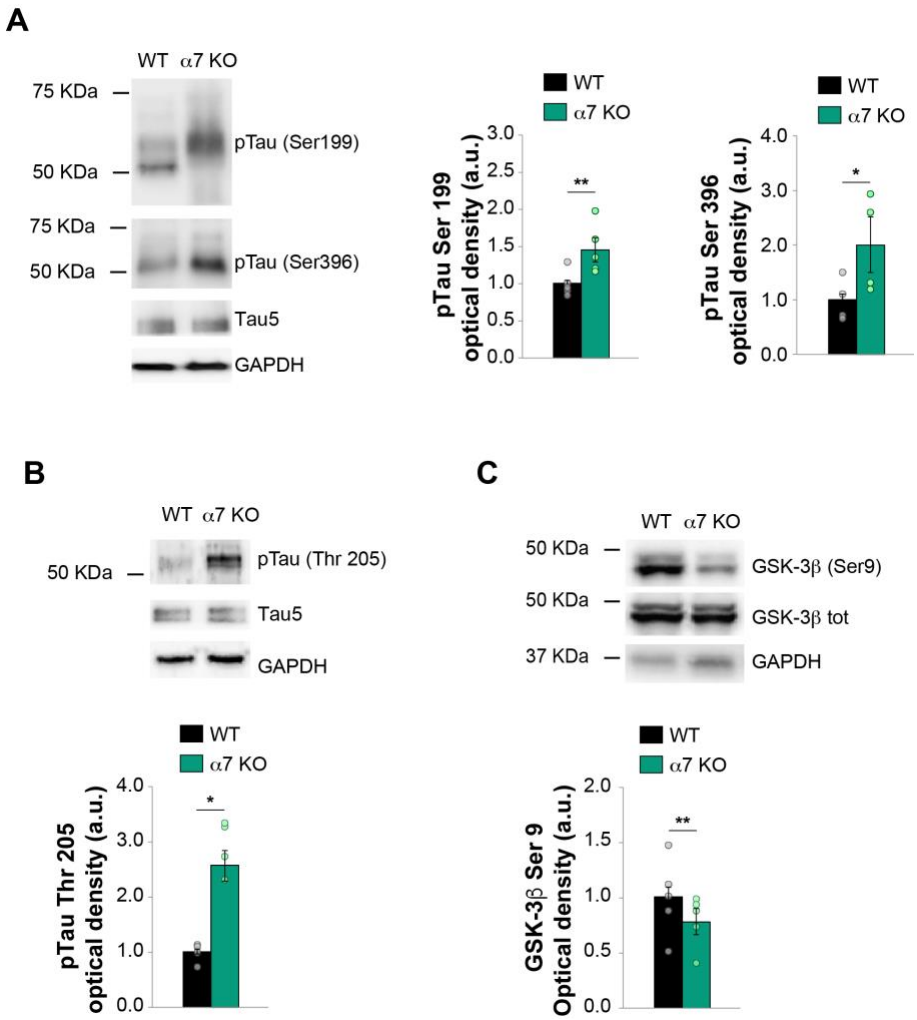

Figure 3 – Tau is hyperphosphorylated and GSK-3β dysregulated in hippocampi from 12M α7 KO mice.

A) Representative images of WB assay (cropped images based on MW here and in the following panels) for the expression of phosphorylated tau (pTau) at Ser 199 and at Ser 396 performed on hippocampi from 12M WT and α7 KO mice. On the right, bar graphs showing the increase of pTau Ser 199 and Ser 396 expression in hippocampi from α7 KO compared to WT (Mann-Whitney Rank Sum Test for pTau Ser 199: P = 0.008; N = 5/5; for pTau Ser 396: P = 0.028; N = 4/4). Tau5, specific for murine tau, was used to normalize pTau densitometric signal from WT and α7 KO tissues. GAPDH was used as loading control. **B)** WB essay for the expression of pTau at Thr

205. Lower panel, bar graph showing the increase of the expression of pTau at Thr 205 in hippocampi of α7 KO compared to WT (Mann-Whitney Rank Sum Test, P = 0.028; N = 4/4). **C)** WB images showing the expression of GSK-3β phosphorylated at Ser9, total GSK-3β and GAPDH as loading control. Lower panel, bar graph showing the decrease of GSK-3β Ser 9 in α7 KO hippocampi compared to WT (Mann-Whitney Rank Sum Test; P = 0.007; N = 5/5). *P < 0.05, **P < 0.01. Data expressed as mean ± SEM.

The lack of endogenous α7nAChRs causes tau accumulation and deposition in neurofibrillary tangles

We then investigated the presence of PHFs in hippocampal slices, suggestive for a more advanced stage of pathology. We used a PHF-1 antibody (a generous gift of Dr. Peter Davies) that detects Ser396/Ser404 phosphorylation sites, known to be associated with NFT formation (Götz et al., 2001).

Confocal microscopy revealed an increased PHF-1 immunoreactivity (IR) in the CA1 area of 12M α7 KO hippocampi compared to WT (Figure 4A), particularly evident in the CA1 *stratum pyramidalis* and *stratum radiatum* (Figure 4B). Analyses of PHF-1 IR revealed an increase of mean size positive puncta in the *stratum oriens*, neuronal-like cells in the *stratum pyramidalis*, and dendritic-like profiles in the *stratum radiatum* (Figure 4C-E). Consistently, Bielschowsky silver staining detected an increase of intraneuronal NFTs in the hippocampus and neocortex from α7 KO (Figure 4F).

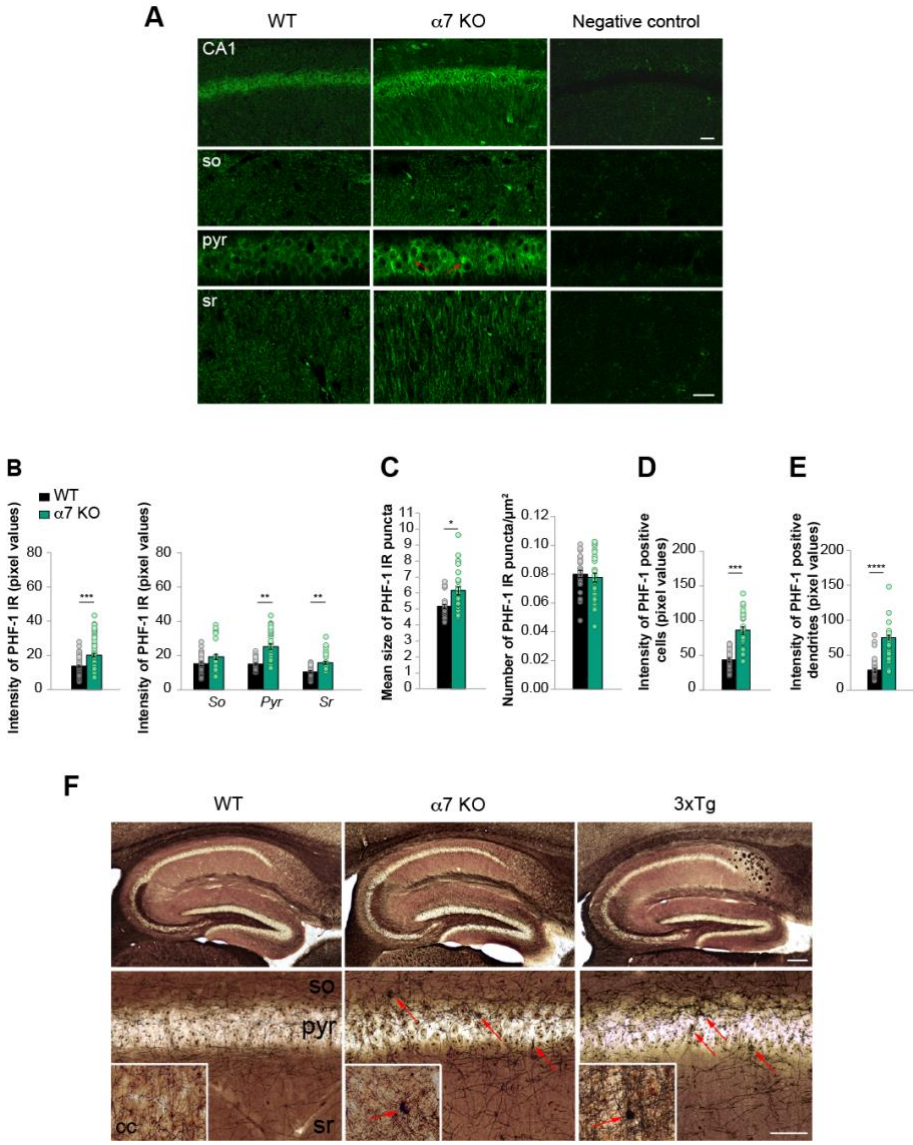

Figure 4 – PHFs immunoreactivity and neurofibrillary tangles in hippocampi from α7 KO mice.

A) Representative confocal images of PHF-1 immunofluorescence in the hippocampus from 12-15M WT and α7 KO mice. Negative control represents WT sections treated with the same immunofluorescence protocol, omitting the primary antibody. Upper panels: CA1 area, 20 ×, scale bar 50 μm; Lower panels: stratum oriens (so), stratum

pyramidalis (pyr) and stratum radiatum (sr), 60 ×, scale bar 25 μm. Red arrows indicate intraneuronal accumulations. **B)** Bar graphs showing the increase of PHF-1 immunoreactivity (IR) in hippocampi from α7 KO (Mann-Whitney test P = 0.0002). On the right, analyses of PHF-1 IR in so, pyr and sr. **C)** Bar graphs showing puncta staining analyses in so. Positive puncta mean size increased in α7 KO (P = 0.0113), whereas number of puncta was not modified (P > 0.99). **D)** Bar graphs showing analyses of cytoplasmic PHF-1 IR intensity in the pyr. Positive cells increased in α7 KO (P = 0.0002). **E)** Bar graphs showing an increase of PHF-1 IR intensity in apical dendrites of the sr in α7 KO (P < 0.0001). N = 32 subfields (4 sections from 2 animals/genotype). **F)** Bielschowsky silver staining showed the presence of silver-positive NFTs in α7 KO. Hippocampi from 3×Tg mice were used as positive control. Representative inserts showing a clear identifiable NFT in α7 KO and 3×Tg cerebral cortex (cc). Red arrows indicate intraneuronal accumulation. Upper panels: 4 ×, scale bar 100 μm; Lower panels: CA1 area, 40 ×, scale bar 50 μm; Inserts: 40 ×, scale bar 50 μm. *P < 0.05, **P < 0.01, ***P < 0.001, ****P < 0.0001. Data expressed as mean ± SEM.

Overall, these data indicated that α7 KO mice present a dysregulation of tau phosphorylation resulting in an increase of PHFs and NFTs.

The lack of endogenous α7nAChRs induces neuronal loss and increases GFAP-positive astrocytes

Besides Aβ and tau pathology, because hippocampal neuronal loss highly correlates with cognitive deficits and AD progression (Donev et al., 2009), we evaluated whether α7 KO mice presented neuronal depletion. We found a decrease in the mean number of NeuN positive cells in hippocampal slices from α7 KO compared to WT controls (Figure 5A).

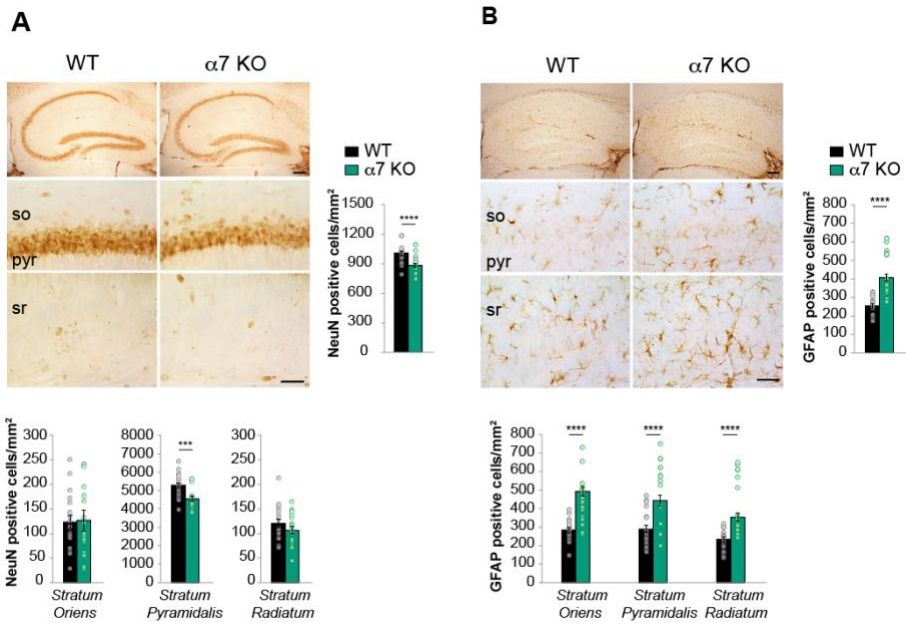

Figure 5 – Neuronal loss and increase of astrocytes in α7 KO hippocampi.

A) Representative images of NeuN staining in the hippocampal formation of 12-15 M WT and α7 KO mice. Upper panels: 4 ×, scale bar 100 μm; Middle panels: stratum oriens (so) and stratum pyramidalis (pyr) of CA1 area, 40 ×; Lower panels: stratum radiatum (sr), 40 ×, scale bar 50 μm. On the right, bar graph showing an increase of neuronal loss in hippocampi from α7 KO ($t_{(34)}$ = 3.938; P < 0.0001). On the bottom, analyses of CA1 layers evidenced a significant loss of neurons in the stratum pyramidalis of α7 KO hippocampi ($t_{(34)}$ = 3.617; P = 0.001). No differences were detected in stratum radiatum and stratum oriens. N = 6 sections from 3 animals/genotype. **B)** Representative images of GFAP staining in the hippocampus of 12-15 M WT and α7 KO mice. Upper panels: 4 ×, scale bar 100 μm; Middle panels: so and pyr of CA1 area, 40 ×; Lower panels: sr, 40 ×, scale bar 50 μm. On the right, bar graph showing an increase of GFAP positive cells in hippocampi from α7 KO animals compared to WT ($t_{(34)}$ = 5.874; P < 0.0001). On the bottom, analyses of CA1 layers showed an increase of astrocytes in the three layers: stratum oriens ($t_{(34)}$ = 4.786; P < 0.0001), stratum pyramidalis ($t_{(34)}$ = 4.621; P < 0.0001), and stratum radiatum ($t_{(34)}$ = 4.321; P < 0.0001). N = 6 sections from 3 animals/genotype. ***P < 0.001, ****P < 0.0001. Data expressed as mean ± SEM.

A statistically significant decrease was found in the *stratum pyramidalis* and *stratum radiatum*, whereas no differences were detected in the *stratum oriens* (Figure 5A).

Finally, because either the increase of Aβ and tau as well as the loss of neuronal function influence astrocytes (González-Reyes et al., 2017; Phatnani and Maniatis, 2015), we evaluated GFAP (Glial Fibrillary Acidic Protein) positive astrocytes. Quantification of GFAP-positive cells revealed an increase that was significant in all the hippocampal strata, i.e. *oriens*, *pyramidalis* and *radiatum*, in hippocampi from α7 KO compared to WT mice (Figure 5B).

Taken together, these findings suggest that α7 KO present a decrease of neurons and an increase of astrocytes in the hippocampus.

DISCUSSION

In this work we showed that genetic deletion of α7nAChRs is sufficient to induce an AD-like pathology characterized by synaptic plasticity and memory impairment, Aβ and tau neuropathology, neuronal loss, and increase of GFAP-positive astrocytes.

We used the α7 KO mouse model that does not overproduce Aβ due to manipulations of genes directly involved in its production (i.e., APP or presenilins). This allowed us to avoid one of the main limitations of research in the AD field, which is the use of models inspired by rare forms of inherited early onset Familial Alzheimer's disease (FAD) characterized by a genetic-driven rise of Aβ production (Hardy et al., 1998). Indeed, FAD only accounts for the 2-3% of AD cases (Qiu et al., 2009), whereas the prevalent form of dementia is sporadic AD, which affects the elderly and it is not associated with genetic mutations directly leading to an increase of Aβ burden (Herrup, 2015).

We first focused on synaptic plasticity, whose disruption is thought to be the early pathogenetic event in AD (Selkoe, 2002). α7 KO mice presented an age-dependent impairment of short- and long-term plasticity, as indicated by the increase of PPF and the reduction of LTP, resulting in memory loss. Previous studies already showed that the deletion of α7nAChRs caused synaptic plasticity deficits, even if at a later age (22-24 months) with respect to our study (Ma et al., 2014). Our results are consistent with data indicating that, at physiological concentrations, Aβ requires α7nAChRs to sustain synaptic functions (Lawrence et al., 2014; Mura et al., 2012; Puzzo et al., 2011, 2008), both at pre-synaptic level, where it enhances release probability (Gulisano et

al., 2019; Koppensteiner et al., 2016; Lazarevic et al., 2017), and at post-synaptic level, where it is needed for long-lasting LTP and memory formation (Garcia-Osta and Alberini, 2009; Gulisano et al., 2019; Morley et al., 2010; Palmeri et al., 2017; Puzzo et al., 2011).

α7nAChRs mediate the raise of pre-synaptic intracellular Ca^{2+} levels during neuronal activity, thus modulating glutamate release, synaptic transmission, and cognitive function (Picciotto, 2000). Hence, it was crucial to exclude that the observed α7 KO phenotype was exclusively due to the failure of cholinergic transmission, as it occurred after an acute pharmacological inhibition of α7nAchRs [for a review see (Yakel, 2014)]. Our finding that the impairment of synaptic plasticity and memory is paralleled by the increase of APP expression and Aβ levels suggests that the loss of α7nAChRs might trigger a chain of events through a negative feedback mechanism aimed at restoring calcium entry inside neurons by stimulating Aβ production. This was further confirmed by the rescue of LTP in slices from α7 KO mice treated with the anti-Aβ antibody M3.2. Notably, treatment with the same antibody impaired LTP in slices from wild type mice, as previously demonstrated (Garcia-Osta and Alberini, 2009; Morley et al., 2010; Puzzo et al., 2011), confirming that caution is needed when proposing treatments

aimed at decreasing Aβ levels, since the protein is physiologically needed to ensure synaptic function.

Our hypothesis that α7nAChRs deletion drives Aβ elevation is supported by extensive literature demonstrating a tight link between α7nAChRs and Aβ (Oz et al., 2013). Aβ and α7nAChRs co-localized inside neurons or at extracellular level in senile plaques (Nagele et al., 2002; Wevers et al., 1999) and high Aβ levels induced α7nAChR alterations (Dineley et al., 2002, 2001; Dougherty et al., 2003; Li et al., 2011; Liu et al., 2001). The lack of α7nAChRs accelerated the pathology in the Tg2576 mouse model of AD ensuing decrease of hippocampal ChAT activity paralleled by a pronounced loss of pyramidal neurons (Hernandez et al., 2010). In 3×Tg mice a reduction of α7nAChRs was found in the same brain regions where intraneuronal Aβ42 accumulation occurred, determining cognitive deficits (Oddo et al., 2005). Interestingly, an increase of α7nAChR-specific antibodies, able to induce Aβ accumulation and memory impairment in animal models (Lykhmus et al., 2015), has been found in plasma samples of early-onset AD patients (Koval et al., 2011).

About the mechanisms underlying α7nAChR regulation of Aβ production, few studies focused on the ability of α7nAChRs activation to reduce Aβ synthesis by shifting APP processing towards the non-

amyloidogenic pathway (Mousavi and Hellström-Lindahl, 2009; Nie et al., 2010; Qi et al., 2007), for example by regulating γ-secretase activity and expression (Nie et al., 2010). This enhanced the production of soluble APPα (sAPPα) recognized for its neuroplasticity and neuroprotective functions able to counteract Aβ neurotoxicity [for reviews (Buckingham et al., 2009; Hefter et al., 2020)]. Hence, the deletion of α7nAChRs might determine an aberrant APP processing leading to Aβ elevation. However, we cannot exclude that the increase of APP expression found in aged α7 KO mice was due to different mechanisms not involving a direct interaction between α7nAChRs and APP. In fact, since the lack of α7nAChRs prevents Aβ to exert its physiological function, this might cause the unbalance of several neuroplasticity pathways (Gulisano et al., 2019) that, in turn, are known to influence APP expression and processing. See for example how cGMP levels regulate Aβ production during LTP by acting on BACE-1/APP approximation (Palmeri et al., 2017).

The increase of APP we found in α7 KO mice raises another series of considerations. Its occurrence in adult age might explain why α7 KO mice do not present a peculiar phenotype until the age of 12 months. Even if it is beyond the scope of this work, we can speculate that in an initial phase other nAChR subtypes, i.e., α4β2nAChRs, might

compensate for the absence of α7nAChRs, a common phenomenon in genetically modified animal models. Moreover, it is conceivable that homeostatic changes occur overtime until a critical stage, when compensation is no longer possible. This trend mirrors the course of the disease since synaptic disruption is thought to begin long before the clinical manifestation. Nevertheless, even if in α7 KO mice the increase of APP is aimed at restoring Aβ function, it eventually leads to a vicious cycle in which Aβ levels reach high concentrations becoming extremely neurotoxic.

In this context, APP might exert a double role as it acts as Aβ precursor and cell surface receptor (Deyts et al., 2016) able to bind Aβ and tau (Fogel et al., 2014; Lorenzo et al., 2000; Shaked et al., 2006; Takahashi et al., 2015; Van Nostrand et al., 2002). APP enhances tau phosphorylation (Greenberg et al., 1994) and serves as a common target for extracellular oligomers of Aβ and tau to enter neurons and impair LTP and memory (Puzzo et al., 2017; Wang et al., 2017). Hence, increased APP expression might contribute to worsening the course of the disease with different mechanisms.

As for the interplay between α7nAChRs and tau in AD, results are conflicting (Rubio et al., 2006). Although some works have shown that the increase of α7nAChRs stimulates tau phosphorylation (Ren et al.,

2007; Wang et al., 2003), most studies showed that a reduction of α7nAChRs is concomitant with tau hyperphosphorylation in brains of AD patients or animal models (Wu et al., 2010). Here, we found that α7nAChRs deletion induced an increased age-dependent expression of tau phosphorylated at Thr 205, Ser 199 and Ser 396, residues known to be involved in AD onset and progression. In particular, pTau at Thr 205 seemed to be involved in tau spreading, as demonstrated in Tg/hTau mice injected with tau (Miao et al., 2019) and, together with pTau at Ser 199, has been correlated with Braak stage V/VI in patients (Neddens et al., 2018). As for pTau at Ser 396, it is considered a key marker of tau hyperphosphorylation since it increases in CA1 pyramidal neurons of AD patients and is crucial for PHFs formation (Furcila et al., 2018; Mondragón-Rodríguez et al., 2014). Consistently, here we found an increase of its expression by WB and PHF-1 immunoreactivity at hippocampal level.

These modifications of tau phosphorylation were accompanied by a concomitant decrease of GSK-3β phosphorylated at Ser 9, a residue involved in the auto-inhibitory regulation of the kinase. In line with our results, α7nAchR agonists reduced tau phosphorylation *in vitro* and *in vivo* by increasing GSK-3β activity in mouse models of AD and hypothermia-induced tau hyperphosphorylation (Bitner et al., 2009; Hu

et al., 2008), effects that are reversed by selective α7nAchR antagonists (Hu et al., 2008).

Another finding of our study is that α7 KO mice exhibited an increase of APP and Aβ levels but no senile plaques. This is in line with several studies demonstrating that soluble oligomers increase in the early stages of AD and appear more toxic than insoluble aggregates [for a review see (Selkoe and Hardy, 2016)]. Consistently, in animal models, low molecular weight Aβ oligomers (dimers), even though unable to initiate plaque formation (Müller-Schiffmann et al., 2016), induce synaptic dysfunction and trigger the AD cascade (Kawarabayashi, 2004; Mc Donald et al., 2015, 2010; Shankar et al., 2008). Studies performed on the arcAβ mice, carrying the Swedish and the Arctic mutations, confirmed that insoluble Aβ deposits are not needed to initiate the cascade of events leading to AD as the impairment of synaptic plasticity and memory occurs before plaques formation (Knobloch et al., 2007). However, we cannot exclude that in our study the absence of plaques might be due to a lower propensity of murine Aβ to form insoluble deposits, as evidenced in previous studies (Puzzo et al., 2015; Puzzo et al., 2014b).

The controversial role of Aβ deposition and its poor correlation with AD symptoms is also supported by several observations in humans showing

that AD patients can manifest dementia without Aβ deposits and, conversely, plaques might be present in cognitively intact elderly subjects (Arriagada et al., 1992; Chételat et al., 2013; Delaère et al., 1990; Driscoll et al., 2006; Iacono et al., 2009; Katzman et al., 1988; Sloane et al., 1997; Zolochevska and Taglialatela, 2016).

On the contrary, tau hyperphosphorylation leading to PHFs and NFTs formation is highly related to cognitive impairment in AD (Nelson et al., 2012), as it also contributes to functional and structural alterations of pyramidal neurons (Merino-Serrais et al., 2011). In this manuscript we have shown that α7 KO mice presented all these tau-related pathologic signs starting at 12 months of age, concomitant to the increase of APP expression and Aβ levels. In this scenario, the initial impairment of LTP found in 9M α7 KO animals might be interpreted as the result of the failure of Aβ physiological function that, when no longer compensated, would trigger the chain of events leading to the AD-like pathology at later age.

Dementia has also been strongly correlated with the degree of neuronal loss especially in the hippocampus and neocortex in humans (Donev et al., 2009). However, AD mouse models do not always mimic this aspect of the disease (Wirths and Bayer, 2010). Here, NeuN experiments have shown a reduction of neuronal number in hippocampi from α7 KO mice.

This might be, in part, independent from the neurotoxic effect exerted by Aβ and/or tau but due to the lack of α7nAChRs in view of their neuroprotective and trophic role. A variety of evidences reported that stimulation of α7nAChRs protected against glutamate neurotoxicity, oxygen and glucose deprivation, neuronal ischemic damage, and neuronal apoptosis [for reviews see (Buckingham et al., 2009; Kume and Takada-Takatori, 2018)], suggesting a general pro-survival function. Notably, α7nAChR-mediated neuroprotection might be mediated by a direct effect on neuronal cells or an indirect action through glial cells. In fact, cultured astrocytes treated with α7nAChR agonists showed a significant reduction of inflammatory cytokines secretion, accompanied by a decrease in neuronal apoptosis (Patel et al., 2017).

Finally, we have documented an increase of GFAP-positive astrocytes in α7 KO hippocampi, in line with previous reports obtained in AD models (Ceyzériat et al., 2018; González-Reyes et al., 2017). Astrocytes have a well-recognized role in modulating synaptic function by uptaking/releasing several gliotransmitters (including glutamate) and regulating the levels of neurotransmitters released from presynaptic terminals as well as glutamate receptor activity [for a review see (Malarkey and Parpura, 2008)]. They overexpress β-secretases and

stimulate Aβ production (Rossner et al., 2005) but also participate in Aβ clearance in physiological conditions (Mulder et al., 2012; Ries and Sastre, 2016). Furthermore, they are involved in the activation of intracellular signaling leading to tau hyperphosphorylation (Chiarini et al., 2017). Several reports have also highlighted a crosstalk between astrocytes and the cholinergic system (Pirttimaki et al., 2013). Septo-hippocampal lesions of cholinergic fibers induce astrocytosis and β-secretase overexpression (Hartlage-Rübsamen et al., 2003), whereas activation of α7nAChRs by physiological and pathological concentrations of Aβ triggers Ca^{2+} elevations and glutamate release from astrocytes (Lee et al., 2014; Pirttimaki et al., 2013), thereby playing a crucial role in regulating neuronal activity and plasticity (Bazargani and Attwell, 2016). Here, the increase of GFAP-positive cells suggests an astrocyte activation/remodeling (Escartin et al., 2021) that might contribute to synaptic dysfunction, even if further studies are needed to better investigate the intricate interplay among Aβ, tau and α7nAChRs at the tripartite synapse.

In conclusion, here we have demonstrated that α7nAChRs malfunction might be upstream the increase of Aβ and tau in the cascade of events leading to AD, supporting the hypothesis that if Aβ lacks its endogenous receptor, a negative feedback mechanism is triggered to overcome the

failure of its physiological function. Even if AD is a multifactorial disease and α7nAChRs malfunction might not be the only etiopathological factor, our findings contribute to understand why ACh-tailored therapies have a time-limited efficacy. In fact, the increase of ACh in the synaptic cleft by cholinesterase inhibitors or the use of AChR agonists might counteract the disease only for a brief period of time after which they might even be responsible for an exhaustion of the cholinergic system. Most importantly, considering the plethora of evidence supporting the importance of Aβ in synaptic function, anti-Aβ therapies might represent a paradox. In fact, they aim at decreasing the level of a physiological protein whose increase might have a compensatory significance. To summarize with a provocative but enlightening conceptual comparison, it would be as administering anti-insulin drugs in type II diabetes, where hyperinsulinemia is the mere consequence of a compensatory mechanism aimed at counterbalancing the lack of its function caused by receptors resistance.

Even if further studies are needed to better delineate Aβ, tau and α7nAChRs crosstalk, our data suggest that the role of Aβ in AD needs to be reassessed, taking into account mechanisms underlying the transition from physiology to pathology to ensure a novel, safe and rational approach to patients. To this end, α7 KO mice might represent

an interesting model to evaluate the cascade of events leading to the increase of Aβ without exploiting FAD human genes.

SUPPLEMENTARY DATA

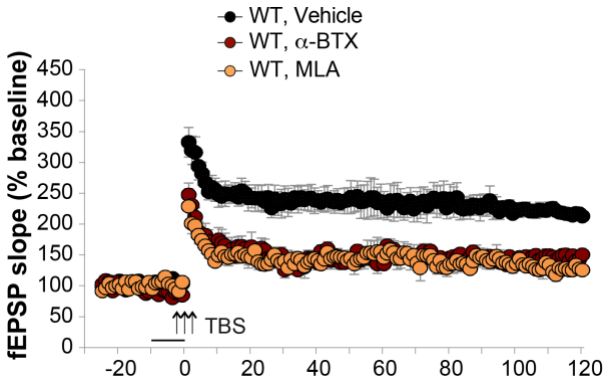

Figure S1. Blocking α7nAchRs impaired LTP. A treatment with α-bungarotoxin (α-BTX) or methyllycaconitine (MLA) for 10 min before tetanus impaired LTP in hippocampal slices from 12 M wild type mice (α-BTX: $F_{(1,12)} = 27.192$, $p < 0.0001$ vs. vehicle-treated slices; N = 7/7 from 5 animals; MLA: $F_{(1,11)} = 27.771$, $p < 0.0001$ vs. vehicle-treated slices; N = 6/7 from 5 animals). TBS = theta-burst stimulation.

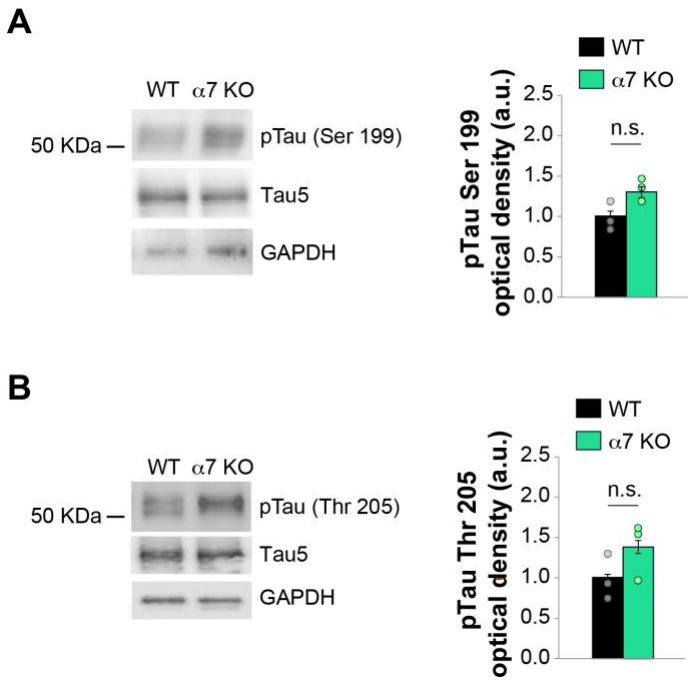

Figure S2. Tau phosphorylation did not change in 9M α7 KO mice. A) Representative images of WB assay (cropped images based on MW here and in the following panel) for the expression of phosphorylated tau (pTau) at Ser 199 performed on hippocampi from 9M WT and α7 KO mice. On the right, bar graphs showing that pTau Ser 199 expression did not change significantly in hippocampi from α7 KO compared to WT (Mann-Whitney Rank Sum Test: P = 0.1; N = 3/3). **B)** WB assay for the expression of pTau at Thr 205. On the right, bar graph showing that pTau at Thr 205 expression did not change in hippocampi of α7 KO compared to WT (Mann-Whitney Rank Sum Test, P = 0.1; N = 3/3). Tau5, specific for murine tau, was used to normalize pTau densitometric signal from WT and α7 KO tissues. GAPDH was used as loading control. n.s. = non significant. Data expressed as mean ± SEM.

Funding

This work was supported by Alzheimer's Association IIRG-09-134220 and University of Catania intramural funds (D.P.), Università Politecnica delle Marche (PSA PJ040046_2018) (F.C.), R01-AG034248 (O.A.).

Declaration of Competing Interest

The authors declare no competing financial interests.

Acknowledgements

We thank Peter Davies (Albert Einstein College of Medicine, Bronx, NY, USA) for providing the PHF-1 antibody.

Author contributions

M.R.T. contributed to conceptualization, behavioral and imaging studies, writing of the original draft; D.D.L.P. performed western blot experiments and contributed to the writing of the manuscript; M.M. contributed to conceptualization, execution and supervision of imaging studies; W.G. contributed to conceptualization, electrophysiological experiments, writing of the original draft; O.A. contributed to the conceptualization, writing, review and editing of the manuscript; CG and FC contributed to the conceptualization, formal analysis of the data, writing, review and editing of the manuscript and provided resources; DP contributed to the conceptualization, formal analysis, visualization, writing of the original draft, supervised the whole work, administered the project. All authors discussed results and commented on the manuscript.

REFERENCES

Anand, P., Singh, B., 2013. A review on cholinesterase inhibitors for Alzheimer's disease. Arch. Pharm. Res. https://doi.org/10.1007/s12272-013-0036-3

Appel, S.H., 1981. A unifying hypothesis for the cause of amyotrophic lateral sclerosis, parkinsonism, and alzheimer disease. Ann. Neurol. 10, 499–505. https://doi.org/10.1002/ana.410100602

Arriagada, P. V, Growdon, J.H., Hedleywhyte, E.T., Hyman, B.T., 1992. Neurofibrillary Tangles But Not Senile Plaques Parallel Duration and Severity of Alzheimers-Disease. Neurology 42, 631–639. https://doi.org/10.1212/WNL.42.3.631

Bazargani, N., Attwell, D., 2016. Astrocyte calcium signaling: The third wave. Nat. Neurosci. https://doi.org/10.1038/nn.4201

Bitner, R.S., Nikkel, A.L., Markosyan, S., Otte, S., Puttfarcken, P., Gopalakrishnan, M., 2009. Selective α7 nicotinic acetylcholine receptor activation regulates glycogen synthase kinase3β and decreases tau phosphorylation in vivo. Brain Res. https://doi.org/10.1016/j.brainres.2009.01.069

Bozdagi, O., Shan, W., Tanaka, H., Benson, D.L., Huntley, G.W., 2000. Increasing numbers of synaptic puncta during late-phase LTP: N-cadherin is synthesized, recruited to synaptic sites, and required for potentiation. Neuron 28, 245–59. https://doi.org/10.1016/s0896-6273(00)00100-8

Bragina, L., Melone, M., Fattorini, G., Torres-Ramos, M., Vallejo-Illarramendi, A., Matute, C., Conti, F., 2006. GLT-1 down-regulation induced by clozapine in rat frontal cortex is associated with synaptophysin up-regulation. J. Neurochem. 99, 134–141. https://doi.org/10.1111/j.1471-4159.2006.04030.x

Buckingham, S.D., Jones, A.K., Brown, L.A., Sattelle, D.B., 2009. Nicotinic acetylcholine receptor signalling: roles in Alzheimer's disease and amyloid neuroprotection. Pharmacol. Rev. 61, 39–61. https://doi.org/10.1124/pr.108.000562

Burghaus, L., Schütz, U., Krempel, U., de Vos, R.A.., Jansen Steur, E.N.H., Wevers, A., Lindstrom, J., Schröder, H., 2000. Quantitative assessment of nicotinic acetylcholine receptor proteins in the cerebral cortex of Alzheimer patients. Mol. Brain Res. 76, 385–388. https://doi.org/10.1016/S0169-328X(00)00031-0

Ceyzériat, K., Ben Haim, L., Denizot, A., Pommier, D., Matos, M., Guillemaud, O., Palomares, M.A., Abjean, L., Petit, F., Gipchtein, P., Gaillard, M.C.,

Guillermier, M., Bernier, S., Gaudin, M., Aurégan, G., Joséphine, C., Déchamps, N., Veran, J., Langlais, V., Cambon, K., Bemelmans, A.P., Baijer, J., Bonvento, G., Dhenain, M., Deleuze, J.F., Oliet, S.H.R., Brouillet, E., Hantraye, P., Carrillo-de Sauvage, M.A., Olaso, R., Panatier, A., Escartin, C., 2018. Modulation of astrocyte reactivity improves functional deficits in mouse models of Alzheimer's disease. Acta Neuropathol. Commun. https://doi.org/10.1186/s40478-018-0606-1

Cheng, Q., Yakel, J.L., 2015. The effect of α7 nicotinic receptor activation on glutamatergic transmission in the hippocampus. Biochem. Pharmacol. 97, 439–444. https://doi.org/10.1016/j.bcp.2015.07.015

Chételat, G., La Joie, R., Villain, N., Perrotin, A., De La Sayette, V., Eustache, F., Vandenberghe, R., 2013. Amyloid imaging in cognitively normal individuals, at-risk populations and preclinical Alzheimer's disease. NeuroImage Clin. https://doi.org/10.1016/j.nicl.2013.02.006

Chiarini, A., Armato, U., Gardenal, E., Gui, L., Dal Prà, I., 2017. Amyloid β-exposed human astrocytes overproduce phospho-tau and overrelease it within exosomes, effects suppressed by calcilytic NPS 2143-Further implications for Alzheimer's therapy. Front. Neurosci. https://doi.org/10.3389/fnins.2017.00217

Connelly, P.J., Prentice, N.P., Fowler, K.G., 2005. Predicting the outcome of cholinesterase inhibitor treatment in Alzheimer's disease. J. Neurol. Neurosurg. Psychiatry 76, 320–4. https://doi.org/10.1136/jnnp.2004.043539

De Chiara, G., Piacentini, R., Fabiani, M., Mastrodonato, A., Marcocci, M.E., Limongi, D., Napoletani, G., Protto, V., Coluccio, P., Celestino, I., Li Puma, D.D., Grassi, C., Palamara, A.T., 2019. Recurrent herpes simplex virus-1 infection induces hallmarks of neurodegeneration and cognitive deficits in mice. PLOS Pathog. 15, e1007617. https://doi.org/10.1371/journal.ppat.1007617

de Vivo, L., 2010. GLT-1 promoter activity in astrocytes and neurons of mouse hippocampus and somatic sensory cortex. Front. Neuroanat. 3. https://doi.org/10.3389/neuro.05.031.2009

Delaère, P., Duyckaerts, C., Masters, C., Beyreuther, K., Piette, F., Hauw, J.J., 1990. Large amounts of neocortical βA4 deposits without neuritic plaques nor tangles in a psychometrically assessed, non-demented person. Neurosci. Lett.

116, 87–93. https://doi.org/10.1016/0304-3940(90)90391-L

Deyts, C., Thinakaran, G., Parent, A.T., 2016. APP Receptor? To Be or Not To Be. Trends Pharmacol. Sci. 37, 390–411. https://doi.org/10.1016/j.tips.2016.01.005

Dickson, D.W., Crystal, H.A., Bevona, C., Honer, W., Vincent, I., Davies, P., 1995. Correlations of synaptic and pathological markers with cognition of the elderly. Neurobiol. Aging 16, 285–298. https://doi.org/10.1016/0197-4580(95)00013-5

Dineley, K.T., Bell, K.A., Bui, D., Sweatt, J.D., 2002. ??-amyloid peptide activates α7 nicotinic acetylcholine receptors expressed in Xenopus oocytes. J. Biol. Chem. 277, 25056–25061. https://doi.org/10.1074/jbc.M200066200

Dineley, K.T., Westerman, M., Bui, D., Bell, K., Ashe, K.H., Sweatt, J.D., 2001. β-Amyloid Activates the Mitogen-Activated Protein Kinase Cascade via Hippocampal α7 Nicotinic Acetylcholine Receptors : In Vitro and In Vivo Mechanisms Related to Alzheimer ' s Disease. In Vivo (Brooklyn). 21, 4125–4133.

Donev, R., Kolev, M., Millet, B., Thome, J., 2009. Neuronal death in Alzheimer's disease and therapeutic opportunities. J. Cell. Mol. Med. 13, 4329–4348. https://doi.org/10.1111/j.1582-4934.2009.00889.x

Dougherty, J.J., Wu, J.L., Nichols, R.A., 2003. β-Amyloid Regulation of Presynaptic Nicotinic Receptors in Rat Hippocampus and Neocortex. J. Neurosci. 23, 6740–6747. https://doi.org/23/17/6740 [pii]

Driscoll, I., Resnick, S.M., Troncoso, J.C., An, Y., O'Brien, R., Zonderman, A.B., 2006. Impact of Alzheimer's pathology on cognitive trajectories in nondemented elderly. Ann. Neurol. https://doi.org/10.1002/ana.21031

Engidawork, E., Gulesserian, T., Balic, N., Cairns, N., Lubec, G., 2001. Changes in nicotinic acetylcholine receptor subunits expression in brain of patients with Down syndrome and Alzheimer's disease. J. Neural Transm. Suppl. https://doi.org/10.1007/978-3-7091-6262-0_17

Escartin, C., Galea, E., Lakatos, A., O'Callaghan, J.P., Petzold, G.C., Serrano-Pozo, A., Steinhäuser, C., Volterra, A., Carmignoto, G., Agarwal, A., Allen, N.J., Araque, A., Barbeito, L., Barzilai, A., Bergles, D.E., Bonvento, G., Butt, A.M., Chen, W.-T., Cohen-Salmon, M., Cunningham, C., Deneen, B., De Strooper, B., Díaz-Castro, B., Farina, C., Freeman, M., Gallo, V., Goldman, J.E., Goldman, S.A., Götz, M., Gutiérrez, A., Haydon, P.G., Heiland, D.H., Hol,

E.M., Holt, M.G., Iino, M., Kastanenka, K. V., Kettenmann, H., Khakh, B.S., Koizumi, S., Lee, C.J., Liddelow, S.A., MacVicar, B.A., Magistretti, P., Messing, A., Mishra, A., Molofsky, A. V., Murai, K.K., Norris, C.M., Okada, S., Oliet, S.H.R., Oliveira, J.F., Panatier, A., Parpura, V., Pekna, M., Pekny, M., Pellerin, L., Perea, G., Pérez-Nievas, B.G., Pfrieger, F.W., Poskanzer, K.E., Quintana, F.J., Ransohoff, R.M., Riquelme-Perez, M., Robel, S., Rose, C.R., Rothstein, J.D., Rouach, N., Rowitch, D.H., Semyanov, A., Sirko, S., Sontheimer, H., Swanson, R.A., Vitorica, J., Wanner, I.-B., Wood, L.B., Wu, J., Zheng, B., Zimmer, E.R., Zorec, R., Sofroniew, M. V., Verkhratsky, A., 2021. Reactive astrocyte nomenclature, definitions, and future directions. Nat. Neurosci. 24, 312–325. https://doi.org/10.1038/s41593-020-00783-4

Fá, M., Puzzo, D., Piacentini, R., Staniszewski, A., Zhang, H., Baltrons, M.A., Li Puma, D.D., Chatterjee, I., Li, J., Saeed, F., Berman, H.L., Ripoli, C., Gulisano, W., Gonzalez, J., Tian, H., Costa, J.A., Lopez, P., Davidowitz, E., Yu, W.H., Haroutunian, V., Brown, L.M., Palmeri, A., Sigurdsson, E.M., Duff, K.E., Teich, A.F., Honig, L.S., Sierks, M., Moe, J.G., D'Adamio, L., Grassi, C., Kanaan, N.M., Fraser, P.E., Arancio, O., 2016. Extracellular Tau Oligomers Produce An Immediate Impairment of LTP and Memory. Sci. Rep. 6, 19393. https://doi.org/10.1038/srep19393

Ferreira-Vieira, T., H., M. Guimaraes, I., R. Silva, F., M. Ribeiro, F., 2016. Alzheimer's disease: Targeting the Cholinergic System. Curr. Neuropharmacol. https://doi.org/10.2174/1570159x13666150716165726

Fogel, H., Frere, S., Segev, O., Bharill, S., Shapira, I., Gazit, N., O'Malley, T., Slomowitz, E., Berdichevsky, Y., Walsh, D.M., Isacoff, E.Y., Hirsch, J.A., Slutsky, I., 2014. APP homodimers transduce an amyloid-β-mediated increase in release probability at excitatory synapses. Cell Rep. 7, 1560–1576. https://doi.org/10.1016/j.celrep.2014.04.024

Furcila, D., DeFelipe, J., Alonso-Nanclares, L., 2018. A Study of Amyloid-β and Phosphotau in Plaques and Neurons in the Hippocampus of Alzheimer's Disease Patients. J. Alzheimer's Dis. 64, 417–435. https://doi.org/10.3233/JAD-180173

Garcia-Osta, A., Alberini, C.M., 2009. Amyloid beta mediates memory formation. Learn. Mem. 16, 267–72. https://doi.org/10.1101/lm.1310209

Glenner, G.G., Wong, C.W., 1984. Alzheimer's disease: Initial report of the

purification and characterization of a novel cerebrovascular amyloid protein. Biochem. Biophys. Res. Commun. 120, 885–890. https://doi.org/10.1016/S0006-291X(84)80190-4

González-Reyes, R.E., Nava-Mesa, M.O., Vargas-Sánchez, K., Ariza-Salamanca, D., Mora-Muñoz, L., 2017. Involvement of Astrocytes in Alzheimer's Disease from a Neuroinflammatory and Oxidative Stress Perspective. Front. Mol. Neurosci. 10. https://doi.org/10.3389/fnmol.2017.00427

Götz, J., Chen, F., van Dorpe, J., Nitsch, R.M., 2001. Formation of neurofibrillary tangles in P301l tau transgenic mice induced by Abeta 42 fibrils. Science 293, 1491–5. https://doi.org/10.1126/science.1062097

Greenberg, S.M., Koo, E.H., Selkoe, D.J., Qiu, W.Q., Kosik, K.S., 1994. Secreted β-amyloid precursor protein stimulates mitogen-activated protein kinase and enhances τ phosphorylation. Proc. Natl. Acad. Sci. U. S. A. https://doi.org/10.1073/pnas.91.15.7104

Grundke-Iqbal, I., Iqbal, K., Quinlan, M., Tung, Y.C., Zaidi, M.S., Wisniewski, H.M., 1986. Microtubule-associated protein tau. A component of Alzheimer paired helical filaments. J Biol Chem 261, 6084–6089. https://doi.org/10.1074/jbc.M111.271320

Gulisano, W., Maugeri, D., Baltrons, M.A., Fà, M., Amato, A., Palmeri, A., D'Adamio, L., Grassi, C., Devanand, D.P., Honig, L.S., Puzzo, D., Arancio, O., 2018a. Role of Amyloid-β and Tau Proteins in Alzheimer's Disease: Confuting the Amyloid Cascade. J. Alzheimers. Dis. 136, 1383–98. https://doi.org/10.3233/JAD-179935

Gulisano, W., Melone, M., Li Puma, D.D., Tropea, M.R., Palmeri, A., Arancio, O., Grassi, C., Conti, F., Puzzo, D., 2018b. The effect of amyloid-β peptide on synaptic plasticity and memory is influenced by different isoforms, concentrations, and aggregation status. Neurobiol. Aging 71, 51–60. https://doi.org/10.1016/j.neurobiolaging.2018.06.025

Gulisano, W., Melone, M., Ripoli, C., Tropea, M.R., Li Puma, D.D., Giunta, S., Cocco, S., Marcotulli, D., Origlia, N., Palmeri, A., Arancio, O., Conti, F., Grassi, C., Puzzo, D., 2019. Neuromodulatory Action of Picomolar Extracellular Aβ42 Oligomers on Presynaptic and Postsynaptic Mechanisms Underlying Synaptic Function and Memory. J. Neurosci. 39, 5986–6000. https://doi.org/10.1523/JNEUROSCI.0163-19.2019

Hanger, D.P., Noble, W., 2011. Functional Implications of Glycogen Synthase Kinase-3-Mediated Tau Phosphorylation. Int. J. Alzheimers. Dis. 2011, 1–11. https://doi.org/10.4061/2011/352805

Hardy, J., Allsop, D., 1991. Amyloid deposition as the central event in the aetiology of Alzheimer's disease. Trends Pharmacol. Sci. https://doi.org/10.1016/0165-6147(91)90609-V

Hardy, J., Duff, K., Hardy, K.G., Perez-Tur, J., Hutton, M., 1998. Genetic dissection of Alzheimer's disease and related dementias: amyloid and its relationship to tau. Nat. Neurosci. 1, 355–8. https://doi.org/10.1038/1565

Hartlage-Rübsamen, M., Zeitschel, U., Apelt, J., Gärtner, U., Franke, H., Stahl, T., Günther, A., Schliebs, R., Penkowa, M., Bigl, V., Roßner, S., 2003. Astrocytic expression of the Alzheimer's disease β-secretase (BACE1) is stimulus-dependent. Glia 41, 169–179. https://doi.org/10.1002/glia.10178

Hefter, D., Ludewig, S., Draguhn, A., Korte, M., 2020. Amyloid, APP, and Electrical Activity of the Brain. Neuroscientist. https://doi.org/10.1177/1073858419882619

Hernandez, C.M., Kayed, R., Zheng, H., Sweatt, J.D., Dineley, K.T., 2010. Loss of alpha7 nicotinic receptors enhances beta-amyloid oligomer accumulation, exacerbating early-stage cognitive decline and septohippocampal pathology in a mouse model of Alzheimer's disease. J. Neurosci. 30, 2442–53. https://doi.org/10.1523/JNEUROSCI.5038-09.2010

Herrup, K., 2015. The case for rejecting the amyloid cascade hypothesis. Nat. Neurosci. 18, 794–799. https://doi.org/10.1038/nn.4017

Hölttä, M., Hansson, O., Andreasson, U., Hertze, J., Minthon, L., Nägga, K., Andreasen, N., Zetterberg, H., Blennow, K., 2013. Evaluating Amyloid-β Oligomers in Cerebrospinal Fluid as a Biomarker for Alzheimer's Disease. PLoS One. https://doi.org/10.1371/journal.pone.0066381

Hu, M., Waring, J.F., Gopalakrishnan, M., Li, J., 2008. Role of GSK-3 activation and 7 nAChRs in A 142 -induced tau phosphorylation in PC12 cells. J. Neurochem. 106, 1371–1377. https://doi.org/10.1111/j.1471-4159.2008.05483.x

Iacono, D., Markesbery, W.R., Gross, M., Pletnikova, O., Rudow, G., Zandi, P., Troncoso, J.C., 2009. The Nun Study: Clinically silent AD, neuronal hypertrophy, and linguistic skills in early life. Neurology.

https://doi.org/10.1212/WNL.0b013e3181b01077

Iqbal, K., Alonso, A. del C., Chen, S., Chohan, M.O., El-Akkad, E., Gong, C.-X., Khatoon, S., Li, B., Liu, F., Rahman, A., Tanimukai, H., Grundke-Iqbal, I., 2005. Tau pathology in Alzheimer disease and other tauopathies. Biochim. Biophys. Acta 1739, 198–210. https://doi.org/10.1016/j.bbadis.2004.09.008

Katzman, R., Terry, R., DeTeresa, R., Brown, T., Davies, P., Fuld, P., Renbing, X., Peck, A., 1988. Clinical, pathological, and neurochemical changes in dementia: A subgroup with preserved mental status and numerous neocortical plaques. Ann. Neurol. 23, 138–144. https://doi.org/10.1002/ana.410230206

Kawarabayashi, T., 2004. Dimeric Amyloid Protein Rapidly Accumulates in Lipid Rafts followed by Apolipoprotein E and Phosphorylated Tau Accumulation in the Tg2576 Mouse Model of Alzheimer's Disease. J. Neurosci. 24, 3801–3809. https://doi.org/10.1523/JNEUROSCI.5543-03.2004

Knobloch, M., Konietzko, U., Krebs, D.C., Nitsch, R.M., 2007. Intracellular Aβ and cognitive deficits precede β-amyloid deposition in transgenic arcAβ mice. Neurobiol. Aging. https://doi.org/10.1016/j.neurobiolaging.2006.06.019

Koppensteiner, P., Trinchese, F., Fà, M., Puzzo, D., Gulisano, W., Yan, S., Poussin, A., Liu, S., Orozco, I., Dale, E., Teich, A.F., Palmeri, A., Ninan, I., Boehm, S., Arancio, O., 2016. Time-dependent reversal of synaptic plasticity induced by physiological concentrations of oligomeric Aβ42: an early index of Alzheimer's disease. Sci. Rep. 6, 32553. https://doi.org/10.1038/srep32553

Koval, L., Lykhmus, O., Kalashnyk, O., Bachinskaya, N., Kravtsova, G., Soldatkina, M., Zouridakis, M., Stergiou, C., Tzartos, S., Tsetlin, V., Komisarenko, S., Skok, M., 2011. The presence and origin of autoantibodies against α4 and α7 nicotinic acetylcholine receptors in the human blood: possible relevance to Alzheimer's pathology. J. Alzheimers. Dis. 25, 747–61. https://doi.org/10.3233/JAD-2011-101845

Kuhn, J., Hardenacke, K., Lenartz, D., Gruendler, T., Ullsperger, M., Bartsch, C., Mai, J.K., Zilles, K., Bauer, A., Matusch, A., Schulz, R.-J., Noreik, M., Bührle, C.P., Maintz, D., Woopen, C., Häussermann, P., Hellmich, M., Klosterkötter, J., Wiltfang, J., Maarouf, M., Freund, H.-J., Sturm, V., 2015. Deep brain stimulation of the nucleus basalis of Meynert in Alzheimer's dementia. Mol. Psychiatry 20, 353–360. https://doi.org/10.1038/mp.2014.32

Kume, T., Takada-Takatori, Y., 2018. Nicotinic Acetylcholine Receptor Signaling:

Roles in Neuroprotection, in: Nicotinic Acetylcholine Receptor Signaling in Neuroprotection. Springer Singapore, Singapore, pp. 59–71. https://doi.org/10.1007/978-981-10-8488-1_4

Lasagna-Reeves, C.A., 2012. Identification of oligomers at early stages of tau aggregation in Alzheimer's disease. FASEB J. 26, 1946–1959.

Lawrence, J.L.M., Tong, M., Alfulaij, N., Sherrin, T., Contarino, M., White, M.M., Bellinger, F.P., Todorovic, C., Nichols, R.A., 2014. Regulation of presynaptic Ca2+, synaptic plasticity and contextual fear conditioning by a N-terminal β-amyloid fragment. J. Neurosci. 34, 14210–8. https://doi.org/10.1523/JNEUROSCI.0326-14.2014

Lazarevic, V., Fieńko, S., Andres-Alonso, M., Anni, D., Ivanova, D., Montenegro-Venegas, C., Gundelfinger, E.D., Cousin, M.A., Fejtova, A., 2017. Physiological concentrations of amyloid beta regulate recycling of synaptic vesicles via alpha7 acetylcholine receptor and CDK5/calcineurin signaling. Front. Mol. Neurosci. https://doi.org/10.3389/fnmol.2017.00221

Lee, L., Kosuri, P., Arancio, O., 2014. Picomolar amyloid-β peptides enhance spontaneous astrocyte calcium transients. J. Alzheimer's Dis. 38, 49–62. https://doi.org/10.3233/JAD-130740

Lemstra, A.W., Richard, E., van Gool, W.A., 2007. Cholinesterase inhibitors in dementia: yes, no, or maybe? Age Ageing 36, 625–7. https://doi.org/10.1093/ageing/afm117

Li Puma, D.D., Piacentini, R., Leone, L., Gironi, K., Marcocci, M.E., De Chiara, G., Palamara, A.T., Grassi, C., 2019. Herpes Simplex Virus Type-1 Infection Impairs Adult Hippocampal Neurogenesis via Amyloid-β Protein Accumulation. Stem Cells 37, 1467–1480. https://doi.org/10.1002/stem.3072

Li, S.F., Wu, M.N., Wang, X.H., Yuan, L., Yang, D., Qi, J.S., 2011. Requirement of ??7 nicotinic acetylcholine receptors for amyloid beta protein-Induced depression of hippocampal long-term potentiation in CA1 region of rats in vivo. Synapse 65, 1136–1143. https://doi.org/10.1002/syn.20951

Liu, Q.-S., Kawai, H., Berg, D.K., 2001. beta -Amyloid peptide blocks the response of alpha 7-containing nicotinic receptors on hippocampal neurons. Proc. Natl. Acad. Sci. U. S. A. 98, 4734–9. https://doi.org/10.1073/pnas.081553598

Llorens-MarÃ-tin, M., Jurado, J., HernÃ¡ndez, F., Ã• vila, J., 2014. GSK-3Î², a pivotal kinase in Alzheimer disease. Front. Mol. Neurosci. 7.

https://doi.org/10.3389/fnmol.2014.00046

Lorenzo, A., Yuan, M., Zhang, Z., Paganetti, P.A., Sturchler-Pierrat, C., Staufenbiel, M., Mautino, J., Vigo, F.S., Sommer, B., Yankner, B.A., 2000. Amyloid beta interacts with the amyloid precursor protein: a potential toxic mechanism in Alzheimer's disease. Nat. Neurosci. 3, 460–4. https://doi.org/10.1038/74833

Lykhmus, O., Voytenko, L., Koval, L., Mykhalskiy, S., Kholin, V., Peschana, K., Zouridakis, M., Tzartos, S., Komisarenko, S., Skok, M., 2015. α7 Nicotinic acetylcholine receptor-specific antibody induces inflammation and amyloid β42 accumulation in the mouse brain to impair memory. PLoS One 10, e0122706. https://doi.org/10.1371/journal.pone.0122706

Ma, L., Turner, D., Zhang, J., Wang, Q., Wang, M., Shen, J., Zhang, S., Wu, J., 2014. Deficits of synaptic functions in hippocampal slices prepared from aged mice null α7 nicotinic acetylcholine receptors. Neurosci. Lett. 570, 97–101. https://doi.org/10.1016/j.neulet.2014.04.018

Malarkey, E.B., Parpura, V., 2008. Mechanisms of glutamate release from astrocytes. Neurochem. Int. 52, 142–154. https://doi.org/10.1016/j.neuint.2007.06.005

Martin, L., Latypova, X., Terro, F., 2011. Post-translational modifications of tau protein: implications for Alzheimer's disease. Neurochem. Int. 58, 458–471.

Mc Donald, J.M., O'Malley, T.T., Liu, W., Mably, A.J., Brinkmalm, G., Portelius, E., Wittbold, W.M., Frosch, M.P., Walsh, D.M., 2015. The aqueous phase of Alzheimer's disease brain contains assemblies built from ∼4 and ∼7 kDa Aβ species. Alzheimer's Dement. 11, 1286–1305. https://doi.org/10.1016/j.jalz.2015.01.005

Mc Donald, J.M., Savva, G.M., Brayne, C., Welzel, A.T., Forster, G., Shankar, G.M., Selkoe, D.J., Ince, P.G., Walsh, D.M., Medical Research Council Cognitive, F., Ageing, S., 2010. The presence of sodium dodecyl sulphate-stable Abeta dimers is strongly associated with Alzheimer-type dementia. Brain 133, 1328–1341. https://doi.org/10.1093/brain/awq065

Melone, M., Burette, A., Weinberg, R.J., 2005. Light microscopic identification and immunocytochemical characterization of glutamatergic synapses in brain sections. J. Comp. Neurol. https://doi.org/10.1002/cne.20743

Melone, M., Ciriachi, C., Pietrobon, D., Conti, F., 2019. Heterogeneity of Astrocytic and Neuronal GLT-1 at Cortical Excitatory Synapses, as Revealed by its

Colocalization With Na+/K+-ATPase α Isoforms. Cereb. Cortex 29, 3331–3350. https://doi.org/10.1093/cercor/bhy203

Merino-Serrais, P., Knafo, S., Alonso-Nanclares, L., Fernaud-Espinosa, I., Defelipe, J., 2011. Layer-specific alterations to CA1 dendritic spines in a mouse model of Alzheimer's disease. Hippocampus. https://doi.org/10.1002/hipo.20861

Miao, J., Shi, R., Li, L., Chen, F., Zhou, Y., Tung, Y.C., Hu, W., Gong, C.-X., Iqbal, K., Liu, F., 2019. Pathological Tau From Alzheimer's Brain Induces Site-Specific Hyperphosphorylation and SDS- and Reducing Agent-Resistant Aggregation of Tau in vivo. Front. Aging Neurosci. 11. https://doi.org/10.3389/fnagi.2019.00034

Mondragón-Rodríguez, S., Perry, G., Luna-Muñoz, J., Acevedo-Aquino, M.C., Williams, S., 2014. Phosphorylation of tau protein at sites Ser396-404 is one of the earliest events in Alzheimer's disease and Down syndrome. Neuropathol. Appl. Neurobiol. https://doi.org/10.1111/nan.12084

Morley, J.E., Farr, S.A., Banks, W.A., Johnson, S.N., Yamada, K.A., Xu, L., 2010. A physiological role for amyloid-beta protein:enhancement of learning and memory. J. Alzheimers. Dis. 19, 441–9. https://doi.org/10.3233/JAD-2009-1230

Mousavi, M., Hellström-Lindahl, E., 2009. Nicotinic receptor agonists and antagonists increase sAPPalpha secretion and decrease Abeta levels in vitro. Neurochem. Int. 54, 237–44. https://doi.org/10.1016/j.neuint.2008.12.001

Mufson, E., Counts, S., Fahnestock, M., Ginsberg, S., 2007. Cholinotrophic Molecular Substrates of Mild Cognitive Impairment in the Elderly. Curr. Alzheimer Res. https://doi.org/10.2174/156720507781788855

Mulder, S.D., Veerhuis, R., Blankenstein, M.A., Nielsen, H.M., 2012. The effect of amyloid associated proteins on the expression of genes involved in amyloid-β clearance by adult human astrocytes. Exp. Neurol. 233, 373–379. https://doi.org/10.1016/j.expneurol.2011.11.001

Müller-Schiffmann, A., Herring, A., Abdel-Hafiz, L., Chepkova, A.N., Schäble, S., Wedel, D., Horn, A.H.C., Sticht, H., De Souza Silva, M.A., Gottmann, K., Sergeeva, O.A., Huston, J.P., Keyvani, K., Korth, C., 2016. Amyloid-β dimers in the absence of plaque pathology impair learning and synaptic plasticity. Brain 139, 509–525. https://doi.org/10.1093/brain/awv355

Mura, E., Zappettini, S., Preda, S., Biundo, F., Lanni, C., Grilli, M., Cavallero, A.,

Olivero, G., Salamone, A., Govoni, S., Marchi, M., 2012. Dual effect of beta-amyloid on α7 and α4β2 nicotinic receptors controlling the release of glutamate, aspartate and GABA in rat hippocampus. PLoS One 7, e29661. https://doi.org/10.1371/journal.pone.0029661

Nagele, R.G., D'Andrea, M.R., Anderson, W.J., Wang, H.-Y., 2002. Intracellular accumulation of beta-amyloid(1-42) in neurons is facilitated by the alpha 7 nicotinic acetylcholine receptor in Alzheimer's disease. Neuroscience 110, 199–211. https://doi.org/S0306452201004602 [pii]

Neddens, J., Temmel, M., Flunkert, S., Kerschbaumer, B., Hoeller, C., Loeffler, T., Niederkofler, V., Daum, G., Attems, J., Hutter-Paier, B., 2018. Phosphorylation of different tau sites during progression of Alzheimer's disease. Acta Neuropathol. Commun. 6, 52. https://doi.org/10.1186/s40478-018-0557-6

Nelson, P.T., Alafuzoff, I., Bigio, E.H., Bouras, C., Braak, H., Cairns, N.J., Castellani, R.J., Crain, B.J., Davies, P., Tredici, K. Del, Duyckaerts, C., Frosch, M.P., Haroutunian, V., Hof, P.R., Hulette, C.M., Hyman, B.T., Iwatsubo, T., Jellinger, K.A., Jicha, G.A., Kövari, E., Kukull, W.A., Leverenz, J.B., Love, S., MacKenzie, I.R., Mann, D.M., Masliah, E., McKee, A.C., Montine, T.J., Morris, J.C., Schneider, J.A., Sonnen, J.A., Thal, D.R., Trojanowski, J.Q., Troncoso, J.C., Wisniewski, T., Woltjer, R.L., Beach, T.G., 2012. Correlation of alzheimer disease neuropathologic changes with cognitive status: A review of the literature. J. Neuropathol. Exp. Neurol. https://doi.org/10.1097/NEN.0b013e31825018f7

Nie, H.Z., Shi, S., Lukas, R.J., Zhao, W.J., Sun, Y.N., Yin, M., 2010. Activation of α7 nicotinic receptor affects APP processing by regulating secretase activity in SH-EP1-α7 nAChR-hAPP695 cells. Brain Res. https://doi.org/10.1016/j.brainres.2010.07.110

Oddo, S., Caccamo, A., Green, K.N., Liang, K., Tran, L., Chen, Y., Leslie, F.M., LaFerla, F.M., 2005. Chronic nicotine administration exacerbates tau pathology in a transgenic model of Alzheimer's disease. Proc. Natl. Acad. Sci. 102, 3046–3051. https://doi.org/10.1073/pnas.0408500102

Oddo, S., Caccamo, A., Shepherd, J.D., Murphy, M.P., Golde, T.E., Kayed, R., Metherate, R., Mattson, M.P., Akbari, Y., LaFerla, F.M., 2003. Triple-Transgenic Model of Alzheimer's Disease with Plaques and Tangles. Neuron

39, 409–421. https://doi.org/10.1016/S0896-6273(03)00434-3

Oz, M., Lorke, D.E., Yang, K.S., Petroianu, G., 2013. On the Interaction of -Amyloid Peptides and 7-Nicotinic Acetylcholine Receptors in Alzheimer ' s Disease. Curr. Alzheimer Res. 10, 618–630.

Palmeri, A., Ricciarelli, R., Gulisano, W., Rivera, D., Rebosio, C., Calcagno, E., Tropea, M.R., Conti, S., Das, U., Roy, S., Pronzato, M.A., Arancio, O., Fedele, E., Puzzo, D., 2017. Amyloid-β Peptide Is Needed for cGMP-Induced Long-Term Potentiation and Memory. J. Neurosci. 37, 6926–6937. https://doi.org/10.1523/JNEUROSCI.3607-16.2017

Patel, H., McIntire, J., Ryan, S., Dunah, A., Loring, R., 2017. Anti-inflammatory effects of astroglial α7 nicotinic acetylcholine receptors are mediated by inhibition of the NF-KB pathway and activation of the Nrf2 pathway. J. Neuroinflammation. https://doi.org/10.1186/s12974-017-0967-6

Phatnani, H., Maniatis, T., 2015. Astrocytes in neurodegenerative disease. Cold Spring Harb. Perspect. Biol. https://doi.org/10.1101/cshperspect.a020628

Picciotto, M., 2000. Nicotinic Receptors in the Brain Links between Molecular Biology and Behavior. Neuropsychopharmacology 22, 451–465. https://doi.org/10.1016/S0893-133X(99)00146-3

Pirttimaki, T.M., Codadu, N.K., Awni, A., Pratik, P., Nagel, D.A., Hill, E.J., Dineley, K.T., Parri, H.R., 2013. α7 Nicotinic Receptor-Mediated Astrocytic Gliotransmitter Release: Aβ Effects in a Preclinical Alzheimer's Mouse Model. PLoS One 8, e81828. https://doi.org/10.1371/journal.pone.0081828

Puzzo, D., Argyrousi, E.K., Staniszewski, A., Zhang, H., Calcagno, E., Zuccarello, E., Acquarone, E., Fa', M., Li Puma, D.D., Grassi, C., D'Adamio, L., Kanaan, N.M., Fraser, P.E., Arancio, O., 2020. Tau is not necessary for amyloid-β–induced synaptic and memory impairments. J. Clin. Invest. 130, 4831–4844. https://doi.org/10.1172/JCI137040

Puzzo, D., Bizzoca, A., Loreto, C., Guida, C.A., Gulisano, W., Frasca, G., Bellomo, M., Castorina, S., Gennarini, G., Palmeri, A., 2015. Role of F3/contactin expression profile in synaptic plasticity and memory in aged mice. Neurobiol. Aging 36, 1702–1715. https://doi.org/10.1016/j.neurobiolaging.2015.01.004

Puzzo, D., Gulisano, W., Arancio, O., Palmeri, A., 2015. The keystone of Alzheimer pathogenesis might be sought in Aβ physiology. Neuroscience 307, 26–36. https://doi.org/10.1016/j.neuroscience.2015.08.039

Puzzo, D., Lee, L., Palmeri, A., Calabrese, G., Arancio, O., 2014a. Behavioral assays with mouse models of Alzheimer's disease: Practical considerations and guidelines. Biochem. Pharmacol. 88, 450–467. https://doi.org/10.1016/j.bcp.2014.01.011

Puzzo, D., Loreto, C., Giunta, S., Musumeci, G., Frasca, G., Podda, M.V., Arancio, O., Palmeri, A., 2014b. Effect of phosphodiesterase-5 inhibition on apoptosis and beta amyloid load in aged mice. Neurobiol. Aging 35, 520–531. https://doi.org/10.1016/j.neurobiolaging.2013.09.002

Puzzo, D., Piacentini, R., Fá, M., Gulisano, W., Li Puma, D.D., Staniszewski, A., Zhang, H., Tropea, M.R., Cocco, S., Palmeri, A., Fraser, P., D'Adamio, L., Grassi, C., Arancio, O., 2017. LTP and memory impairment caused by extracellular Aβ and Tau oligomers is APP-dependent. Elife 6, 1–21. https://doi.org/10.7554/eLife.26991

Puzzo, D., Privitera, L., Fa', M., Staniszewski, A., Hashimoto, G., Aziz, F., Sakurai, M., Ribe, E.M., Troy, C.M., Mercken, M., Jung, S.S., Palmeri, A., Arancio, O., 2011. Endogenous amyloid-β is necessary for hippocampal synaptic plasticity and memory. Ann. Neurol. 69, 819–30. https://doi.org/10.1002/ana.22313

Puzzo, D., Privitera, L., Leznik, E., Fà, M., Staniszewski, A., Palmeri, A., Arancio, O., 2008. Picomolar amyloid-β positively modulates synaptic plasticity and memory in hippocampus. J. Neurosci. 28. https://doi.org/10.1523/JNEUROSCI.2692-08.2008

Qi, X.-L., Nordberg, A., Xiu, J., Guan, Z.-Z., 2007. The consequences of reducing expression of the alpha7 nicotinic receptor by RNA interference and of stimulating its activity with an alpha7 agonist in SH-SY5Y cells indicate that this receptor plays a neuroprotective role in connection with the pathogenes. Neurochem. Int. 51, 377–83. https://doi.org/10.1016/j.neuint.2007.04.002

Qiu, C., Kivipelto, M., von Strauss, E., 2009. Epidemiology of Alzheimer's disease: occurrence, determinants, and strategies toward intervention. Dialogues Clin. Neurosci. 11, 111–28. https://doi.org/10.1097/ALN.0b013e318212ba87

Ren, K., Thinschmidt, J., Liu, J., Ai, L., Papke, R.L., King, M.A., Hughes, J.A., Meyer, E.M., 2007. ??7 Nicotinic receptor gene delivery into mouse hippocampal neurons leads to functional receptor expression, improved spatial memory-related performance, and tau hyperphosphorylation. Neuroscience 145, 314–322. https://doi.org/10.1016/j.neuroscience.2006.11.023

Ricciarelli, R., Puzzo, D., Bruno, O., Canepa, E., Gardella, E., Rivera, D., Privitera, L., Domenicotti, C., Marengo, B., Marinari, U.M., Palmeri, A., Pronzato, M.A., Arancio, O., Fedele, E., 2014. A novel mechanism for cyclic adenosine monophosphate-mediated memory formation: Role of amyloid beta. Ann. Neurol. 75, 602–607. https://doi.org/10.1002/ana.24130

Ries, M., Sastre, M., 2016. Mechanisms of Aβ clearance and degradation by glial cells. Front. Aging Neurosci. https://doi.org/10.3389/fnagi.2016.00160

Rossner, S., Lange-Dohna, C., Zeitschel, U., Perez-Polo, J.R., 2005. Alzheimer's disease beta-secretase BACE1 is not a neuron-specific enzyme. J. Neurochem. 92, 226–34. https://doi.org/10.1111/j.1471-4159.2004.02857.x

Rubio, A., Pérez, M., Ávila, J., 2006. Acetylcholine Receptors and Tau Phosphorylation. Curr. Mol. Med. 6, 423–428. https://doi.org/10.2174/156652406777435444

Schneider, C.A., Rasband, W.S., Eliceiri, K.W., 2012. NIH Image to ImageJ: 25 years of image analysis. Nat. Methods 9, 671–5. https://doi.org/10.1038/nmeth.2089

Selkoe, D.J., 2002. Alzheimer's disease is a synaptic failure. Science 298, 789–91. https://doi.org/10.1126/science.1074069

Selkoe, D.J., Hardy, J., 2016. The amyloid hypothesis of Alzheimer's disease at 25 years. EMBO Mol. Med. 8, 595–608. https://doi.org/10.15252/emmm.201606210

Sengupta, U., Portelius, E., Hansson, O., Farmer, K., Castillo-Carranza, D., Woltjer, R., Zetterberg, H., Galasko, D., Blennow, K., Kayed, R., 2017. Tau oligomers in cerebrospinal fluid in Alzheimer's disease. Ann. Clin. Transl. Neurol. 4, 226–235. https://doi.org/10.1002/acn3.382

Shaked, G.M., Kummer, M.P., Lu, D.C., Galvan, V., Bredesen, D.E., Koo, E.H., 2006. Abeta induces cell death by direct interaction with its cognate extracellular domain on APP (APP 597-624). FASEB J. 20, 1254–6. https://doi.org/10.1096/fj.05-5032fje

Shankar, G.M., Li, S., Mehta, T.H., Garcia-Munoz, A., Shepardson, N.E., Smith, I., Brett, F.M., Farrell, M.A., Rowan, M.J., Lemere, C.A., Regan, C.M., Walsh, D.M., Sabatini, B.L., Selkoe, D.J., 2008. Amyloid-β protein dimers isolated directly from Alzheimer's brains impair synaptic plasticity and memory. Nat. Med. 14, 837–842. https://doi.org/10.1038/nm1782

Sloane, J.A., Pietropaolo, M.F., Rosene, D.L., Moss, M.B., Peters, A., Kemper, T., Abraham, C.R., 1997. Lack of correlation between plaque burden and cognition in the aged monkey. Acta Neuropathol. 94, 471–478. https://doi.org/10.1007/s004010050735

Strada, O., Vyas, S., Hirsch, E.C., Ruberg, M., Brice, A., Agid, Y., Javoy-Agid, F., 1992. Decreased choline acetyltransferase mRNA expression in the nucleus basalis of Meynert in Alzheimer disease: an in situ hybridization study. Proc. Natl. Acad. Sci. 89, 9549–9553. https://doi.org/10.1073/pnas.89.20.9549

Takahashi, M., Miyata, H., Kametani, F., Nonaka, T., Akiyama, H., Hisanaga, S. ichi, Hasegawa, M., 2015. Extracellular association of APP and tau fibrils induces intracellular aggregate formation of tau. Acta Neuropathol. 129, 895–907. https://doi.org/10.1007/s00401-015-1415-2

Van Nostrand, W.E., Melchor, J.P., Keane, D.M., Saporito-Irwin, S.M., Romanov, G., Davis, J., Xu, F., 2002. Localization of a fibrillar amyloid β-protein binding domain on its precursor. J. Biol. Chem. 277, 36392–36398. https://doi.org/10.1074/jbc.M204676200

Wang, H.-Y., Li, W., Benedetti, N.J., Lee, D.H.S., 2003. α 7 Nicotinic Acetylcholine Receptors Mediate β-Amyloid Peptide-induced Tau Protein Phosphorylation. J. Biol. Chem. 278, 31547–31553. https://doi.org/10.1074/jbc.M212532200

Wang, H.Y., Lee, D.H., Davis, C.B., Shank, R.P., 2000. Amyloid peptide Abeta(1-42) binds selectively and with picomolar affinity to alpha7 nicotinic acetylcholine receptors. J. Neurochem. 75, 1155–61. https://doi.org/10.1046/j.1471-4159.2000.0751155.x

Wang, Y., Mandelkow, E., 2015. Tau in physiology and pathology. Nat. Rev. Neurosci. 17, 22–35. https://doi.org/10.1038/nrn.2015.1

Wang, Z., Jackson, R.J., Hong, W., Taylor, W.M., Corbett, G.T., Moreno, A., Liu, W., Li, S., Frosch, M.P., Slutsky, I., Young-Pearse, T.L., Spires-Jones, T.L., Walsh, D.M., 2017. Human Brain-Derived Aβ Oligomers Bind to Synapses and Disrupt Synaptic Activity in a Manner That Requires APP. J. Neurosci. 37, 11947–11966. https://doi.org/10.1523/JNEUROSCI.2009-17.2017

Wevers, A., Monteggia, L., Nowacki, S., Bloch, W., Schutz, U., Lindstrom, J., Pereira, E.F.R., Eisenberg, H., Giacobini, E., De Vos, R.A.I., Steur, E.N.H.J., Maelicke, A., Albuquerque, E.X., Schroder, H., 1999. Expression of nicotinic acetylcholine receptor subunits in the cerebral cortex in Alzheimer's disease:

Histotopographical correlation with amyloid plaques and hyperphosphorylated-tau protein. Eur. J. Neurosci. 11, 2551–2565. https://doi.org/10.1046/j.1460-9568.1999.00676.x

Whitehouse, P.J., Price, D.L., Clark, A.W., Coyle, J.T., DeLong, M.R., 1981. Alzheimer disease: Evidence for selective loss of cholinergic neurons in the nucleus basalis. Ann. Neurol. 10, 122–126. https://doi.org/10.1002/ana.410100203

Wilcock, D.M., Gordon, M.N., Morgan, D., 2006. Quantification of cerebral amyloid angiopathy and parenchymal amyloid plaques with Congo red histochemical stain. Nat. Protoc. 1, 1591–1595. https://doi.org/10.1038/nprot.2006.277

Wirths, O., Bayer, T.A., 2010. Neuron Loss in Transgenic Mouse Models of Alzheimer's Disease. Int. J. Alzheimers. Dis. 2010, 1–6. https://doi.org/10.4061/2010/723782

Wu, J., Ishikawa, M., Zhang, J., Hashimoto, K., 2010. Brain imaging of nicotinic receptors in Alzheimer's disease. Int. J. Alzheimers. Dis. 2010, 548913. https://doi.org/10.4061/2010/548913

Yakel, J.L., 2014. Nicotinic ACh receptors in the hippocampal circuit; functional expression and role in synaptic plasticity. J. Physiol. 592, 4147–53. https://doi.org/10.1113/jphysiol.2014.273896

Zolochevska, O., Taglialatela, G., 2016. Non-Demented Individuals with Alzheimer's Disease Neuropathology: Resistance to Cognitive Decline May Reveal New Treatment Strategies. Curr Pharm Des 22, 4063–4068.

Chapter 3: Innate preferences affect results of object recognition task in wild type and Alzheimer's disease mouse models

Tropea MR[1], Sanfilippo G[1], Giannino F[1], Davì V[1], Gulisano W[1], Puzzo D[1,2].

[1]Department of Biomedical and Biotechnological Sciences, Section of Physiology, University of Catania, 95125, Catania, Italy; [2]Oasi Research Institute-IRCCS, 94018, Troina, Italy.

In: J Alzheimers Dis. 2022;85(3):1343-1356.

doi: 10.3233/JAD-215209.

ABSTRACT

Background: Object recognition task (ORT) is a widely used behavioral paradigm to assess memory in rodent models, due to its easy technical execution, the lack of aversive stressful stimuli and the possibility to repeat the test on the same animals. However, mouse exploration might be strongly influenced by a variety of variables.

Objective: To study whether innate preferences influenced exploration in male and female wild type mice and the Alzheimer's disease (AD) model 3xTg.

Methods: We first evaluated how object characteristics (material, size, and shape) influence exploration levels, latency, and exploration modality. Based on these findings, we evaluated whether these innate preferences biased the results of ORT performed in wild type mice and AD models.

Results: Assessment of Exploration levels, i.e., the time spent in exploring a certain object in respect to the total exploration time, revealed an innate preference for objects made in shiny materials, such as metal and glass. A preference for bigger objects characterized by higher affordance was also evident, especially in male mice. When performing ORT, exploration was highly influenced by these innate preferences. Indeed, both wild type and AD mice spent more time in exploring the metal object, regardless of its novelty. Furthermore, the

use of objects with higher affordance such as the cube was a confounding factor leading to “false” results that distorted ORT interpretation.

Conclusion: When designing exploration-based behavioral experiments aimed at assessing memory in healthy and AD mice, object characteristics should be carefully evaluated to improve scientific outcomes and minimize possible biases.

INTRODUCTION

Memory is the faculty of our brain to store and recall information learnt by experience during life and it is tightly related to learning, which is the ability to acquire new skills, actions, bearing, significance and concepts. Different types of memory have been described and, among these, recognition memory is considered a subtype of declarative memory used to recognize already encountered items, people, and situations [1].

During the last decades, the study of recognition memory has gained the interest of several neuroscientists and a wide number of studies has been performed. A great contribution has been provided by studies in animal models such as rodents and non-human primates. However, while recognition memory can be accessible through oral and written language in humans, when using animal models an accurate ethological knowledge of the species is needed. In this context, behavioral paradigms aimed at investigating recognition memory are based on the spontaneous exploration of novel items. If two stimuli are simultaneously presented to a rat or a mouse and one of these two items was already experienced by the animal whereas the other one is new, the animal would spend more time exploring the novel item [2,3]. The Object Recognition Task (ORT) relies on this concept, and it is one of the most used behavioral paradigms to study recognition memory, its

impairment in neurodegenerative disorders such as Alzheimer's disease (AD), and the efficacy of cognitive-enhancing drugs [4]. Different ORT paradigms have been adopted, but beside the specific protocol used, the test usually consists of two phases: i) familiarization or training phase, in which the animal encounters two (or more) identical objects; ii) testing phase, in which the animal is exposed to one (or more) novel objects. The time spent exploring the familiar versus the novel object during the test phase is used as an index of recognition memory. Although ORT is relatively easy to perform, does not require expensive equipment nor a long animal training, or positive/negative reinforcement, several variables can influence the test risking to invalidate the results [5,6]. For example, recognition performance might be affected by the context [7], the exposure time to the objects during the familiarization phase or the delay between familiarization and test phase [3] [3], the number and characteristics of presented objects [8-10] or their position [11], animal strain [12], and sex [13,14]. Among these aspects, we focused on the characteristics of the objects used to evaluate memory in animal models of AD. In fact, it frequently occurs that the difference in exploration of the familiar vs. the novel object does not depend upon a difference in memory performance but on an innate preference for a certain object due to its intrinsic characteristics. If so, the exploration time will change *a priori* because of the higher attractive

properties of the object and ORT results will be doubtful or not reliable. Here, we first studied whether exploration was influenced by exposure to objects of different material, size and shape in wild type mice. Based on these findings, we evaluated how these innate preferences influenced ORT performances in male and female wild type mice and the 3×Tg mouse model of AD.

MATERIALS AND METHODS

Animals

We used young male and female wild type mice (C57BL/6J) and 3×Tg (APPSwe, PS1M146V, and tauP301L) AD mice [15] aged 7-8 months. Mice were kept in the animal facility of the University of Catania, maintained on a 12h light/dark cycle (with lights on at 6.00 AM) in a temperature (23 ± 1° C) and humidity (57 ± 3%) controlled ventilated cabinet. Mice were housed in IVC standard cages enriched with a plastic object used as a nest and crease paper. Food (standard diet cubes) and water (filtered drinking water by particle filter, active carbon filter and UV light) were available *ad libitum*. The experiments complied with the ARRIVE guidelines, were carried out in accordance with the EU Directive 2010/63/EU for animal experiments and received approval by the Institutional Animal Care and Use Committee.

Object Preference Assessment

Object preference assessment was performed by using an apparatus of our design and construction, consisting in an arena (45x45x40cm) made by white matte polymethyl methacrylate non reflective panels. The floor of the arena was coated with a self-adhesive anti reflective film to further avoid reflections. Illumination was provided by a perpendicular diffused light source located 65 cm from the floor of the arena (Fig. 1).

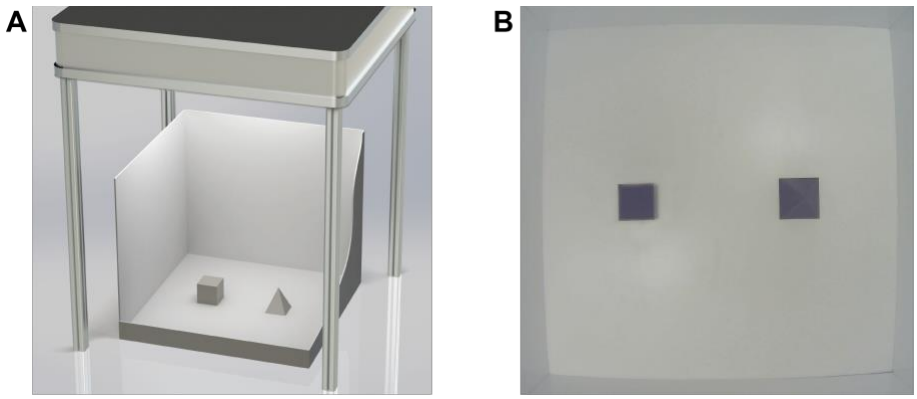

Figure 1 – Arena used to perform behavioral studies. A) Computer rendering of the apparatus. The arena is represented in a sectioned view to allow the visualization of objects placement. Light bulbs are inserted in a lid mounted perpendicular to the arena to ensure a diffuse and homogeneous illumination, avoiding object shadows as much as possible. B) Screenshot obtained from the recording camera placed on top of the arena.

Based on preliminary studies, we chose to use two 6 W light bulbs providing 80 lux on the floor of the arena. Mice underwent a two-day

period of habituation to the arena, where they were allowed to explore the environment for 5 minutes per day. Then, each mouse underwent four days of testing in a random order. The animal was put into the arena with three objects different in material, size, shape or color and allowed to explore them for a total time of 10 minutes. After each trial, the arena and the objects were cleaned with 70% ethanol and dried with absorbent paper. For each object we measured: i) horizontal exploration, considered as the mouse pointing its nose toward the object at a distance not >2 cm, with the mouse standing with all four paws on the floor of the arena [t explor horiz (s)]; ii) vertical exploration, considered as the mouse exploring the object with the two anterior paws lean on the object and the two posterior paws on the floor of the arena [t explor vert (s)]; iii) on-top exploration, considered as the mouse exploring the object standing on it [t explor on-top (s)]; iv) on-top non exploration, time spent sitting or standing on the object, without exploring it [t on top (s)]; v) latency to first approach to each object [latency (s)]. Based on these measurements we calculated Exploration levels and Exploration type.

$$Exploration\ levels = \frac{t\ explor\ [object\ 1] \times\ 100}{t\ total}$$

where t = time and:

- t explor [object1] = t explor horiz [object1] (s) + t explor vert [object1] (s) + t explor on-top [object1] (s)
- t total = t explor [object1] (s) + t explor [object2] (s) + t explor [object3] (s)

Exploration type: horizontal, vertical or on-top, where:

$$Horizontal\ Exploration\ type = \frac{t\ explor\ horiz\ [object\ 1] \times\ 100}{t\ explor\ [object\ 1]}$$

$$Vertical\ Exploration\ type = \frac{t\ explor\ vert\ [object\ 1] \times\ 100}{t\ explor\ [object\ 1]}$$

$$On - top\ Exploration\ type = \frac{t\ explor\ on - top\ [object\ 1] \times\ 100}{t\ explor\ [object\ 1]}$$

Mice with a total exploration time < 5 s were excluded [16].

Choice of objects

All the 3D printed objects were realized as previously described in polylactic acid (PLA) [17]. Briefly, after their design by a computer aided design software (Solidworks, France), 3D models were sliced and converted in g-code by a slicer software (Simplify3D, USA). For 3D printing we used a Prusa-inspired 3D printer customized according to our needs to obtain a 100 μm resolution on z-axis and a printing nozzle diameter of 200 μm.

To assess the preference for materials, we used three cylindrical objects with similar size made by three different materials: glass, metal and PLA. To assess the preference for size, we used three 3D printed cylinders made of PLA, with increasing size. The small object (25 x 22.5 Ø mm) measured half of the medium object (50 x 45 Ø mm), whereas the big object was one third bigger than the medium one (75 x 67.5 Ø mm). To assess the preference for shape, we used a pyramid, a cube and a truncated sphere in PLA. The objects were designed to have comparable dimensions (mean height = 54 ± 2.9 mm).

Object Recognition Task

ORT test was performed as described previously [18] by using the same environmental conditions described for the Object Preference Assessment. After 3 days of habituation (5 min/day), mice underwent the training phase (T1). The mouse was put into the arena and allowed to explore two identical objects placed in the central part of the box, equally distant from the perimeter and the center for 10 min. Twenty-four hours after T1, mice underwent the second trial (T2) to test memory retention for 10 min. In T2, mice were presented with two different objects, respectively a "familiar" (i.e., the one used for T1) and a "novel" object. To understand whether innate preferences might influence memory, we alternated the use of preferred objects identified

in the Object Preference Assessment. In different series of experiments we used: i) Familiar objects: two identical metal cylinders in T1; Novel object: PLA cylinder in T2; ii) Familiar objects: two identical PLA cylinders in T1; Novel object: metal cylinder in T2; iii) Familiar objects: two identical PLA cubes in T1; Novel object: PLA sphere in T2; iv) Familiar objects: two identical PLA spheres in T1; Novel object: PLA cube in T2; v) Familiar objects: two identical PLA spheres in T1; Novel object: PLA pyramid in T2. Animal exploration was defined as the mouse pointing its nose toward the object from a distance not <2 cm. We calculated:

$$Discrimination\ index = \frac{t\ explor\ [novel\ object](s) - \ explor\ [familiar\ object](s)}{t\ explor\ [novel\ object](s) - \ explor\ [familiar\ object](s)}$$

Exploration was scored using a personal computer and mice with a total exploration time <5 s were excluded [16].

Statistical analysis

Data were expressed as mean ± standard error mean (SEM). Statistical analyses were performed by using Systat software (Chicago, IL, USA). We used: two-tailed t-test for comparisons between two groups, one-way ANOVA with Bonferroni post-hoc for comparisons among

different groups, two-way ANOVA for interactions between variables. To assess if mice were able to discriminate between the two objects, we compared the performance obtained in our experimental groups with a fictive group (mean value of 10 independent experiments = 0; standard error = 0.7), as previously described [6].

The level of significance was set at $p < 0.05$.

RESULTS

Assessment of preference in exploring objects of different materials

To investigate whether mice showed a preference for a certain material, they were exposed to three cylinders of similar size but different materials, i.e. metal, glass and PLA (Fig. 2A), randomly positioned in the arena.

Exploration levels (time of exploration of each object/total exploration time) analyses showed that mice spent more time exploring glass (43.21 ± 2.04 % total exploration time) and metal (41.52 ± 2.12 %) objects in respect to PLA ones (15.25 ± 1.31 %), as confirmed by ANOVA ($F_{(2,57)} = 70.74$, $p < 0.0001$; Bonferroni's $p = 0$ for PLA vs. glass or metal; Fig. 2B).

We then evaluated different types of explorations to understand whether the possible influence of object affordance on Exploration Levels. To this end, we distinguished among horizontal exploration, vertical exploration, and on-top exploration. We found that animals spent more time in exploring the three objects by horizontal exploration (one-way ANOVA $F_{(2,57)} = 63.609$, $p < 0.0001$; Bonferroni's $p = 0$ for horizontal exploration vs. vertical or on-top), regardless the object material (two-way ANOVA exploration type*material interaction: $F_{(4,171)} = 0.055$, $p = 0.994$; Fig. 2C). To evaluate the affordance of the chosen objects, we scored the time spent on-top without exploring them (on-top non exploration time). We found that mice climbed on top of all the three objects, suggesting that the cylinder is an object with higher affordance. In particular, mice spent a higher percentage of non-exploration time on-top of the metal cylinder, reflecting a general preference for the metal material (metal: 42.01 ± 6.44 %; glass: 29.91 ± 5.36 %; PLA: 13.07 ± 3.8%; $F_{(2,57)} = 7.47$, $p = 0.001$; Bonferroni's $p = 0.001$ for on-top non exploration between metal and PLA; Fig. 2D).

Finally, to evaluate if animals were particularly attracted by an object, we scored latency, i.e. how many seconds were needed for the mouse to approach a certain object for the first time. As expected, we found a lower latency for glass (8.55 ± 1.9 sec) and metal (20.65 ± 8.42 sec) in respect to PLA (56.7 ± 11.98 sec), suggesting that mice were

preferentially attracted by these materials ($F_{(2,57)}$ = 0.001; Bonferroni's p = 0.001 and 0.012 for metal and glass vs. PLA, respectively; Fig. 2E).

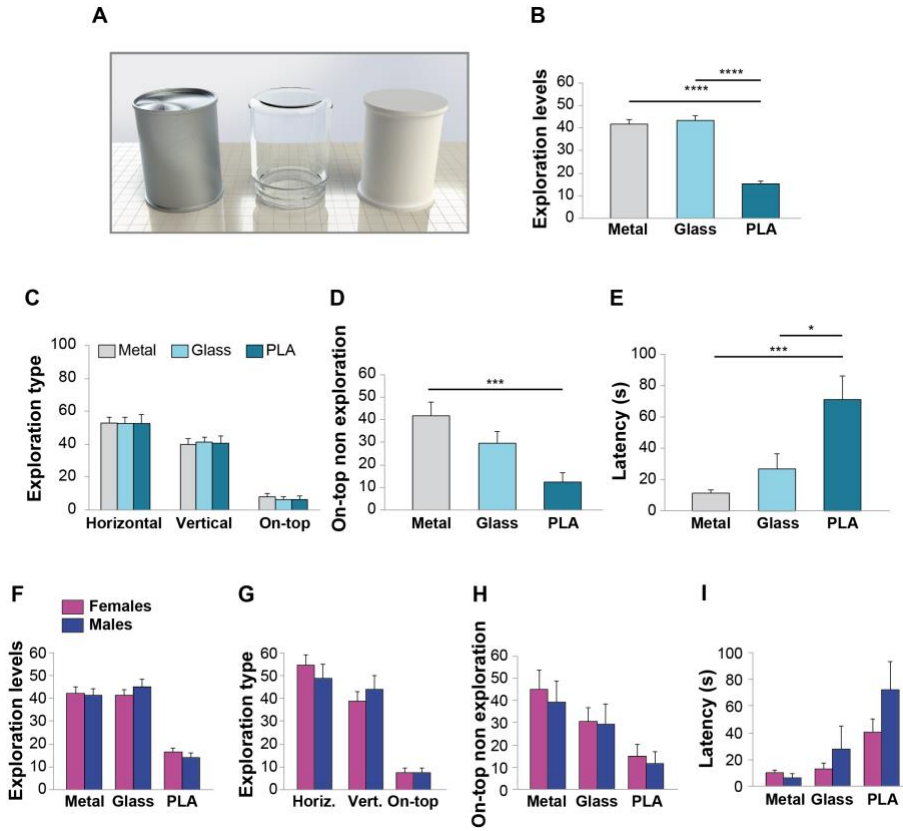

Figure 2 - Mice preferred to explore objects made in metal or glass. A) Metal, glass and PLA objects used to evaluate preference for materials. B) Exploration levels (time of exploration of each object/total exploration time) was higher for metal and glass compared to PLA objects (n = 20 sex-balanced animals). C) Horizontal and vertical exploration were mainly used to approach the objects. Exploration modality was not affected by object material. D) Mice spent more time on top of the metal object. E) Latency to the first approach indicated that mice were preferentially attracted by metal and glass objects. F) Exploration levels as well as Exploration type G), On-top non exploration H) and Latency for different materials I) did not change between males and females. Data expressed as mean ± SEM. *p < 0.05, ***p ≤ 0.001, ****p ≤ 0.0001.

We then analyzed results in respect to sex, to evaluate possible gender differences. We found no differences between females and males in: i) preferences for material (Two-way ANOVA sex*object material interaction: $F_{(2,54)} = 0.559$, $p = 0.575$; Fig. 2F); ii) exploration type (Two-way ANOVA sex*exploration type interaction: $F_{(2,54)} = 0.868$, $p = 0.425$; Fig. 2G), iii) on-top non exploration (Two-way ANOVA sex*on-top non exploration interaction: $F_{(2,54)} = 0.384$, $p = 0.683$; Fig. 2H); iv) latency for different materials (Two-way ANOVA sex*latency interaction: $F_{(2,54)} = 1.161$, $p = 0.321$; Fig. 2I).

Assessment of preference in exploring objects of different size

To investigate whether exploration might be influenced by object size, mice were exposed to three cylinders defined as small, medium and big (Fig. 3A). Exploration levels analysis showed that mice preferentially explored the big object (46.37 ± 1.4 % total exploration time), followed by the medium size object (37.7 ± 1.58 %), whereas they had little interest in the small one (15.93 ± 1.43 %). Thus, preference paralleled the object size as confirmed by statistical analyses ($F_{(2,57)} = 112.762$, $p < 0.0001$; Bonferroni's $p < 0.0001$ for big and medium vs. small and big vs. medium; Fig. 3B).

Object size also influenced exploration type (two-way ANOVA exploration type*material interaction: $F_{(4,171)} = 17.404$, $p < 0.0001$; Fig. 3C). We found a significant difference between the modality used to explore the small object versus the medium and the big one (Fig. 3C). Horizontal modality was mainly dedicated to the small object ($F_{(2,57)} = 16.820$, $p < 0.0001$; Bonferroni's $p = 0.001$ between small and medium; $p < 0.0001$ between small and big; Fig. 3C), whereas vertical and on-top exploration to the medium and big object (vertical: $F_{(2,57)} = 6.594$, $p = 0.003$; Bonferroni's $p = 0.026$ between small and medium; $p = 0.003$ between small and big; on-top: $F_{(2,57)} = 9.37$, $p < 0.0001$; Bonferroni's $p = 0.038$ between small and medium; $p < 0.0001$ between small and big; Fig. 3C). Also, the big object was equally explored by horizontal and vertical modality (Fig. 3C). Analyses of on-top non exploration confirmed this difference, due to the fact that mice could only climb bigger objects, being unable to sit on the small one (small: no time spent on-top; medium: 30.2 ± 5.93 %; big: 44.25 ± 7.37 %; $F_{(2,57)} = 17.489$, $p < 0.0001$; Bonferroni's $p = 0.001$ between small and medium; $p < 0.0001$ between small and big; Fig. 3D).

The preference for objects with higher dimensions and affordance was confirmed by the lower latency for the medium and big object (small: 108.35 ± 12.9 sec; medium: 34.2 ± 6.65 sec; big: 31.7 ± 18.86 sec; $F_{(2,57)}$

= 7.18, p = 0.002; Bonferroni's p = 0.006 and p = 0.005 for small vs. medium and big, respectively; Fig. 3E).

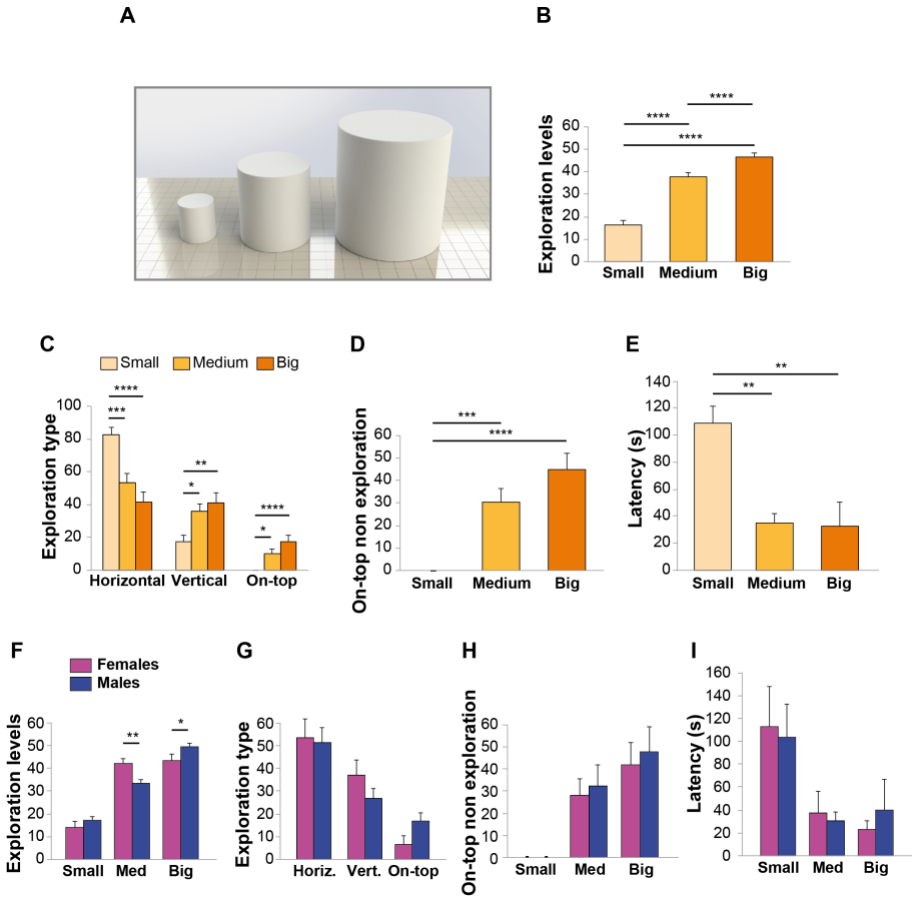

Figure 3 - Mice preferred to explore big and medium size objects. A) Small, medium and big PLA cylinders to evaluate preference for size. B) Exploration levels indicated that mice spent more time exploring the big object followed by the medium size one (n = 20 sex-balanced animals). C) Exploration type depended upon object size. The small object was mainly approached by horizontal exploration, the medium and especially big object also by vertical and on-top exploration. D) The medium and big objects were used for on-top non exploration. E) Latency to the first approach indicated that mice were preferentially attracted by medium and big objects. F) Total exploration time did not differ between males and females. F) Females equally

explored the medium and big object, whereas males preferred the big object. G) No sex differences were recorded in exploration type, on-top non exploration H), and Latency for different size objects I). Data expressed as mean ± SEM. *p < 0.05, **p ≤ 0.01, ***p ≤ 0.001, ****p ≤ 0.0001.

Analyses of performance in female and male mice confirmed that object size influenced exploration time, although a sex-related difference was found (Two-way sex*object size interaction: $F_{(2,54)} = 8.056$, $p = 0.001$; Fig. 3F).

In particular, both females and males preferred to explore the medium and the big object compared to the small one. However, females spent more time than males in exploring the medium object ($p = 0.004$; Fig. 3F), whereas males spent more time than females in exploring the big object ($p = 0.036$; Fig. 3F). Conversely, no sex differences were found when analyzing exploration type, as both females and males preferred horizontal exploration (Two-way sex*exploration type interaction: $F_{(2,54)} = 1.324$, $p = 0.274$; Fig. 3G). Concerning on-top non exploration, both sexes preferred the medium and big object not being able to climb the small one (Two-way ANOVA sex*on-top non exploration interaction: $F_{(2,54)} = 0.072$, $p = 0.931$; Fig. 3H). Latency was not different in males and females (Two-way ANOVA sex*latency interaction: $F_{(2,54)} = 0.191$, $p = 0.827$; Fig. 3I).

Assessment of preference in exploring objects of different shapes

To assess whether shape might influence preference and exploration modality, mice were exposed to three objects of similar size, material (PLA) and color (grey), but different shape, i.e. a pyramid, a cube and a truncated sphere (Fig. 4A).

Exploration levels analysis showed that mice preferentially explored the pyramid (37.20 ± 2.22 % total exploration time) and the cube (41.45 ± 2.76 % total exploration time) in respect to the truncated sphere (21.33 ± 2.02 % total exploration time) ($F_{(2,57)} = 20.2$, $p < 0.0001$; Bonferroni's $p < 0.0001$ comparing sphere with pyramid or cube; Fig. 4B).

Animals preferred the horizontal exploration modality compared to the vertical or the on-top exploration ($F_{(2,57)} = 39.299$, $p < 0.0001$; Bonferroni's $p < 0.0001$ comparing horizontal vs. vertical or on-top; Fig. 4C). The preference for horizontal exploration was evident for all of the three objects, whereas on-top exploration was mainly dedicated to the cube, due to the difficulty in climbing the pyramid or the truncated sphere ($F_{(2,57)} = 23.749$, $p < 0.0001$; Bonferroni's $p < 0.0001$ comparing cube vs. pyramid or sphere; Fig. 4C). This was confirmed by analyses of on-top non exploration (pyramid: no time spent on-top; cube: 47 ± 8.07 %; truncated sphere: 4.08 ± 1.87 %; $F_{(2,57)} = 29.608$, $p < 0.0001$; Bonferroni's $p < 0.0001$ comparing cube vs. pyramid or sphere; Fig. 4D). Finally, objects' shape did not influence latency (pyramid: 25.85 ±

10.42 %; cube: 24.75 ± 6.02 %; truncated sphere: 13.09 ± 3.47 %; $F_{(2,57)}$ = 0.833, p = 0.44; Fig. 4E).

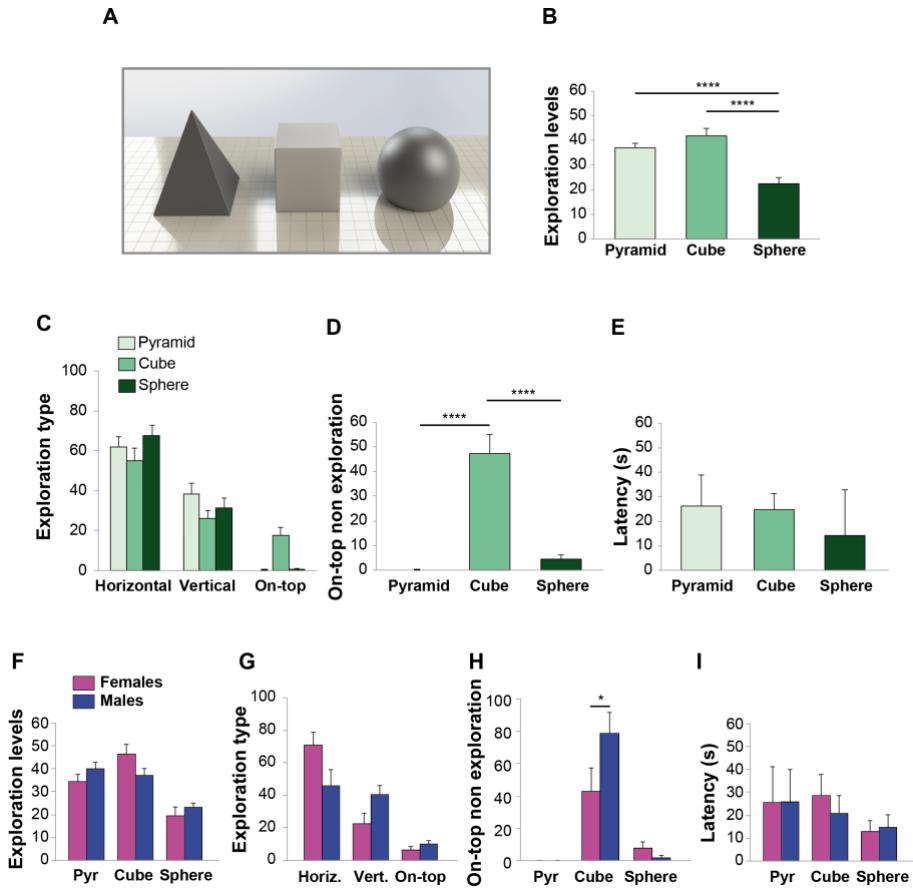

Figure 4 - Mice preferred to explore objects with higher affordance. A) PLA pyramid, cube and truncated sphere to evaluate preference for different shapes. B) Exploration levels indicated that mice spent more time exploring objects with higher affordance such as the pyramid and the cube (n = 20 sex-balanced animals). C) Horizontal and vertical exploration were mainly used to approach the objects and were not influenced by object shape. On-top exploration and D) On-top non exploration was essentially performed for the cube. E) Latency to the first approach was similar for the three objects. E) Exploration levels and Exploration type G) did not significantly differ

between males and females. However, females preferred horizontal vs. vertical exploration, whereas males equally explored object by horizontal and vertical exploration. H) On-top non exploration for the cube was higher in males. I) Latency for different shapes did not change between males and females. Data expressed as mean ± SEM. *$p < 0.05$, ****$p \leq 0.0001$.

No differences were found between males and females in preference for different shapes (Two-way ANOVA sex*object shape interaction: $F_{(2,54)} = 3.031$, $p = 0.057$; Fig. 4F). Analyses of results showed a difference in exploration type between females and males (Two-way ANOVA sex*exploration type interaction: $F_{(2,54)} = 6.732$, $p = 0.002$; Fig. 4G). In particular, females preferred horizontal exploration ($p < 0.0001$; Fig. 4G), whereas males spent a similar amount of time in exploring objects by horizontal and vertical exploration ($p = 1$; Fig. 4G). However, male mice showed a higher on-top non exploration for the cube compared with females ($p = 0.038$; Fig. 4G). No differences were found when latency (Two-way ANOVA sex*latency interaction: $F_{(2,54)} = 0.064$, $p = 0.871$; Fig. 4I).

Innate object preference prejudiced ORT results in wild type and Alzheimer's disease mice

Based on the Object Preference assessment, we investigated how the choice of objects influenced results of exploration-based behavioral test

commonly used to investigate memory. To this end, we performed ORT in wild type and AD mice to evaluate recognition memory by assessing the differences in exploration of a familiar versus a novel object [4,18]. In particular, we exposed mice to the objects toward which mice showed an innate preference and to neutral objects. We selected the most representative objects of a certain category and showed an example of ORT performed by using two objects with an evident difference in brightness (metal vs. PLA) or affordance (cube vs. sphere).

In a series of experiments, we evaluated the impact of objects made by different materials. During the training phase (T1), mice were exposed to two identical metal cylinders for 10 minutes. After a 24 hrs interval, mice were exposed to a metal cylinder (familiar object) and PLA cylinder (novel object) (Fig. 5A). We found that both wild type and AD mice spent a similar amount of time in exploring the familiar and the novel object during the testing phase (t-test wild type: $t_{(18)} = 1.274$, $p = 0.219$; AD: $t_{(18)} = 0.818$, $p = 0.424$ between familiar and novel object; Fig. 5B). Analyses of Discrimination Index confirmed that there was no difference between wild type and AD mice (0.09 ± 0.07 vs. 0.06 ± 0.07; $t_{(18)} = 0.282$; $p = 0.781$; Fig. 5C) and that both genotypes were (apparently) unable to learn since Discrimination Index was not different than zero when compared with the fictive group (t-test wild type: $t_{(18)} = 0.936$, $p = 0.362$; AD: $t_{(18)} = 0.673$, $p = 0.510$; Fig. 5C). No

differences were recorded in total exploration time ($t_{(18)}$ = 0.445, p = 0.662; Fig. 5D). Males and females of both experimental groups behaved similarly when analyzing the time spent in exploring the familiar and novel object (Two-way ANOVA sex*familiar-novel object interaction in wild type: $F_{(1,16)}$ = 1.020, p = 0.328; in AD mice: $F_{(1,16)}$ = 0.052, p = 0.822; Fig. 5E) and Discrimination Index (sex*genotype interaction: $F_{(1,16)}$ = 0.104, p = 0.751; Fig. 5F).

Thus, in this experimental condition, wild type did not present the increase in exploration of the novel object expected when memory is intact.

Conversely, when we used two identical PLA cylinders as familiar objects during the training phase, and a PLA cylinder paired with a metal cylinder as a novel object during the testing phase (Fig. 4G), both wild type and AD mice spent more time in exploring the novel object (t-test wild type: $t_{(18)}$ = 6.256, p < 0.0001; AD: $t_{(18)}$ = 3.363, p = 0.003 between familiar and novel object; Fig. 5H). These results were confirmed by analyses of Discrimination Index that suggested no significant differences between wild type and AD performances (0.36 ± 0.08 vs. 0.20 ± 0.08; $t_{(18)}$ = 1.320; p = 0.203; Fig. 5I). Notably, both genotypes resulted able to learn as Discrimination Index was different than zero when compared with the fictive group (t-test wild type: $t_{(18)}$ =

3.372, p = 0.003; AD: $t_{(18)} = 2.363$, p = 0.030; Fig. 5I). Total exploration time did not differed between the two genotypes ($t_{(18)} = 0.750$; p = 0.463; Fig. 5J).

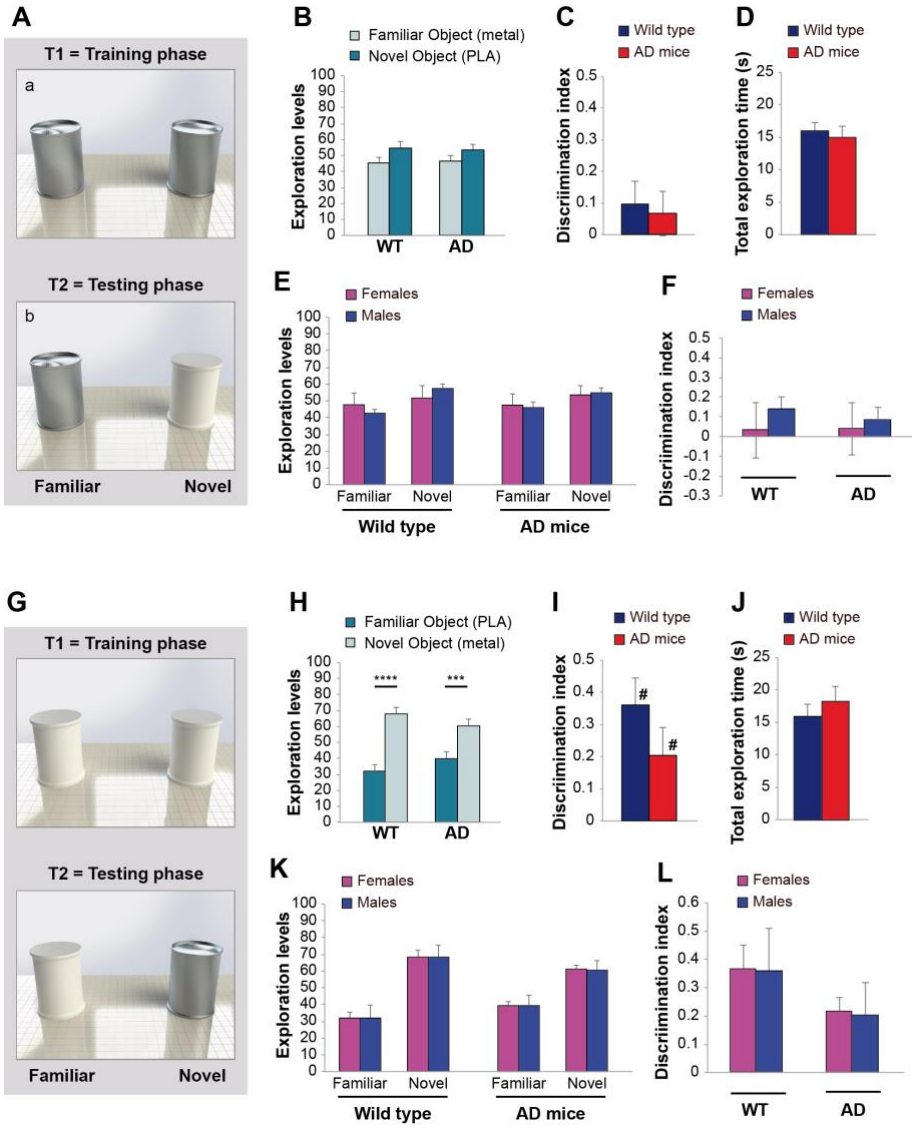

Figure 5. The use of metal objects biased results of object recognition task in wild type and AD mice. A) Objects used during the T1 training phase (a) and the T2 testing phase (b). B) Both wild type and AD mice dedicated the same amount of time in exploring the familiar and the novel object (n = 10/10 sex-balanced animals). C)

Discrimination Index indicated an impairment of recognition memory in both wild type and AD mice. D) Total exploration time was similar in wild type and AD mice. E) Males and females of both genotypes spent a similar amount of time in exploring the familiar and the novel object; F) No gender differences were found in Discrimination Index of wild type and AD mice. G) Objects used during the T1 training phase (a) and the T2 testing phase (b) in another series of experiments. H) Both wild type and AD mice dedicated a higher amount of time in exploring the novel object (n = 10/10 sex-balanced animals). I) Discrimination Index indicated a normal recognition memory in both wild type and AD mice. J) Total exploration time was similar in wild type and AD mice. K) No gender differences were found in exploration of novel vs. familiar object and L) Discrimination Index in wild type and AD mice. Data expressed as mean ± SEM. ***$p < 0.005$, ****$p \leq 0.0001$, # difference with zero (comparison with fictive group).

No gender differences were found in time spent exploring the familiar vs. novel object (Two-way ANOVA sex*familiar-novel object interaction in wild type: $F_{(1,16)} = 0.004$, $p = 0.952$; in AD mice: $F_{(1,16)} = 0.008$, $p = 0.929$; Fig. 5K) or Discrimination Index (sex*genotype interaction: $F_{(1,16)} = 0.486$, $p = 0.496$; Fig. 5L).

Thus, in this experimental condition, AD mice did not present the expected impairment of memory. Overall, these experiments suggested that the use of an attractive metal object either used as familiar or novel object prejudiced results of ORT that erroneously indicated an impairment of memory in wild type mice or a normal memory in AD mice.

In a second series of experiments, we evaluated whether objects of different shapes might influence ORT. During the training phase mice were exposed to two identical PLA cubes (Fig. 6Aa). As expected, no differences were found in exploration levels of the two cubes (wild type: $t_{(22)} = 1.465$, $p = 0.154$; AD: $t_{(22)} = 1.794$, $p = 0.087$ between familiar and novel object; Fig. 6B) or in total exploration time ($t_{(22)} = 0.294$, $p = 0.771$; Fig. 6C). After 24 hrs, mice were exposed to a PLA sphere as a novel object (Fig. 6Ab). We found that both genotypes spent a higher amount of time in exploring the familiar object (t-test wild type: $t_{(22)} = 9.435$, $p < 0.0001$; AD: $t_{(18)} = 2.937$, $p = 0.008$ between familiar and novel object; Fig. 6D), with no differences in total exploration time ($t_{(22)} = 0.392$; $p = 0.699$; Fig. 6E). Discrimination Index confirmed that wild type and AD mice behaved similarly, both preferring the exploration of the familiar object (-0.32 ± 0.04 vs. -0.17 ± 0.08; $t_{(22)} = 1.613$, $p = 0.121$; Fig. 6F). This was particularly evident for wild type mice that showed a Discrimination Index different than zero but negative (comparison with the fictive group: t-test wild type: $t_{(20)} = 2.913$, $p = 0.001$; Fig. 6F). No differences were found in males and females in time spent exploring the familiar vs. the novel object (Two-way ANOVA sex*familiar-novel object interaction in wild type: $F_{(1,20)} = 0.602$, $p = 0.447$; in AD mice: $F_{(1,20)} = 0.023$, $p = 0.882$; Fig. 6G), as confirmed by the analyses of

Discrimination Index (sex*genotype interaction: $F_{(1,20)} = 0.136$, $p = 0.716$; Fig. 6H).

This result was opposite to that normally expected, since wild type mice should dedicate more time in exploring the novel object, whereas AD mice, due to their memory deficit, usually spent the same amount of time in exploring the familiar and the novel object. Thus, in this experimental setting, the use of objects with higher affordance such as the cube during the training phase did not allow a correct evaluation of memory.

We then inverted the objects and used two identical PLA spheres as familiar objects and a PLA cube as a novel object (Fig. 6Ib-c). Also in this case, no differences were found in Exploration levels of the two spheres during the training phase (wild type: $t_{(22)} = 1.432$, $p = 0.166$; AD: $t_{(22)} = 1.921$, $p = 0.368$ between familiar and novel object; Fig. 6J) or in total exploration time ($t_{(20)} = 0.021$, $p = 0.983$; Fig. 6K). However, a higher total exploration time in T1 was recorded in wild type mice exposed to cubes (Fig. 6C) in respect to spheres (Fig. 6K) ($t_{(22)} = 3.037$, $p = 0.006$).

During the training phase, wild type mice spent a higher % of time in exploring the novel object (t-test: $t_{(22)} = 5.322$, $p < 0.0001$), whereas AD mice dedicated the same amount of time in exploring the two objects

($t_{(20)}$ = 0.814, p = 0.425 between familiar and novel object; Fig. 6L). Total exploration time was unchanged ($t_{(21)}$ = 0.081; p = 0.936; Fig. 6M). Analyses of Discrimination Index confirmed the difference between wild type and AD mice (0.27 ± 0.07 vs. 0.04 ± 0.08; $t_{(21)}$ = 2.136, p = 0.045) and that only wild type mice were able to learn (t-test vs. fictive group wild type: $t_{(20)}$ = 2.695, p = 0.014; AD: $t_{(19)}$ = 0.429, p = 0.673; Fig. 6N). No gender differences were found in exploration (sex*familiar-novel object interaction in wild type: $F_{(1,20)}$ = 0.356, p = 0.558; in AD mice: $F_{(1,18)}$ = 1.026, p = 0.325; Fig. 6O) and Discrimination Index (sex*genotype interaction: $F_{(1,19)}$ = 0.056, p = 0.816; Fig. 6P).

Thus, when we used the sphere in the training phase and the cube in the testing phase, ORT results allowed to distinguish between a normal cognition in wild type animals and the expected impairment in AD mice.

Even if this choice of objects could be appropriate, considering that the use of objects with higher affordance such as the cube might represent a bias, we performed another series of experiments maintaining the sphere as a familiar object and substituting the cube with the pyramid as a novel object (Fig. 6Ic).

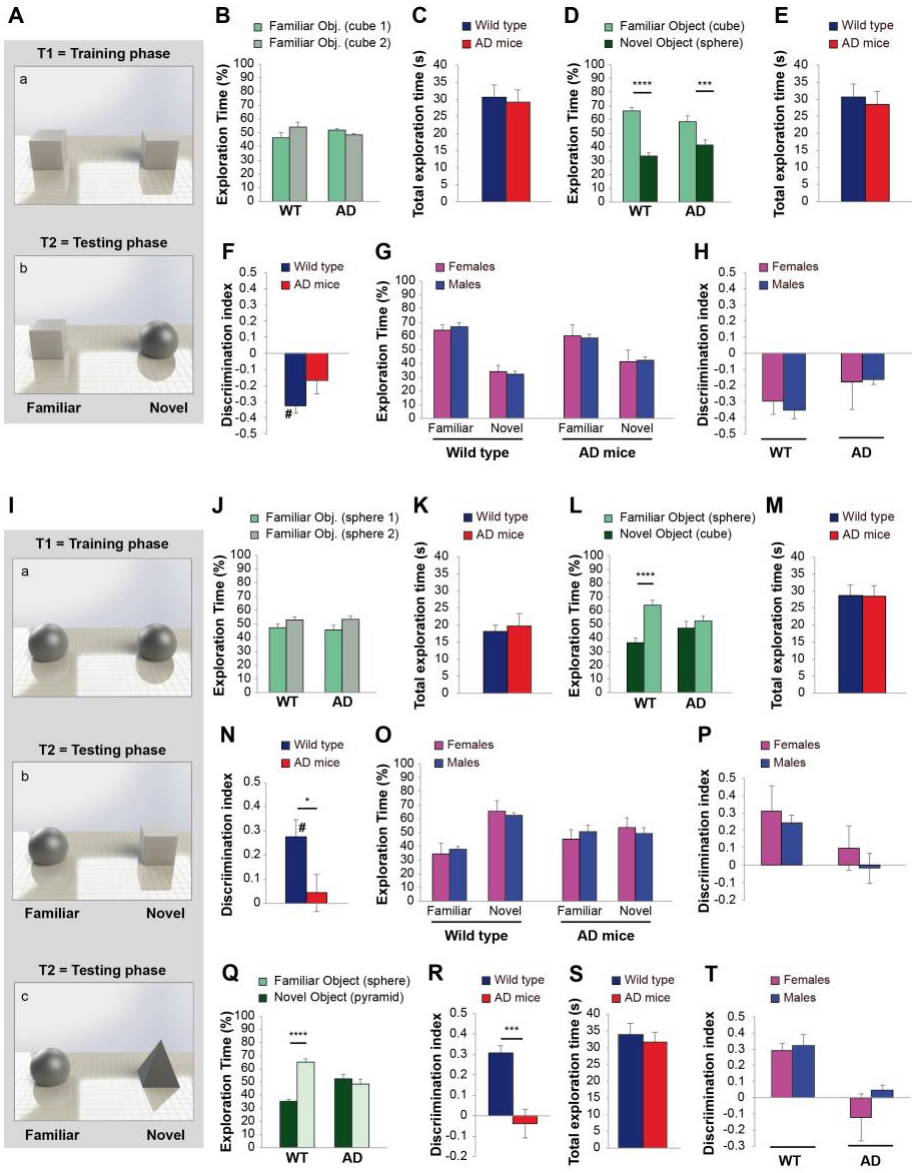

Figure 6. Shape of the objects affects results of object recognition task. A) Objects used during the training (a) and the testing phase (b). B) Mice spent the same amount of time in exploring the two identical objects during the training phase. C) No difference was found between wild type and AD mice in total exploration time. D) Both wild type and AD mice dedicated a higher amount of time in exploring the familiar object (n = 12/12 sex-balanced animals). H) Total exploration time was

similar in wild type and AD mice. F) Discrimination Index indicated a strong impairment of recognition memory in both genotypes, particularly evident for wild type mice. G) No gender differences were found in exploration of novel vs. familiar object and H) Discrimination Index in wild type and AD mice. I) Objects used during the training (a) and the testing phases (b,c). J) Mice spent the same amount of time in exploring the two identical objects during the training phase. K) No difference was found between wild type and AD mice in total exploration time. L) Wild type mice dedicated a higher amount of time in exploring the novel object, whereas AD mice explored indifferently the familiar and the novel object (n = 12/11 sex-balanced animals). M) Total exploration time was similar in wild type and AD mice. N) Discrimination Index indicated a normal recognition memory in wild type mice, and impairment in AD mice. O) No gender differences were found in exploration of novel vs. familiar object and P) Discrimination Index in wild type and AD mice. Q) Exploration times of familiar and novel object during the testing phase (setting c) showed that wild type but not AD mice spent a higher amount of time exploring the novel object (n = 10/10 sex-balanced animals). R) Discrimination Index indicated a normal recognition memory in wild type mice, and impairment in AD mice. S) Total exploration time was similar in wild type and AD mice. T) No gender differences were found in Discrimination Index in wild type and AD mice. Data expressed as mean ± SEM. * < 0.05, ***p < 0.005, ****p ≤ 0.0001, # difference with zero.

These experiments confirmed that the use of neutral objects is the most appropriate as wild type mice spent more time in exploring the novel object, i.e. the pyramid, compared to the familiar object (t-test: $t_{(18)}$ = 10.318, p < 0.0001; Fig. 6Q), whereas AD mice dedicated a similar

amount of time in exploring the two objects (t-test: $t_{(18)} = 0.691$, $p = 0.498$; Fig. 6Q).

The Discrimination Index was different between wild type and AD mice (0.30 ± 0.03 vs. -0.03 ± 0.07; t-test: $t_{(18)} = 3.914$, $p = 0.001$; Fig. 6R), and indicated that only wild type animals were able to learn (t-test vs. fictive group wild type: $t_{(18)} = 3.775$, $p = 0.001$; AD: $t_{(18)} = 0.363$, $p = 0.721$; Fig. 6R). No differences were recorded in total exploration time ($t_{(18)} = 0.487$; $p = 0.632$; Fig. 6S) nor gender differences in exploration levels (sex*familiar-novel object interaction in wild type: $F_{(1,16)} = 0.246$, $p = 0.627$; in AD mice: $F_{(1,16)} = 2.428$, $p = 0.139$; data not shown) and Discrimination Index (sex*genotype interaction: $F_{(1,16)} = 0.605$, $p = 0.448$; Fig. 6T).

Thus, the use of neutral objects allowed distinguishing between normal and impaired memory in wild type and AD mice, avoiding the possible biases due to the use of attractive objects toward which mice manifest an innate preference.

DISCUSSION

Exploration is an innate behavior aimed at providing information about the environment and particular items or individuals. Given its

ubiquitous nature across species, exploratory behavior has been considered a powerful tool to study cognitive and affective performance in pre-clinical research. A variety of tests aimed to investigate memory are based on novelty exploration [19]. Several objects, such as pyramids, parallelepipeds, cubes, hemispheres, truncated pyramids but even complex objects such as coffee mugs, cans, Playmobil and Lego toys, PVC pipes, glass vases and candlesticks, have been used to perform ORT or other exploration-based studies in rodents [20]. The choice of materials is also variable, since objects used can be made of glass, porcelain, metal, plastic, rubber, and wood [20].

In this manuscript we have confirmed that intrinsic object qualities might influence exploration behavior and affect the results of test aimed at investigating memory in animal models.

We found that shining objects made of metal or glass elicited a greater curiosity in mice, consistent with previous studies [10,20]. In fact, although rats and mice have limited color vision and show poor color discrimination, they are able to discriminate between stimuli that differ in brightness [21,22]. This implies that, when using these objects to perform ORT or similar studies, the experimenter might not distinguish between memory performance and the innate attraction towards shiny objects. Our results demonstrated that when pairing a metal with a PLA

object, ORT results were clearly biased. When the metal cylinder was used either as a familiar or a novel object, both wild type and AD mice spent more time in exploring it during the testing phase. Therefore, if a shiny object is used as a familiar object, one can wrongly interpret that wild type mice had memory impairment. Conversely, if it is used as a novel object, results might be read as AD mice having a normal memory. Thus, the use of metal objects is not recommended, especially if paired with plastic ones. It would be more appropriate to randomly alternate metal and glass as familiar or novel objects, and not to use them together with neutral objects made in plastic or, as in our experiments, in PLA. Otherwise, PLA objects might be used alone, considering that total exploration time is maintained in an acceptable range and that, if brilliant objects are not present during the test, mice will spend more time in exploring PLA objects, as previously demonstrated [18].

When studying exploration behavior related to objects of different size, we found that the objects with big and medium dimensions appeared more suitable for exploration, even if the bigger object was mainly used for climbing or sitting. Conversely, the small object resulted the less explored and attractive. This is in line with previous studies suggesting that object size influenced exploration and preference [23] probably

because an object with a similar size to the animal, results in a higher affordance. Indeed, affordance is referred to what animals could perceive, recognize, and memorize of an object [10], and depends upon the relationship between the properties of objects and the abilities of animals [24]. Therefore, affordance is influenced by those characteristics of the object that attract the animal because of a possible interaction with it [25]. In general, an object with higher affordance is the one that the mouse could lean on, climb onto, grasp or perform other actions belonging to common rodent activities, or an object able to elicit sensory perceiving. Consistently, our findings showed that the small object, approachable only by horizontal exploration, was less explored in respect to the medium and the big object that could be also explored by vertical and on-top exploration. Consequently, if the aim of the study is to evaluate memory, it would be better to choose an object with high affordance that mice are interested to explore but with characteristics that do not allow an excessive active interaction to avoid distraction and a decrease of exploration time. In agreement with previous findings, a medium size object, i.e., comparable to mouse dimension, should be preferentially chosen [26], and, in any case, it would be better not to associate objects of different size in the same experimental protocol.

Concerning possible sex-differences, we found that females equally explored the medium and the big object, whereas males preferred the

big object. Although we cannot explain this different behavior, we can speculate that it might depend upon the mouse size, being males bigger than females (mean weight = 33 ± 2 vs. 26 ± 2 grams).

Affordance also addressed the preference related to the object shape. Previous studies have demonstrated that mice explored objects that can be climbed significantly longer than objects that can only be touched [10]. In our experimental setting, mice mainly explored the cube and the pyramid, compared to the truncated sphere. However, they spent a higher amount of time sitting on the cube that was used as a sort of "observation tower" to explore the surrounding environment.

This behavior was particularly evident in male mice and influenced exploration type. In fact, while female behavior mirrored the common exploration type preference (horizontal > vertical > on-top), males displayed no differences between horizontal and vertical exploration, and spent more time standing on the cube to visualize the surrounding environment. This might be related to sex differences in navigation and object exploration [1,2]. In fact, it has been previously demonstrated that females navigate using both landmarks and Euclidean geometry, preferentially encoding information based on objects characteristics and

locations, whereas males are inclined to use geometric cues using the shape of the environment as a reference [3,5,6].

Here, the use of objects with high affordance such as the cube affected ORT results especially in wild type mice that spent a very high amount of time exploring the cube during the testing phase. This resulted in a clear inversion of Discrimination Index that indicates memory impairment. Furthermore, the higher time spent in exploring the familiar cube versus the novel object, determined a false alteration of novelty preferences, which is a characteristic of autism spectrum disorders and other stereotyped behaviors [27]. This bias was avoided by using a different object that, although with good affordance, cannot be climbed, i.e., the pyramid.

In conclusion, in line with previous findings, we have shown that intrinsic characteristics of the object used affect total exploration time, latency, recognition and Discrimination Index. Objects in PLA, with a similar size to that of the animal and shapes preserving a good affordance resulted more appropriate to perform behavioral tests based on exploration. These findings should be considered when performing memory tests based on novelty to provide reliable data.

Acknowledgements

This work was supported by University of Catania intramural funds (Progetto Piaceri) to D.P.

Conflict of Interest/Disclosure Statement

The authors have no conflict of interest to report.

REFERENCES

[1] Squire LR, Wixted JT, Clark RE (2007) Recognition memory and the medial temporal lobe: a new perspective. *Nat Rev Neurosci* **8**, 872–883.

[2] Eichenbaum H, Yonelinas AP, Ranganath C (2007) The Medial Temporal Lobe and Recognition Memory. *Ann Rev Neurosci* **30**, 123–152.

[3] Ennaceur A, Delacour J (1988) A new one-trial test for neurobiological studies of memory in rats. 1: Behavioral data. *Behav Brain Res* **31**, 47–59.

[4] Zhang R, Xue G, Wang S, Zhang L, Shi C, Xie X (2012) Novel object recognition as a facile behavior test for evaluating drug effects in AβPP/PS1 Alzheimer's disease mouse model. *J Alzheimers Dis* **31**, 801–12.

[5] Ameen-Ali KE, Easton A, Eacott MJ (2015) Moving beyond standard procedures to assess spontaneous recognition memory. *Neurosci Biobehav Rev* **53**, 37–51.

[6] Akkerman S, Prickaerts J, Steinbusch HWM, Blokland A (2012) Object recognition testing: Statistical considerations. *Behav Brain Res* **232**, 317–322.

[7] Piterkin P, Cole E, Cossette M-P, Gaskin S, Mumby DG (2008) A limited role for the hippocampus in the modulation of novel-object preference by contextual cues. *Learn Mem* **15**, 785–791.

[8] Oliveira AMM, Hawk JD, Abel T, Havekes R (2010) Post-training reversible inactivation of the hippocampus enhances novel object recognition memory. *Learn Mem* **17**, 155–160.

[9] Hale G, Good M (2005) Impaired Visuospatial Recognition Memory but Normal Object Novelty Detection and Relative Familiarity Judgments in Adult Mice Expressing the APPswe Alzheimer's Disease Mutation. *Behav Neurosci* **119**, 884–891.

[10] Ennaceur A (2010) One-trial object recognition in rats and mice: Methodological and theoretical issues. *Behav Brain Res* **215**, 244–254.

[11] Williams MT, Herring NR, Schaefer TL, Skelton MR, Campbell NG, Lipton JW, McCrea AE, Vorhees C V. (2007) Alterations in Body Temperature, Corticosterone, and Behavior Following the Administration of 5-Methoxy-Diisopropyltryptamine ('Foxy') to Adult Rats: a New Drug of Abuse. *Neuropsychopharmacology* **32**, 1404–1420.

[12] Şık A, van Nieuwehuyzen P, Prickaerts J, Blokland A (2003) Performance of different mouse strains in an object recognition task. *Behav Brain Res* **147**, 49–54.

[13] Frick KM, Gresack JE (2003) Sex Differences in the Behavioral Response to Spatial and Object Novelty in Adult C57BL/6 Mice. *Behav Neurosci* **117**, 1283–1291.

[14] Bettis T, Jacobs LF (2012) Sex differences in object recognition are modulated by object similarity. *Behav Brain Res* **233**, 288-92.

[15] Oddo S, Caccamo A, Shepherd JD, Murphy MP, Golde TE, Kayed R, Metherate R, Mattson MP, Akbari Y, LaFerla FM (2003) Triple-Transgenic Model of Alzheimer's Disease with Plaques and Tangles. *Neuron* **39**, 409–421.

[16] Gulinello M, Mitchell HA, Chang Q, O'Brien WT, Zhou Z, Abel T , Wang L , Corbin JC, Veeraragavan S, Samaco RC, Andrews NA, Fagiolini M, Cole TB, Burbacher TM, Crawley JN (2019) Rigor and reproducibility in rodent behavioral research. *Neurobiol Lear Mem* **165**, 106780.

[17] Gulisano W, Tropea MR, Arancio O, Palmeri A, Puzzo D (2018) Sub-efficacious doses of phosphodiesterase 4 and 5 inhibitors improve memory in a mouse model of Alzheimer's disease. *Neuropharmacology* **138**, 151–159.

[18] Gulisano W, Melone M, Ripoli C, Tropea MR, Li Puma DD, Giunta S, Cocco S, Marcotulli D, Origlia N, Palmeri A, Arancio O, Conti F, Grassi C, Puzzo D (2019) Neuromodulatory Action of Picomolar Extracellular Aβ42 Oligomers on Presynaptic and Postsynaptic Mechanisms Underlying Synaptic Function and Memory. *J Neurosci* **39**, 5986–6000.

[19] Leger M, Quiedeville A, Bouet V, Haelewyn B, Boulouard M, Schumann-Bard P, Freret T (2013) Object recognition test in mice. *Nature Prot* **8**, 2531–2537.

[20] Antunes M, Biala G (2012) The novel object recognition memory: neurobiology, test procedure, and its modifications. *Cogn Process* **13**, 93–110.

[21] Jacobs GH, Fenwick JA, Williams GA (2001) Cone-based vision of rats for ultraviolet and visible lights. *J Exp Biol* **204**, 2439–46.

[22] Jacobs GH (1993) The distribution and nature of colour vision among the mammals. *Biol Rev* **68**, 413–471.

[23] Buccafusco JJ (2000) Methods of behavior analysis in neuroscience. 1st ed. Boca Raton (FL): CRC Press/Taylor & Francis.

[24] Chemero A, Heyser C (2005) Object Exploration and a Problem with Reductionism. *Synthese* **147**, 403–423.

[25] Blaser R, Heyser C (2015) Spontaneous object recognition: a promising approach to the comparative study of memory. *Front Behav Neurosci* **9**, 183.

[26] Levin ED, Buccafusco JJ (2006) Introduction. In: Levin ED, Buccafusco JJ, editors. Animal Models of Cognitive Impairment. Boca Raton (FL): CRC Press/Taylor & Francis.

[27] Jacob S, Landeros-Weisenberger A, Leckman JF (2009) Autism spectrum and obsessive-compulsive disorders: OC behaviors, phenotypes and genetics. *Autism Res* **2**, 293–311.

General Discussion

Aβ peptides presents a characteristic biphasic dose-response curve, where low pM doses, in the range of the concentration physiologically present in the brain, exert a cognitive enhancing effect, while high concentrations are detrimental.

This hormetic behavior might hold the key in understanding AD pathophysiology.

Indeed, our findings evidenced interesting differences and similarities between low versus high oAβ_{42} concentrations.

Aβ crosstalk with cyclic nucleotides

Low and high oAβ42 levels affect the same key intracellular pathways involved in synaptic plasticity and memory (i.e., cAMP/PKA/p-CREB, NO/cGMP/PKG/p-CREB cascade, CaMKII, BDNF), leading to their stimulation when at pM concentrations, or inhibition when at nM concentrations (Puzzo et al., 2005, 2009; Ghosh and Giese, 2015; Song et al., 2015; Opazo et al., 2018).

In physiological conditions, cAMP and cGMP are both able to stimulate Aβ production. This increase of Aβ, in turn, induces a series of pre- and post-synaptic modifications involving cyclic nucleotides to ensure memory formation.

In particular, studies aimed at understanding the molecular mechanisms underlying cAMP regulation of Aβ production have evidenced that cAMP induces a *de novo* synthesis of APP by stimulating PKA (Su et al., 2003; Ricciarelli et al., 2014). This cAMP/PKA/APP/Aβ cascade is

decisive to elicit LTP and memory consolidation. Differently from cAMP, which stimulates Aβ production by increasing APP synthesis, cGMP does not modify APP expression but affects APP processing. Specifically, cGMP stimulates APP and BACE-1 to converge in the endolysosomal compartment (Palmeri et al., 2017) where amyloidogenic processing is favored (Tam et al., 2014). The role of the cyclic nucleotides in mediating the physiological effect of Aβ is, however, not confined to the regulation of Aβ production. Indeed, in the project described in Chapter 1 (Gulisano et al., 2019), we have shown that the enhancement of LTP and memory by low pM Aβ is blocked by inhibitors of the NO/cGMP/PKG pathway and correlates with an increased expression of nNOS. Additionally, pM Aβ increased p-CREB levels, known to be critical in cyclic nucleotides regulation of gene expression during late-LTP and long-term memory formation. Thus, in the healthy synapse, cGMP acts both upstream of Aβ, by regulating its production, and downstream, by modulating its effects, thus suggesting the existence of a cGMP-Aβ-cGMP loop.

Therefore, in physiological conditions, Aβ and cyclic nucleotides interaction is beneficial leading to CREB phosphorylation, LTP and memory.

Conversely, AD patients precent a decrease of both cAMP and cGMP levels (Bonkale et al., 1999; Hesse et al., 2017; Ugarte et al., 2015) and preclinical studies have demonstrated that intrahippocampal infusion of nM Aβ decreases cAMP levels in the hippocampus of mice (Zhang et al., 2014) and Aβ treatment of cultured hippocampal neurons leads to the inactivation of PKA (Vitolo et al., 2002). Also, Aβ inhibits the physiological increase in cGMP immunoreactivity occurring after LTP induction in murine hippocampal slices (Puzzo et al., 2005). Interfering

with cyclic nucleotides pathways, high concentrations of Aβ result in a reduction of CREB phosphorylation and consequent synaptic plasticity impairment (Rosa et al., 2015; Puzzo et al., 2009; Puzzo et al., 2005).

Interestingly, high nM concentrations of oAβ42 require APP to impair synaptic plasticity and memory, as APP mediates Aβ and tau neuronal internalization at toxic concentrations. (Ripoli et al., 2014; Puzzo et al., 2017).

Aβ crosstalk with α7nAChRs

Our findings, described in chapter 1 (Gulisano et al., 2019) demonstrated that, when at low concentrations, $oA\beta_{42}$ exerts a positive effect acting at the extracellular level trough α7nAChRs, increasing glutamate release at the hippocampus and boosting the formation of l-LTP and long-term memory.

In physiological conditions Aβ works as a neuromodulator, ensuring synaptic plasticity and memory processes through α7nAChRs, and the lack of the α7nAChR suppresses Aβ physiological function impairing LTP and memory.

On the other hand, several studies indicate that cholinergic transmission is impaired in early AD. Indeed, the most consistent neuronal loss throughout the progression of AD is found in long projection neurons, particularly cholinergic neurons of the basal forebrain (Mufson et al., 2003). Significantly, loss of cholinergic neurons in the nucleus basalis of Meynert, decrease of choline acetyltransferase (ChAT) activity and reduction of nAChRs have been highly correlated with AD progression (Burghaus et al., 2000; Dickson et al., 1995; Engidawork et al., 2001;

Kuhn et al., 2015; Mufson et al., 2007; Strada et al., 1992; Whitehouse et al., 1981). Taken together these findings strongly suggest a fundamental role of the cholinergic system in AD pathophysiology.

We therefore hypothesized that the lack of the α7nAChRs (i.e., a receptor resistance) might induce a compensatory increase of Aβ production, triggering a dysfunctional loop that would lead to Aβ accumulation to toxic concentrations, ultimately resulting in structural alterations at the synapse and the consequent memory loss. Indeed, in the project described in chapter 2 (Tropea et al., 2021), we have demonstrated that the lack of α7nAChRs can trigger a feedback response with the increase of APP and Aβ production, accompanied by tau hyperphosphorylation and accumulation in the neurofibrillary tangles, causing memory loss associated with the structural signs of neurodegeneration (as summarized in Fig. 1).

Feedback mechanisms finely regulate most of physiological processes in the maintenance of the organism homeostasis and failure of these mechanisms invariably results in the onset of several pathologies. In Type II diabetes the insulin receptor resistance, induces a negative feedback maladaptive response, with an increase of insulin production that cannot exert its effect in the glycemic regulation. In a similar fashion an α7nAChR resistance (e.g., receptor polymorphism inactivation, auto-antibodies, etc.) can determine the shift from the positive to the negative effects of Aβ hormetic behavior.

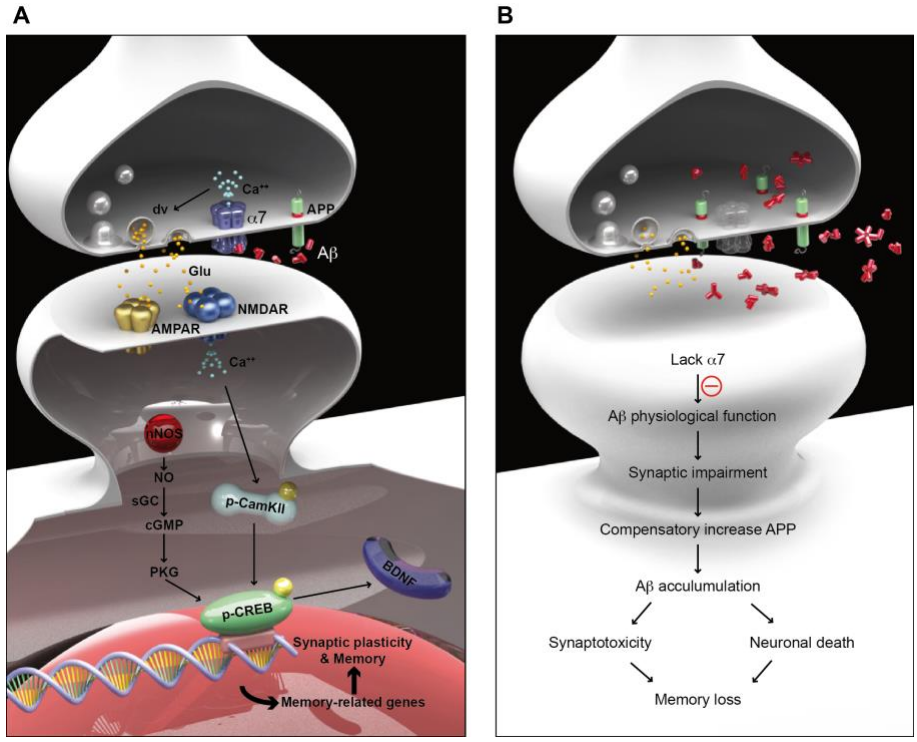

Figure 1. Failure of Aβ physiology triggers an Alzheimer-like pathology: a working hypothesis. A) In physiological conditions Aβ activates α7nAChRs leading to Ca^{2+} entry thus increasing neurotransmitter release. This, in turn, would trigger a cascade of intracellular events involving the NO/cGMP/PKG pathway and the plasticity-related molecules p-CREB, p-CaMKII and BDNF leading to the enhancement of synaptic plasticity and memory. B) The lack of α7nAChRs suppresses Aβ physiological function at the synapse and induces an increase of Aβ production that leads to Aβ accumulation and consequent synaptotoxicity.

Concluding remarks

Our work strongly suggests that α7nAChRs malfunction might precede the increase of Aβ and tau in the cascade of events leading to AD. Aβ

accumulation would therefore not represent the *primum movens* of AD pathology but a consequence of the failure of Aβ physiology.

This newfound perspective on the Aβ role in AD might be particularly relevant in understanding the current failure of AD therapeutic strategies based on lowering Aβ levels. Indeed, our findings question the very rational of the anti-Aβ approaches, suggesting this *Occam's razor strategy* "if Aβ is increased in AD patients, reducing Aβ levels is the answer" might not represent a good strategy for AD treatment.

Even if further studies are necessary to better delineate Aβ, tau and α7nAChRs crosstalk at the synapse, the data presented in this thesis suggest that the role of Aβ in AD needs to be reevaluated, considering mechanisms underlying the transition from physiology to pathology.

Up to now, one of the greatest limitations in the use of rodent models in AD research has been the need to rely upon transgenic animals overexpressing human genes mutated in Familiar forms of AD (FAD). FAD only account to the 2-3% of AD forms (Bird, 2008); therefore, these rodent models cannot provide dependable indications on the development of sporadic AD pathology. Our data suggest that α7 KO mice might represent an interesting model to evaluate the cascade of events leading to the increase of Aβ without exploiting FAD human genes.

The results presented in this thesis contribute to shine new light on the role of Aβ in AD. Our work might also represent a bridge between the two most accepted theories on AD pathophysiology: the amyloid hypothesis, that finds in Aβ increase and accumulation the cause of the disease, and the cholinergic hypothesis, that focuses on the loss of cholinergic transmission.

As Aβ shift from physiology to pathology plays an undeniable pivotal role in AD, further investigations are required to deepen the knowledge on the physiological role of Aβ at the synapse and its interplay with α7nAChRs and the cyclic nucleotides, as well as the intracellular pathways underlying Aβ compensatory increase. Understanding the dysfunctional loop regulating Aβ production might represent a key piece in the conceptualization of novel therapeutic strategies.

REFERENCES

Bird TD (2008) Genetics aspects of Alzheimer disease. Genetics in Medicine 10, 231-239

Bonkale WL, Cowburn RF, Ohm TG, Bogdanovic N, Fastbom J. A quantitative autoradiographic study of [3H]cAMP binding to cytosolic and particulate protein kinase A in post-mortem brain staged for Alzheimer's disease neurofibrillary changes and amyloid deposits. Brain Res. 1999 Feb 13;818(2):383-96. doi: 10.1016/s0006-8993(98)01307-9.

Burghaus, L., Schütz, U., Krempel, U., de Vos, R.A.., Jansen Steur, E.N.H., Wevers, A., Lindstrom, J., Schröder, H., 2000. Quantitative assessment of nicotinic acetylcholine receptor proteins in the cerebral cortex of Alzheimer patients. Mol. Brain Res. 76, 385–388.

Dickson, D.W., Crystal, H.A., Bevona, C., Honer, W., Vincent, I., Davies, P., 1995. Correlations of synaptic and pathological markers with cognition of the elderly. Neurobiol. Aging 16, 285–298. https://doi.org/10.1016/0197-4580(95)00013-5

Engidawork, E., Gulesserian, T., Balic, N., Cairns, N., Lubec, G., 2001. Changes in nicotinic acetylcholine receptor subunits expression in brain of patients with Down syndrome and Alzheimer's disease. J. Neural Transm. Suppl. https://doi.org/10.1007/978-3-7091-6262-0_17

Ghosh, A., Giese, K.P. Calcium/calmodulin-dependent kinase II and Alzheimer's disease. Mol Brain 8, 78 (2015). https://doi.org/10.1186/s13041-015-0166-2

Gulisano, W., Melone, M., Ripoli, C., Tropea, M.R., Li Puma, D.D., Giunta, S., Cocco, S., Marcotulli, D., Origlia, N., Palmeri, A., Arancio, O., Conti, F.,

Grassi, C., Puzzo, D., 2019. Neuromodulatory Action of Picomolar Extracellular Aβ42 Oligomers on Presynaptic and Postsynaptic Mechanisms Underlying Synaptic Function and Memory. J. Neurosci. 39, 5986–6000. https://doi.org/10.1523/JNEUROSCI.0163-19.2019

Hesse R, Lausser L, Gummert P, Schmid F, Wahler A, Schnack C, Kroker KS, Otto M, Tumani H, Kestler HA, Rosenbrock H, von Arnim CA. Reduced cGMP levels in CSF of AD patients correlate with severity of dementia and current depression. Alzheimers Res Ther. 2017 Mar 9;9(1):17. doi: 10.1186/s13195-017-0245-y.

Kuhn, J., Hardenacke, K., Lenartz, D., Gruendler, T., Ullsperger, M., Bartsch, C., Mai, J.K., Zilles, K., Bauer, A., Matusch, A., Schulz, R.-J., Noreik, M., Bührle, C.P., Maintz, D., Woopen, C., Häussermann, P., Hellmich, M., Klosterkötter, J., Wiltfang, J., Maarouf, M., Freund, H.-J., Sturm, V., 2015. Deep brain stimulation of the nucleus basalis of Meynert in Alzheimer's dementia. Mol. Psychiatry 20, 353–360. https://doi.org/10.1038/mp.2014.32

Mufson, E., Counts, S., Fahnestock, M., Ginsberg, S., 2007. Cholinotrophic Molecular Substrates of Mild Cognitive Impairment in the Elderly. Curr. Alzheimer Res. https://doi.org/10.2174/156720507781788855

Palmeri A, Ricciarelli R, Gulisano W, Rivera D, Rebosio C, Calcagno E, Tropea MR, Conti S, Das U, Roy S, Pronzato MA, Arancio O, Fedele E, Puzzo D (2017) Amyloid-β Peptide Is Needed for cGMP-Induced Long-Term Potentiation and Memory. The Journal of neuroscience : the official journal of the Society for Neuroscience 37:6926–6937

Puzzo D, Vitolo O, Trinchese F, Jacob JP, Palmeri A, Arancio O (2005) Amyloid-beta peptide inhibits activation of the nitric oxide/cGMP/cAMP-responsive element-binding protein pathway during hippocampal synaptic plasticity. The Journal of neuroscience : the official journal of the Society for Neuroscience 25:6887–6897

Puzzo D, Staniszewski A, Deng SX, Privitera L, Leznik E, Liu S, Zhang H, Feng Y, Palmeri A, Landry DW, Arancio O (2009) Phosphodiesterase 5 inhibition improves synaptic function, memory, and amyloid-beta load in an Alzheimer's disease mouse model. The Journal of neuroscience : the official journal of the Society for Neuroscience 29:8075–8086

Puzzo D, Piacentini R, Fá M, Gulisano W, Li Puma DD, Staniszewski A, Zhang H,

Tropea MR, Cocco S, Palmeri A, Fraser P, D'Adamio L, Grassi C, Arancio O (2017) LTP and memory impairment caused by extracellular Aβ and Tau oligomers is APP-dependent. eLife 6:1–21

Ricciarelli R, Puzzo D, Bruno O, Canepa E, Gardella E, Rivera D, Privitera L, Domenicotti C, Marengo B, Marinari UM, Palmeri A, Pronzato MA, Arancio O, Fedele E. A novel mechanism for cyclic adenosine monophosphate-mediated memory formation: Role of amyloid beta. Ann Neurol. 2014 Apr;75(4):602-7. doi: 10.1002/ana.24130.

Ripoli C, Cocco S, Li Puma DD, Piacentini R, Mastrodonato A, Scala F, Puzzo D, D'Ascenzo M, Grassi C (2014) Intracellular accumulation of amyloid-β (Aβ) protein plays a major role in Aβ-induced alterations of glutamatergic synaptic transmission and plasticity. The Journal of neuroscience : the official journal of the Society for Neuroscience 34:12893–12903

Opazo P, Viana da Silva S, Carta M, Breillat C, Coultrap SJ, Grillo-Bosch D, Sainlos M, Coussen F, Bayer KU, Mulle C, Choquet D. CaMKII Metaplasticity Drives Aβ Oligomer-Mediated Synaptotoxicity. Cell Rep. 2018 Jun 12;23(11):3137-3145. doi: 10.1016/j.celrep.2018.05.036.

Rosa E, Fahnestock M. (2015) CREB expression mediates amyloid β-induced basal BDNF downregulation. Neurobiology of Aging 36(8):2406-13. doi: 10.1016 j.neurobiolaging.2015.04.014

Song, JH., Yu, JT. & Tan, L. Brain-Derived Neurotrophic Factor in Alzheimer's Disease: Risk, Mechanisms, and Therapy. Mol Neurobiol 52, 1477–1493 (2015). https://doi.org/10.1007/s12035-014-8958-4

Strada, O., Vyas, S., Hirsch, E.C., Ruberg, M., Brice, A., Agid, Y., Javoy-Agid, F., 1992. Decreased choline acetyltransferase mRNA expression in the nucleus basalis of Meynert in Alzheimer disease: an in situ hybridization study. Proc. Natl. Acad. Sci. 89, 9549–9553. https://doi.org/10.1073/pnas.89.20.9549

Su Y, Ryder J, Ni B (2003) Inhibition of Aβ production and APP maturation by a specific PKA inhibitor https://doi.org/10.1016/S0014-5793(03)00645-8

Tam JH, Seah C, Pasternak SH. The Amyloid Precursor Protein is rapidly transported from the Golgi apparatus to the lysosome and where it is processed into beta-amyloid. Mol Brain. 2014 Aug 1;7:54. doi: 10.1186/s13041-014-0054-1.

Ugarte A, Gil-Bea F, García-Barroso C, Cedazo-Minguez Á, Ramírez MJ, Franco R,

García-Osta A, Oyarzabal J, Cuadrado-Tejedor M. Decreased levels of guanosine 3', 5'-monophosphate (cGMP) in cerebrospinal fluid (CSF) are associated with cognitive decline and amyloid pathology in Alzheimer's disease. Neuropathol Appl Neurobiol. 2015 Jun;41(4):471-82. doi: 10.1111/nan.12203.

Vitolo OV, Sant'Angelo A, Costanzo V, Battaglia F, Arancio O, Shelanski M (2002) Amyloid beta -peptide inhibition of the PKA/CREB pathway and long-term potentiation: reversibility by drugs that enhance cAMP signaling. Proc Natl Acad Sci USA. 2002 Oct 1;99(20):13217-21. doi: 10.1073/pnas.172504199.

Whitehouse, P.J., Price, D.L., Clark, A.W., Coyle, J.T., DeLong, M.R., 1981. Alzheimer disease: Evidence for selective loss of cholinergic neurons in the nucleus basalis. Ann. Neurol. 10, 122–126. https://doi.org/10.1002/ana.410100203

Zhang C, Cheng Y, Wang H, Wang C, Wilson SP, Xu J, Zhang HT. RNA interference-mediated knockdown of long-form phosphodiesterase-4D (PDE4D) enzyme reverses amyloid-β42-induced memory deficits in mice. J Alzheimers Dis. 2014;38(2):269-80. doi: 10.3233/JAD-122236.

Author's publications and awards

Original Peer Reviewed Research Articles

1. **Tropea MR**, Sanfilippo G, Giannino F, Davì V, Gulisano W, Puzzo D. Innate preferences affect results of object recognition task in wild type and Alzheimer's disease mouse models. J Alzheimers Dis. 2022;85(3):1343-1356. doi: 10.3233/JAD-215209.
2. Caruso G, Grasso M, Fidilio A, Torrisi SA, Musso N, Geraci F, **Tropea MR**, Privitera A, Tascedda F, Puzzo D, Salomone S, Drago F, Leggio GM, Caraci F. Antioxidant activity of fluoxetine and vortioxetine in a non-transgenic animal model of Alzheimer's disease. Front Pharmacol. 2021 Dec 24;12:809541. doi: 10.3389/fphar.2021.809541.
3. **Tropea MR**, Li Puma DD, Melone M, Gulisano W, Arancio O, Grassi C, Conti F, Puzzo D. Genetic deletion of α7 nicotinic acetylcholine receptors induces an age-dependent Alzheimer's disease-like pathology. Prog Neurobiol. 2021 Nov; 206:102154. doi: 10.1016/j.pneurobio.2021.102154.
4. Torrisi SA*, Geraci F*, **Tropea MR***, Grasso M, Caruso G, Fidilio A, Musso N, Sanfilippo G, Tascedda F, Palmeri A, Drago F, Salomone S, Puzzo D, Leggio GM, Caraci F. Fluoxetine and Vortioxetine reverse depressive-like phenotype and memory deficits induced by Aβ1-42 oligomers in mice: a key role of Transforming Growth Factor-β1. Front Pharmacol. ***Co-first author**.
5. Gulisano W, Melone M, Ripoli C, **Tropea MR**, Li Puma DD, Giunta S, Cocco S, Marcotullli D, Origlia N, Palmeri A, Arancio O, Conti F, Grassi G, Puzzo D. Neuromodulatory action of picomolar extracellular Aβ42 oligomers on pre- and postsynaptic mechanisms underlying synaptic function and memory. J Neurosci. 2019 May 24; 0163:19. doi: 10.1523/JNeurosci.0163-19.2019.
6. Costa L, Sardone LM, Bonaccorso CM, D'Antoni S, Spatuzza M, Gulisano W, **Tropea MR**, Puzzo D, Leopoldo M, Lacivita E, Catania MV, Ciranna L. Activation of Serotonin 5-HT7 Receptors

Modulates Hippocampal Synaptic Plasticity by Stimulation of Adenylate Cyclases and Rescues Learning and Behavior in a Mouse Model of Fragile X Syndrome. Front Mol Neurosci. 2018 Oct 2;11:353. doi: 10.3389/fnmol.2018.00353.

7. Gulisano W, Melone M, Li Puma DD, **Tropea MR**, Palmeri A, Arancio O, Grassi C, Conti F, Puzzo D. The effect of amyloid-beta peptide on synaptic plasticity and memory is influenced by different isoforms, concentrations and aggregation status. Neurobiol Aging. Neurobiol Aging. 2018 Jul 18;71:51-60. doi: 10.1016/j.neurobiolaging.2018.06.025.
8. Gulisano W*, **Tropea MR***, Arancio O, Palmeri A, Puzzo D. Sub-efficacious doses of phosphodiesterase 4 and 5 inhibitors improve memory in a mouse model of Alzheimer's disease. Neuropharmacology. 2018 Jun 6;138:151-159. doi: 10.1016/j.neuropharm.2018.06.002. ***Co-first author**.
9. Puzzo D, Piacentini R, Fá M, Gulisano W, Li Puma DD, Staniszewski A, Zhang H, **Tropea MR**, Cocco S, Palmeri A, Fraser P, D'Adamio L, Grassi C, Arancio O. LTP and memory impairment caused by extracellular Aβ and Tau oligomers is APP-dependent. Elife. 2017 Jul 11;6. pii: e26991. doi: 10.7554/eLife.26991.
10. Palmeri A, Ricciarelli R, Gulisano W, Rivera D, Rebosio C, Calcagno E, **Tropea MR**, Conti S, Das U, Roy S, Pronzato MA, Arancio O, Fedele E, Puzzo D. Amyloid-β Peptide Is Needed for cGMP-Induced Long-Term Potentiation and Memory. J Neurosci. 2017 Jul 19;37(29):6926-6937. doi: 10.1523/JNEUROSCI.3607-16.2017.
11. Palmeri A, Mammana L, **Tropea MR**, Gulisano W, Puzzo D. Salidroside, a Bioactive Compound of Rhodiola Rosea, Ameliorates Memory and Emotional Behavior in Adult Mice. J Alzheimers Dis. 2016 Feb 26;52(1):65-75. doi: 10.3233/JAD-151159.

Oral communications

1. **Tropea MR**, Gulisano W, Li Puma DD, Melone M, Arancio O, Grassi C, Conti F, Puzzo D. A failure of Amyloid-β physiological function due to the deletion of α7 nicotinic acetylcholine receptors triggers an Alzheimer's disease-like pathology. In: 71st SIF National Congress Milan (Online). 7-9 September 2021.
2. **Tropea MR**. Neuromodulatory role of Amyloid-beta peptide at the synapse: pre- and post-synaptic mechanisms. In: BIOMETEC Retreat. Nov 30 – Dec 1, 2019.
3. **Tropea MR**, Gulisano W, Teich A, Arancio O, Palmeri A, Puzzo D. Oligomeric Amyloid-beta at physiological concentrations rescues the impairment of hippocampal synaptic plasticity and memory in aged Amyloid Precursor Protein knockout mice. In: FEPS 2019. Bologna, Sept 10-13, 2019.
4. **Tropea MR.** Oligomeric amyloid-beta peptide at picomolar concentrations converts early-LTP into late-LTP, and short-term into long-term memory through the NO/cGMP/PKG/CREB pathway. In: 13th Annual Meeting of Young Researchers in Physiology. Anacapri (NA), May 10-12, 2019.
5. **Tropea MR**. Synaptic plasticity and Memory in physiological conditions and Neurodegenerative disorders. Workshop in: The International Medical Students' Congress of Bucharest. Bucharest (Romania), Dec 5-9, 2018 (invited speaker).
6. **Tropea MR**, Gulisano W, Arancio O, Prickaerts J, Palmeri A, Puzzo D. cAMP and cGMP specific phosphodiesterase inhibitors enhance memory in physiological conditions and Alzheimer's disease. In: 69° Congress of the Italian Physiological Society. Florence, Sept 19-21, 2018.
7. **Tropea MR**, Puzzo D. Amyloid-beta peptide is required for the cGMP-induced long-term potentiation and memory. In: The International Medical Students' Congress of Bucharest. Bucharest (Romania), Dec 6-10, 2017.
8. **Tropea MR**, Mammana L, Gulisano W, Puzzo D, Palmeri A. Effects of Salidroside, a bioactive compound of Rhodiola Rosea, on memory and emotional behavior in adult mice. In: 67° Congress of the Italian Physiological Society. Catania, Sept 21-23, 2016 (poster pitch context).

Posters

1. **Tropea MR**, Gulisano W, Romano A, Giannino F, Leggio GM, Puzzo D. Physiological role of dopamine D3 receptors in hippocampal synaptic plasticity and memory. In SfN Virtual Neuroscience 2021. Nov 8-11, 2021 (poster presenter).
2. **Tropea MR,** Gulisano W, Li Puma DD, Melone M, Arancio O, Grassi C, Conti F, Puzzo D. A failure of Amyloid-β physiological function due to deletions of α7 nicotinic acetylcholine receptors triggers an Alzheimer's disease-like pathology. In SfN Global Connectome: a virtual event. Jan 11-13, 2021 (poster presenter).
3. **Tropea MR,** Gulisano W, Puzzo D. A novel modular behavioral apparatus to standardize experimental context in recognition memory assessment. In: Neuroscience 2019, Oct 19 23 2019, Chicago, IL, USA (poster presenter).
4. Gulisano W, **Tropea MR**, Puzzo D. The relevance of a standardized experimental context to assess recognition memory: realization of a novel modular behavioral apparatus. In FEPS 2019. Bologna, Sept 10-13, 2019.
5. **Tropea MR**, Gulisano W, Melone M, Li Puma DD, Palmeri A, Arancio O, Grassi C, Conti F, Puzzo D. Unraveling the role of different isoforms, concentrations, and aggregation status of amyloid-β peptide in hippocampal synaptic plasticity and memory. In: National Meeting of PhD Students in Neuroscience 2019. Naples, Mar 1, 2019. (poster presenter).
6. Puzzo D, Gulisano W, **Tropea MR**, Arancio O, Palmeri A. A combination of sub-efficacious doses of phosphodiesterase 4 and 5 inhibitors rescued spatial, recognition and fear memory in a mouse model of Alzheimer's disease. In: Society for Neuroscience Meeting. San Diego, USA, Nov 3-7, 2018.
7. Ciranna L, Costa L, Spatuzza M, Bonaccorso CM, D'Antoni S, Gulisano W, **Tropea MR**, Leopoldo M, Lacivita E, Puzzo D,

Catania MV. In vivo treatment with a 5-HT7 receptor agonist rescues synaptic plasticity, dendritic spine morphology, learning and behavior in a mouse model of Fragile X Syndrome. In: 11th FENS Forum. Berlin (Germany), July 7-11, 2018.

8. Puzzo D, Piacentini R, Fá M, Gulisano W, Li Puma DD, Staniszewski A, Zhang H, **Tropea MR**, Cocco S, Palmeri A, Fraser PE, D'Adamio L, Grassi C, Arancio O. Oligomers of amyloid-beta and tau impair synaptic plasticity and memory in an APP-dependent fashion. In: SOCIETY FOR NEUROSCIENCE ABSTRACT. Neuroscience 2017. Washington D.C. (CA), USA. Nov 11-15, 2017.
9. Sanfilippo G, Melone M, Gulisano W, **Tropea MR**, Palmeri A, Conti F, Puzzo D. Both monomers and oligomers of Amyloid-β peptide are involved in synaptic plasticity in physiological and pathological conditions. In: 68° Congress of the Italian Physiological Society. Pavia, Sept 6-8, 2017.
10. **Tropea MR**, Gulisano W, Puzzo D, Palmeri A. The effect of 200 pM Amyloid-beta on short- and long-term plasticity depends upon endogenous α7-nicotinic ACh receptors. In: 68° Congress of the Italian Physiological Society. Pavia, Sept 6-8, 2017 (poster presenter).
11. Puzzo D, Ricciarelli R, Gulisano W, **Tropea MR**, Rebosio C, Arancio O, Fedele E, Palmeri A. Amyloid-beta peptide is required for the cGMP-induced long-term potentiation and memory. In: SOCIETY FOR NEUROSCIENCE ABSTRACT. Neuroscience 2016. San Diego (CA), USA. Nov 3-7, 2016.
12. Puzzo D, Ricciarelli R, Gulisano W, **Tropea MR**, Rebosio C, Arancio O, Fedele E, Palmeri A. Amyloid-beta peptide is needed for cGMP-induced long-term potentiation and memory. In: 10th FENS Forum. Copenhagen (Denmark), July 2-6, 2016.
13. **Tropea MR**, Mammana L, Gulisano W, Puzzo D, Palmeri A. Enhancing effects of Salidroside, a bioactive compound of Rhodiola Rosea, on cognition and emotional behavior in adult mice. In: Controversies in Neurodegeneration, Joint Meeting of the SIF Workgroups "neurodegenerative diseases" and "Inflammation". Catania, Jun 9, 2016 (poster presenter).

Awards

1. Special Mention. In: Young Researchers in Physiology. Anacapri, May 10-12, 2019.
2. Chair Oral Presentation Session. In: National Meeting of PhD Students in Neuroscience 2019. Naples, Mar 1, 2019.
3. Best Oral Presentation in Fundamental Sciences, Medical Students' Society of Bucharest, Romania. Bucharest, Dec 10, 2017.
4. Best Poster Award, Italian Society of Physiology. Catania, Sept 23, 2016.